
Electronic Thesis and Dissertation Repository

9-24-2018 11:00 AM

Brachypodium distachyon Histone Deacetylase BdHD1: A Positive Regulator in ABA Sensitivity and Drought Tolerance

Jingpu Song, *The University of Western Ontario*

Supervisor: Tian, Lining, *The University of Western Ontario*

Co-Supervisor: Henry, Hugh, *The University of Western Ontario*

A thesis submitted in partial fulfillment of the requirements for the Doctor of Philosophy degree in Biology

© Jingpu Song 2018

Follow this and additional works at: <https://ir.lib.uwo.ca/etd>



Part of the [Molecular Genetics Commons](#)

Recommended Citation

Song, Jingpu, "Brachypodium distachyon Histone Deacetylase BdHD1: A Positive Regulator in ABA Sensitivity and Drought Tolerance" (2018). *Electronic Thesis and Dissertation Repository*. 5728. <https://ir.lib.uwo.ca/etd/5728>

This Dissertation/Thesis is brought to you for free and open access by Scholarship@Western. It has been accepted for inclusion in Electronic Thesis and Dissertation Repository by an authorized administrator of Scholarship@Western. For more information, please contact wlsadmin@uwo.ca.

Abstract

Despite evidence that specific histone deacetylases (HDACs) play important roles in the abiotic stress responses of plants, their roles in the stress responses of monocots remain largely unexplored. I investigated a HDAC gene, *Bradi3g08060* (*BdHDI*), in the monocot *Brachypodium distachyon* (*Brachypodium*). The *Brachypodium BdHDI*-overexpression (OE) plants displayed a hypersensitive phenotype to abscisic acid (ABA) and exhibited higher survival under drought conditions. Conversely, the *BdHDI*-RNAi plants were insensitive to ABA and had low survival under drought stress. Based on ChIP-Seq at the genome-wide level, overexpressing *BdHDI* led to lower acetylation on lysine residue 9 of histone 3 at the transcriptional start sites of 230 genes than in wild type plants under the drought treatment. I validated the ChIP-Seq data for 10 transcription factor genes from the 230 drought-specific genes. These genes exhibited much lower expression in *BdHDI*-OE compared to the wild type plants under drought stress. I further identified an ABA-inducible transcription factor gene, *BdWRKY24* and analysis showed this gene was repressed in *BdHDI*-OE plants but highly expressed in *BdHDI*-RNAi plants under drought stress. These results indicate that *BdHDI* plays a positive role in ABA sensitivity and drought stress tolerance, and they provide a link between the role of *BdHDI* and the drought stress response at a genome-wide level in *Brachypodium*.

Key Words

BdHD1, *Brachypodium*, CHIP-Seq, drought stress, histone acetylation, histone deacetylase, H3K9ac

Acknowledgements

I thank my supervisor Dr. Lining Tian for giving me such an opportunity to pursue my PhD in his research team. His supervising style has led to my growth as an independent researcher. I really appreciate the freedom and support that have been given from him to pursue my own ideas. I am grateful to my co-supervisor Dr. Hugh Henry for the guidance and advice during the five years of graduate school. Especially, my thesis writing has improved because of his help.

I thank my advisory committee members Dr. Shiva Singh and Dr. Frederic Marsolais for their valuable time and advice throughout this project.

I would also like to thank all my fellow lab mates: Dr. Gang Tian, lab technician Mimmie Lu and other graduate students in the lab. I am grateful for their encouragement and helpful discussion on my project.

My special thanks go to Dr. Chen Chen, Dr. Chenlong Li and Jie Shu for their help with ChIP-Seq data analysis. I thank Dr. Benjamin Rubin for his help on data statistical analysis. Many thanks to all the people at the London Research and Development Center for their friendships.

Last but not least, I appreciate my parents for their support!

Table of Contents

Abstract	i
Key Words	ii
Acknowledgements	iii
Table of Contents	iv
List of Tables	vii
List of Figures	viii
List of Appendices	x
Abbreviations	xi
Chapter 1 Introduction	1
1.1 Drought is a threat to crop production.....	1
1.2 ABA regulatory networks in response to drought stress	2
1.2.1 The core ABA-signaling pathway	2
1.2.2 Other ABA-signaling pathways.....	6
1.3 Histone deacetylases in drought stress responses	11
1.4 <i>Brachypodium distachyon</i> , a genetic model system for studying monocots	16
1.5 Hypothesis and objectives	18
Chapter 2 Materials and Methods	19
2.1 Plant materials and growth conditions	19
2.2 Phylogenetic analysis	19
2.3 Plant RNA extraction and gene cloning	19
2.4 Subcellular localization	20
2.5 Generation of stable transgenic <i>Brachypodium</i> plants	20
2.6 Homozygous transgenic plant selection using a progeny test.....	22
2.7 Plant genome DNA isolation.....	23
2.8 General polymerase chain reaction setup.....	23
2.9 Stress treatments.....	23
2.10 Soil water content and leaf water potential (Ψ_1) measurements	25
2.11 Protein extraction and protein gel blotting	26
2.12 Chromatin immunoprecipitation assays	26
2.13 ChIP-Seq and data analysis	28

2.14 Gene ontology analysis	29
2.15 Gene expression analysis.....	29
2.16 Primer design.....	30
2.17 Statistical analysis	30
Chapter 3 Results	31
3.1 Characterization of <i>BdHDI</i> in response to drought stress in <i>Brachypodium</i>	31
3.1.1 <i>BdHDI</i> is an homologous gene of <i>HDAC1</i>	31
3.1.2 Expression of <i>BdHDI</i> is reduced by drought stress and ABA.....	39
3.1.3 Development of <i>BdHDI</i> -overexpression lines and <i>BdHDI</i> -RNA interference lines.....	44
3.1.4 Overexpression of <i>BdHDI</i> enhances drought tolerance in <i>Brachypodium</i>	49
3.1.5 <i>bdhd1-30</i> plants exhibit lower survival under drought stress.....	49
3.1.6 Overexpression of <i>BdHDI</i> leads to a ABA-hypersensitive phenotype during seed germination and post-germination growth	54
3.1.7 <i>BdHDI</i> -RNAi plants show insensitivity to ABA.....	57
3.1.8 Overexpressing <i>BdHDI</i> does not affect the expression of <i>PYL4</i> , <i>AGH3</i> and <i>ABI5</i>	57
3.2 <i>BdHDI</i> reduces H3K9ac and represses gene expression under drought stress	62
3.2.1 Overexpression of <i>BdHDI</i> leads to a decrease of H3K9ac in <i>Brachypodium</i> ..	62
3.2.2 H3K9ac modification patterns under drought stress conditions.....	65
3.2.3 Identification of differentially H3K9ac modified genes under drought stress in OE22	68
3.2.4 Association of H3K9ac modification changes with differential gene expression under drought stress.....	73
3.2.5 <i>BdWRKY24</i> is a drought- and ABA-inducible transcription factor	80
Chapter 4 Discussion	83
4.1 <i>BdHDI</i> positively regulates ABA sensitivity and drought tolerance in <i>Brachypodium</i>	83
4.2 <i>BdHDI</i> represses gene expression through H3K9 deacetylation	85
4.3 <i>BdHDI</i> affects the expression of <i>BdWRKY24</i>	87
4.4 Concluding remarks and perspectives	88
References	91

Appendices 100
Curriculum Vitae 104

List of Tables

Table 1. Histone deacetylases in <i>Brachypodium</i>	32
--	----

List of Figures

Figure 1. Model of the core ABA signaling pathway involved in drought stress response	4
Figure 2. A model of regulation of WRKY40 in the ABA response	9
Figure 3. Histone acetylation and its regulation by HDACs and HATs	12
Figure 4. Phylogenetic analysis of histone deacetylases of <i>Brachypodium</i> and <i>Arabidopsis</i>	33
Figure 5. Domain organization of HDACs in HDA6, HDA9, HDA19 and BdHD1	35
Figure 6. Subcellular localization of BdHD1-YFP fusion proteins	37
Figure 7. Drought-induced changes in <i>Brachypodium</i> using the soil drying method.....	40
Figure 8. Gene expression of <i>BdHD1</i> under drought, PEG-6000, mannitol and ABA	42
Figure 9. Generation of <i>BdHD1</i> -overexpression lines.....	45
Figure 10. Generation of <i>BdHD1</i> -RNAi lines	47
Figure 11. Survival of <i>BdHD1</i> -OE plants under drought stress	50
Figure 12. Survival of <i>BdHD1</i> -RNAi plants under drought stress	52
Figure 13. <i>BdHD1</i> -OE plants are hypersensitive to ABA during germination and during post-germination growth.	55
Figure 14. Knocking down <i>BdHD1</i> in <i>bdhd1-30</i> leads to an ABA insensitive phenotype during post-germination growth.....	58
Figure 15. Gene expression of <i>PYL4</i> , <i>ABI5</i> and <i>AGH3</i> in <i>BdHD1</i> -OE plants.....	60
Figure 16. Overexpressing <i>BdHD1</i> leads to a decrease of H3K9ac at the genome-wide level	63
Figure 17. The distribution of H3K9ac modification in Bd21-3 and OE22 plants under control and drought conditions.....	66
Figure 18. Regions with decreased H3K9ac in OE22	69

Figure 19. Gene ontology analysis of the 230 drought-specific genes	71
Figure 20. Profiling of H3K9ac on the 10 transcription factor genes under control conditions.	74
Figure 21. Profiling of H3K9ac on the 10 transcription factor genes under drought conditions	76
Figure 22. Expression of the “binding activity” genes	78
Figure 23. Expression analysis of <i>BdWRKY24</i> under drought stress and ABA	81

List of Appendices

Appendix 1. Primers used for gene amplification of <i>BdHDI</i>	101
Appendix 2. Primers used for genotyping of <i>BdHDI</i> -RNAi plants	102
Appendix 3. Primers used for ChIP-qPCR	103
Appendix 4. Primers used for RT-qPCR	104

Abbreviations

Abbreviation	Full name
1/2 MS	half strength of MS medium
ABA	abscisic acid
ABAR	ABA receptor
ABF	ABA-responsive element binding factors
ABI1	ABA-insensitive 1
ABI2	ABA-insensitive 2
ABI3	ABA-insensitive 3
ABI4	ABA-insensitive 4
ABI5	ABA-insensitive 5
ac	acetylation
AGH3	ABA-hypersensitive germination 3
AREB	ABA-responsive element binding protein
bp	base pair
bZIP	basic-domain leucine zipper
CBF	C-repeat binding factor
cDNA	complementary DNA
CDS	coding DNA sequence
ChIP	chromatin immunoprecipitation

ChIP-qPCR	ChIP followed by quantitative real-time PCR
ChIP-Seq	ChIP followed by next generation sequencing
C _T	cycle threshold value
CTAB	hexadecyltrimethylammonium bromide
DNA	deoxyribonucleic acid
EDTA	ethylenediaminetetraacetic acid
ERF	ethylene response factor
gDNA	genomic DNA
GFP	green fluorescent protein
GO	gene ontology
H2A	histone 2 A
H2B	histone 2 B
H3	histone 3
H3K9	lysine residue 9 of histone 3
H3K9ac	acetylation of H3K9
H4	histone 4
HAT	histone acetyltransferase
HD-tuin	histone deacetylase-tuin
HD-Zip	homeodomain-leucine zipper
HDAC	histone deacetylase

IGB	integrated genome browser
kb	kilo base pair
MACS	model-based analysis for ChIP-Seq
MS	Murashige and Skoog
MYB	myeloblastosis
NAC	no apical meristem/cup-shaped cotyledon
NAD-	nicotinamide adenine dinucleotide-
OE	overexpression
PCR	polymerase chain reaction
PEG	polyethylene glycol
PMSF	phenylmethylsulfonyl
PP2C	type 2C protein phosphatases
PYR/PYL/RCAR	pyrabactin resistance/pyrabactin-like or regulatory components of ABA receptor
RNA	ribonucleic acid
RNA-Seq	RNA sequencing
RNAi	RNA interference
RPD3	reduced potassium dependency protein 3
RT-qPCR	real-time quantitative PCR
SamDC	S-adenosylmethionine decarboxylase

SDS	sodium dodecyl sulfate
SE	standard error
SICER	spatial clustering for identification of ChIP-enriched regions
SIR2	silent information regulator protein 2
SnRK2	sucrose nonfermenting 1-related protein kinase 2
SRT	sirtuin
T-DNA	transfer DNA
TSS	transcription start site
TTS	transcription termination site
v/v	volume/volume
w/v	weight/volume
WIG	wiggle
WRKY	WRKY transcription factor
YFP	yellow fluorescent protein
β -ME	β -mercaptoethanol

Chapter 1 Introduction

1.1 Drought is a threat to crop production

Water availability is a key factor for plant growth and survival. A lack of water causes drought, which is one of the largest threats to plant productivity throughout the world (Rosegrant, 2003; Lesk et al., 2016). The intensity and duration of drought events have been increasing globally since the 1970s, and the number of severe drought events is likely to increase during the 21st century (Burke et al., 2006; Blunden et al., 2011). In the 2000s, long-term drought events were experienced in the western United States, northeast China and southeast Australia, while the central United States, Russia and Ukraine also suffered short-term but severe drought events (Sternberg, 2011). The effects of drought are expected to increase and spread with growing water scarcity and global climate change (Harb et al., 2010). Drought can be a major challenge for agriculture by severely affecting crop growth and reducing yields (Daryanto et al., 2016; Lesk et al., 2016). Meanwhile, the global demand for food is projected to increase for at least another 40 years (Godfray et al., 2010; Fita et al., 2015). To help meet this increasing food demand under such circumstances, the development of crop plants tolerant to drought stress is a promising approach.

The effects of drought stress in plants can be evident at all stages, including germination, plant growth and seed production (Farooq et al., 2009). Understanding the physiological mechanisms and genetic control of drought responses is required for the development of crops with enhanced drought tolerance. Because plants are sessile, and are thus limited in their ability to search for additional water in their environment, they have adapted at the physiological, molecular and cellular levels to respond to and survive drought stress. Plant response to drought is a complex process (Mickelbart et al., 2015). Plants can exhibit drought stress responses through drought resistance. Drought resistance includes drought avoidance and drought tolerance (Price, 2002). Drought avoidance is when plants maintain high tissue water potential by improving water uptake and the capacity of plant cells to hold water and reduce water loss despite a soil water deficit (Price, 2002). Drought tolerance is when plants can withstand a water deficit with low tissue water potential and survive drought stress (Ingram and Bartels, 1996).

Understanding the mechanisms of drought responses has been an active topic of plant research. Plants respond to drought stress via a range of physiological and biochemical changes. These changes include stomatal closure, repression of photosynthesis and cell growth (reviewed by Osakabe et al., 2014). At the molecular level, drought stress triggers the activation or repression of drought-responsive genes (Kapazoglou and Tsafaris, 2011). The products of gene expression may function in drought response and tolerance at the cellular level (Shinozaki and Yamaguchi-Shinozaki, 2007). Studying the physiological and molecular mechanisms of drought responses offers the opportunity to advance a more holistic understanding of drought resistance. This understanding of drought stress can lead to development of drought-tolerant crops.

1.2 ABA regulatory networks in response to drought stress

Plants respond to drought stress by inducing the expression of a variety of genes. The products of these genes are thought to enhance stress tolerance and to regulate gene expression through signal transduction pathways (Shinozaki et al., 2003). Under water deficit conditions, the plant hormone abscisic acid (ABA) is produced, and it plays crucial roles in plant stress responses (Finkelstein, 2013). ABA accumulates in guard cells to promote stomatal closure, which reduces water loss from transpiration (Schroeder et al., 2001; Hosy et al., 2003). ABA induces the expression of many genes that respond to drought stress in plants (Finkelstein, 2013). Current evidence has demonstrated that the existence of both ABA-dependent and ABA-independent regulatory systems governs drought stress-inducible gene expression (Yamaguchi-Shinozaki and Shinozaki, 2005). ABA regulates the expression of many stress-responsive genes whose products may prevent vegetative tissues from dehydration or high osmotic pressure (Umezawa et al., 2010). Thus, ABA is a drought stress-related phytohormone.

1.2.1 The core ABA-signaling pathway

Numerous studies have been conducted to increase understanding of the cellular and molecular basis of ABA responses. The ABA signaling model has been dramatically updated since the breakthrough discovery in 2009 of the ABA receptors PYRABACTIN RESISTANCE1/PYR1-LIKE/REGULATORY COMPONENTS OF ABA RECEPTOR

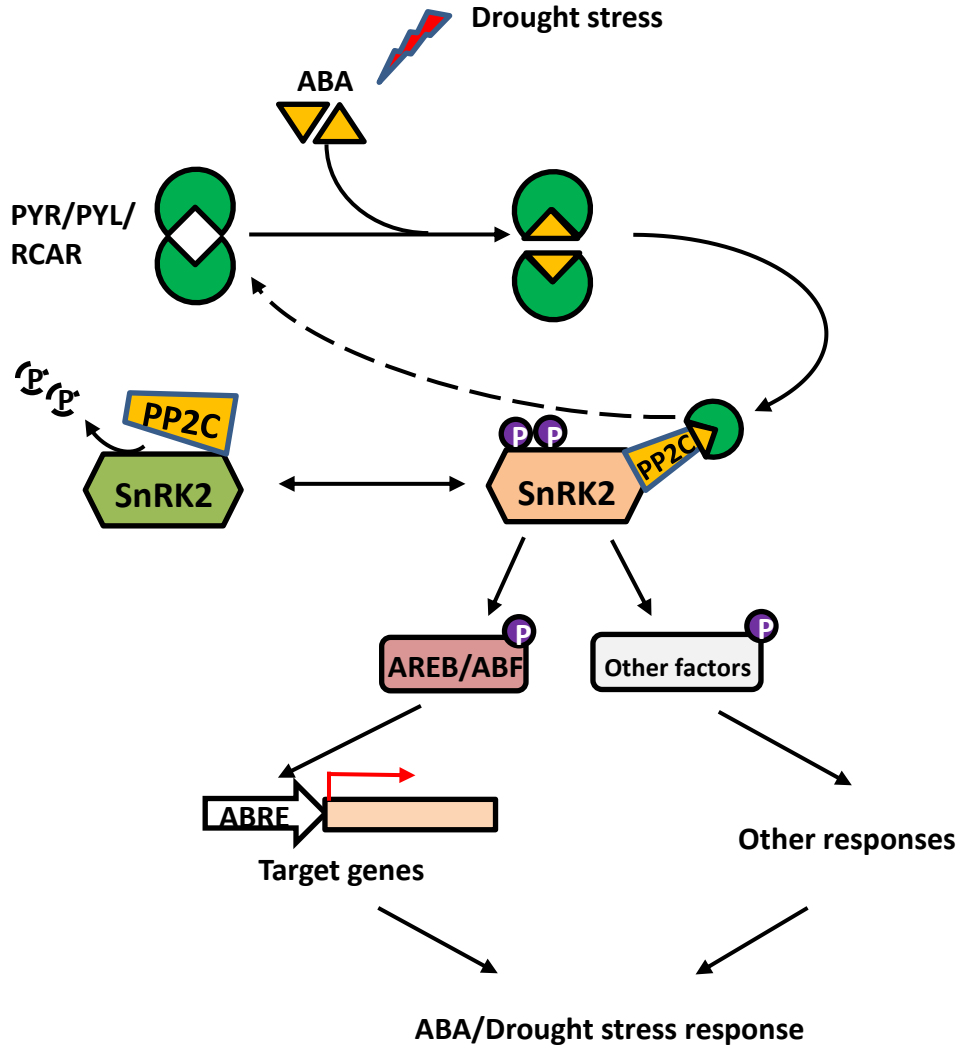
(P_{YR}/P_{YL}/R_{CAR}) (Ma et al., 2009; Park et al., 2009) and the identification of a protein phosphatase-kinase complex as downstream component of P_{YR}/P_{YL}/R_{CAR} (Umezawa et al., 2009). A double negative regulatory system of the ABA signaling pathway has been proposed and supported by several studies. The regulatory system consists of four components: the ABA receptors P_{YR}/P_{YL}/R_{CAR}, PROTEIN PHOSPHATASES 2C (PP2Cs), protein kinases SUCROSE NONFERMENTING-1-RELATED KINASES 2 (SnRK2s) and their downstream target genes (basic-domain leucine zipper (bZIP) transcription factors) (Melcher et al., 2009; Santiago et al., 2009; Umezawa et al., 2009). The core signaling model was well reviewed in 2010 (Umezawa et al., 2010). Briefly, as shown in Figure 1, SnRK2 is inactivated by the direct dephosphorylation of PP2C in the presence of ABA. Under drought stress, ABA promotes the interaction of P_{YL}/P_{YL}/R_{CAR} and PP2C, resulting in the inhibition of PP2C and the activation of SnRK2. SnRK2 phosphorylates ABA-RESPONSIVE ELEMENT BINDING/ ABA-RESPONSIVE ELEMENT BINDING FACTOR (AREB/ABF)-type bZIP transcription factors to regulate gene expression of downstream targets. Transcription factors regulate gene clusters through specifically binding to the cis-acting element in the promoters of the respective target genes. A single transcription factor can control the expression of many targets (Nakashima et al., 2009). AREB/ABF are bZIP transcription factors that regulate ABA-dependent gene expression under drought stress conditions (Fujita, 2005). It has been demonstrated that the phosphorylation of ABRE/ABFs by SnRK2s is crucial in the regulatory system for ABA responses (Fujita et al., 2009; Umezawa et al., 2013).

The first two protein phosphatase genes, *ABA-INSENSITIVE1* (*ABI1*) and *ABI2*, were identified from a genetic screen in the mid-1990s (Leung et al., 1997). *ABI1* and *ABI2* belong to a subgroup of the PP2C family, group A (Schweighofer et al., 2004). The mutant plants, *abi-1* or *abi-2*, showed ABA insensitive phenotypes. However, the loss-of-function type mutants of other group A members are hypersensitive to ABA. These observations suggest that PP2Cs are major negative regulators of ABA signaling (Hirayama and Shinozaki, 2007). PP2C functions are well conserved, because they play negative regulatory roles in ABA signaling in different plant species (Komatsu et al., 2009; Tougane et al., 2010). SnRK2 was first identified as an ABA-activated protein kinase and later was

Figure 1. Model of the core ABA signaling pathway involved in drought stress response

Under control conditions, PP2C negatively regulates SnRK2 by direct interactions and dephosphorylation of multiple residues of SnRK2. Once drought stress up-regulates endogenous ABA, PYR/PYL/RCAR binds ABA and interacts with PP2C to inhibit protein phosphatase activity. In turn, SnRK2 is released from PP2C-dependent regulation and activated to phosphorylate downstream factors, such as the AREB/ABF bZIP-type transcription factor or membrane proteins involving ion channels. The products of these genes respond to ABA/drought stress.

This figure is modified from Umezawa et al. (2010)



characterized as a global regulator of ABA signaling in plants (Mikołajczyk et al., 2000; Umezawa et al., 2004). Overexpressing SnRK2 positively regulates drought tolerance in plants (Umezawa et al., 2004). The double negative regulation system in ABA signaling suggests that the ABA receptors PYR/PYL/RCAR positively regulate ABA signaling. Thus, perception and receptor factors, such as PYL4, can be used to improve drought stress tolerance (Pizzio et al., 2013). The transcriptional activities of AREB/ABF transcription factors are controlled by ABA-dependent phosphorylation. Overexpression of AREB enhances ABA hypersensitivity and drought tolerance in plants (Yoshida et al., 2010; Barbosa et al., 2013).

1.2.2 Other ABA-signaling pathways

In addition to the core ABA-signaling pathway, many other ABA-dependent transcription factors function in regulating drought stress responsive genes under water deficit conditions. It has been demonstrated that some members of the myeloblastosis (MYB) and MYC families (Abe et al., 1997), homeodomain-leucine zipper (HD-Zip) (Zhang et al., 2012), the No Apical Meristem/Cup-Shaped Cotyledon (NAC) (Tran et al., 2004a; Nakashima et al., 2007) and WRKY factors (Rushton et al., 2012) play critical roles in ABA and abiotic responses.

The positive or negative roles of MYB/MYC, HD-Zip and NAC in ABA responses have been studied in many plant species (Nakashima et al., 2014). In *Arabidopsis thaliana* (*Arabidopsis*), drought stress induces a dehydration-responsive gene, *RD22*, which is dependent on ABA biosynthesis (Yamaguchi-Shinozaki and Shinozaki, 1993). The induction of *RD22* is mediated by two transcription factors, MYC and MYB. MYC2, a MYC transcription factor, and MYB2, a MYB transcription factor, can bind to these cis-acting elements and cooperatively activate the gene expression of this gene (Abe et al., 1997). HD-Zip proteins have been found and characterized in a wide variety of plant species. Many HD-Zip family members are involved in responses to abiotic stress, including drought stress (Ariel et al., 2007; Agalou et al., 2008). Two HD-Zip genes, *AtHB7* and *AtHB12*, strongly induced by ABA and drought stress, function as negative regulators of the ABA response pathway in *Arabidopsis* (Valdés et al., 2012). NAC transcription factors also regulate stress-responsive genes through the ABA-dependent pathway (Valdés

et al., 2012). Overexpressing the *STRESS-RESPONSIVE NAC1(SNAC1)* gene enhanced ABA sensitivity and improved drought tolerance in *Oryza sativa* (rice) (Hu et al., 2006). In *Arabidopsis*, the expression of three NAC transcription factors, *ANAC019*, *ANAC055* and *ANAC072*, was induced by drought stress and ABA. Overexpressing either *ANAC019*, *ANAC055* or *ANAC072* gene led to up-regulation of several stress-inducible genes and the plants showed increased drought tolerance (Tran et al., 2004).

WRKY proteins comprise one of the largest families of transcription factors found in plants (Rushton et al., 2010). Although the involvement of WRKY transcription factors in plant pathogen responses has been well documented, it was only recently that some of the family members were shown to respond to ABA and drought stress (Ren et al., 2010; Rushton et al., 2012; He et al., 2016; Wu et al., 2017). The WRKY factors work at different levels in the ABA response. Whether WRKY factors are playing positive or negative roles in the ABA response depends on the family member (Rushton et al., 2012).

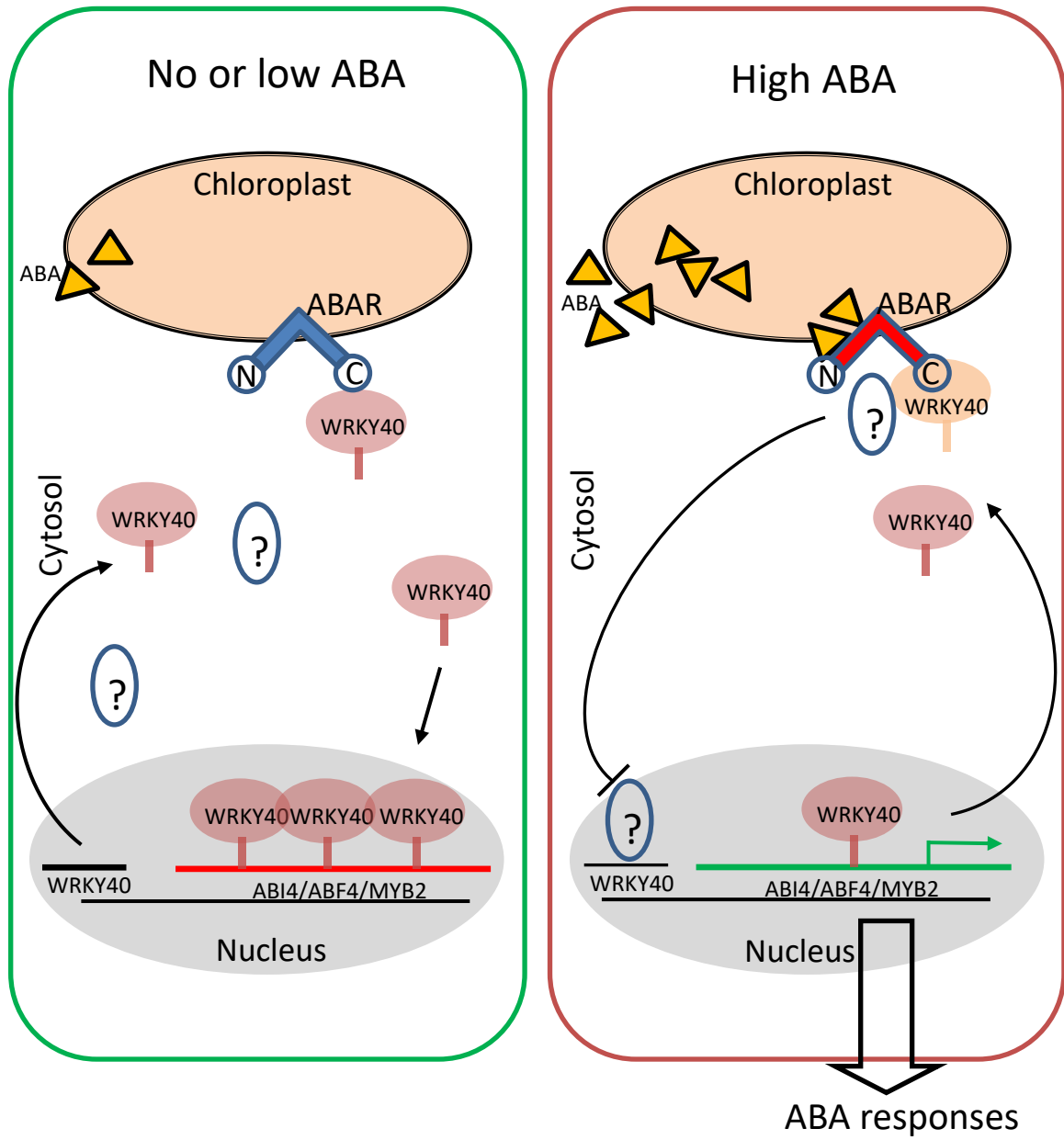
WRKY proteins contain highly conserved WRKY DNA-binding domains (Xie et al., 2005). Current evidence has shown that the WRKY domain is mirrored by the W box (TTGACC/T), which is a remarkable conservation of the cognate binding site of the WRKY domain (Eulgem et al., 2000; Rushton et al., 2010). W boxes have been found in many stress-inducible promoters in studies of plant promoters, and recently, the binding of WRKY proteins to W boxes in the promoters of abiotic stress-inducible genes has been clearly demonstrated (Shang et al., 2010). The importance of WRKY in ABA signaling has been illustrated by recent studies of the binding activity of WRKY to the ABA receptor (Shang et al., 2010). The ABA receptor ABAR spans the chloroplast envelope and the N- and C- terminal portions are exposed to the cytoplasm. It has been reported that the C-terminal part of the ABAR protein binds ABA (Wu et al., 2009a). The C-terminal also binds to a WRKY protein, AtWRKY40 (Shang et al., 2010) in *Arabidopsis*. It is proposed that ABA simulates the interaction of AtWRKY40, and AtWRKY40 is recruited from the nucleus to the cytoplasm. Based on Shang et al. (2010), a mechanism of ABA signaling is suggested that operates by the removal of AtWRKY40 from the nucleus (Figure 2). Further study has shown that the knockout mutants of *AtWRKY40* exhibited an ABA-hypersensitive phenotype in ABA-induced post-germination growth arrest (Shang et al., 2010). The

expression of many ABA-responsive genes is altered in *AtWRKY40* knockout plants. Additionally, *AtWRKY40* directly targets and binds to W box-containing fragments of the promoters of several ABA-responsive genes, such as *ABI4*, *ABI5* and *MYB18* (Shang et al., 2010). This observation suggests that *AtWRKY40* negatively regulates ABA signaling by repressing many ABA-responsive genes through W box-binding activity. An additional report also demonstrated that the knockout of *AtWRKY40* enhanced plant sensitivity to drought stress (Chen et al., 2010a). In rice, *OsWRKY45*-overexpressing plants had a lower rate of water loss than wild type plants, leading to greater drought tolerance under water stress conditions (Qiu and Yu, 2009). Overexpression of *OsWRKY11*, another rice WRKY gene, resulted in significant drought tolerance (Wu et al., 2009b). Very recent research has identified three drought-responsive WRKY genes in wheat and has demonstrated that overexpression of these genes enhances drought tolerance in *Arabidopsis* (He et al., 2016). These new insights into the role of WRKY transcription factors in ABA and drought responses have provided more information regarding the involvement of WRKY genes in the improvement of crop drought tolerance. On the other hand, for the purpose of improving crop drought tolerance, further investigation is needed to understand the specific roles of individual WRKY genes, and the gene regulation mechanism of *WRKY* in drought response (Rushton et al., 2012).

Figure 2. A model of regulation of WRKY40 in the ABA response

The N and C termini of ABA receptor (ABAR) are sticking out from the chloroplast envelop to the cytosol. In the condition of no to low ABA, the C terminus of ABAR interacts with several WRKY transcription factors, such as WRKY40, which negatively regulates ABA signaling. WRKY40 binds to the W-box on the promoter of ABA-responsive genes to inhibit their expression. To respond to a high level of ABA, WRKY40 is recruited from the nucleus to promote the ABAR-WRKY interaction, which relieves ABA-responsive genes of inhibition by downregulating *WRKY40* expression to respond to ABA. In this model, the symbol “?” indicates an unknown factor or signaling cascade that may repress the *WRKY40* gene expression.

This figure is modified from Shang et al. (2010)



1.3 Histone deacetylases in drought stress responses

Gene expression driven by environmental stress cues often depends on chromatin structure, governed by histone post-translational modifications and DNA methylation (Chinnusamy and Zhu, 2009). Numerous regulators of epigenetic effects on the expression of ABA- or stress-regulated genes have been reported (Chinnusamy et al., 2008). Chromatin, consisting of nucleosomes, is where the heritable and instructional information is stored in a cell. Each nucleosome is composed of octameric protein complexes with two molecules each of the four core histones – H2A, H2B, H3 and H4, and approximately 146 base pair (bp) of DNA. The histones with positively charged amino-terminal tails are tightly associated with the negatively charged phosphate backbone of DNA. The amino-terminal tails of H3 and H4 can be reversibly modified, in what are described as histone modifications. The histone modifications of H3 and H4, such as acetylation (Figure 3A), alter the interactions between the DNA and core histones, and thus change the chromatin structure. Histone modifications play a key role in gene expression under drought stress (Chinnusamy and Zhu, 2009). Previous research has discovered that specific histone modifications at certain residues of the H3 and H4 amino-terminal tails constitute the “histone code.” Histone modifications can determine the accessibility of *cis*-elements of genes to transcription factors by leading to either an “open” or “closed” chromatin configuration (Jenuwein, 2001).

Histone acetylation is a dynamic reversible process that is regulated by histone acetyltransferases (HATs) and histone deacetylases (HDACs). HATs add acetyl groups to the lysine residues of histone tails to neutralize the positive charge of histone tails and to decrease their affinity for DNA. On the other hand, HDACs remove acetyl groups from the lysine residues of histone amino-terminal tails, resulting in histone hypoacetylation, which enables the histones to bind more tightly to DNA. The dynamic equilibrium between HATs and HDACs controls the histone acetylation of nucleosomes, which affects chromatin structure, thus regulating gene expression (Liu et al., 2014). In general, histone acetylation mediated by HATs is associated with gene activation, while histone deacetylation regulated by HDACs leads to gene repression (Figure 3B) (Hebbes et al., 1988; Lusser et al., 2001).

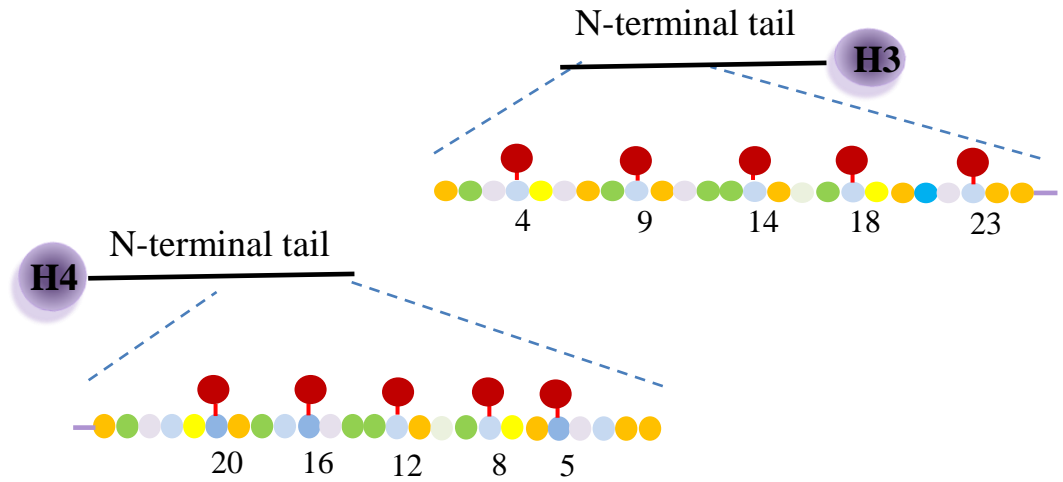
Figure 3. Histone acetylation and its regulation by HDACs and HATs

(A) Schematic representation of various lysine residues of histone acetylation on H3 and H4. Purple circles represent histones. Dark lines represent N-terminal tails of H3 and H4. Dark red represents an acetyl group. Dark blue circle labeled with “K” represents lysine residues.

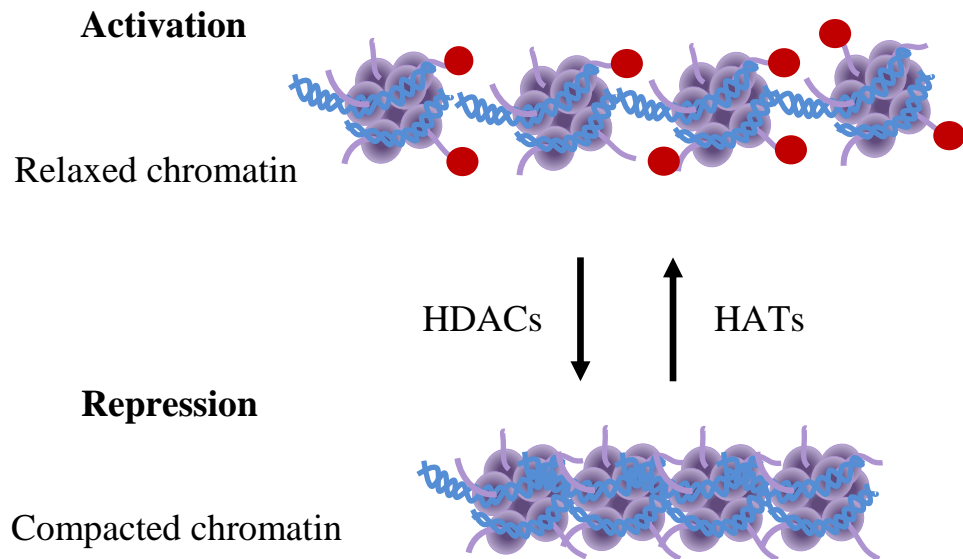
(B) Expression of gene regulated via targeted histone acetylation and histone deacetylation activities. In the upper panel, histones are modified with an acetyl group (dark red) via histone acetyltransferase activity, which causes a loose chromatin structure and gene activation. In the lower panel, histone acetyl groups are removed by histone deacetylases. The compacted chromatin structure leads to gene repression.

This figure is modified from DE Ruijter et al. (2003)

A



B



Plant HDACs are classified into three types, namely reduced potassium dependency protein 3 (RPD3)/HDA1, histone deacetylase 2 (HD2) and the silent information regulator protein 2 (SIR2) (Ruijter et al., 2003). The RPD3/HDA1 group is homologous to yeast RPD3 and is most widely studied throughout eukaryotes. All RPD3/HDA1 family members possess a characteristic histone deacetylase domain. In *Arabidopsis*, there are 12 putative members, and they are further divided into three classes based on sequence similarity (Napoli et al., 2002). Class I includes HDA19, HDA6, HDA7 and HDA9. Class II encompasses HDA5, HDA15 and HDA18. HDA2 and its isoforms comprise the third class. A second type of HD2 was originally identified in maize (Lusser et al., 1997) and it appears to be plant-specific (Dangl et al., 2001). The SIR2 histone deacetylases are nicotinamide adenine dinucleotide (NAD)-dependent enzymes.

Previous studies have demonstrated the involvement of some RPD3/HDA1 class I members in response to ABA and abiotic stresses (Chen and Wu, 2010; Chen et al., 2010b; Zheng et al., 2016). HDA6 and HDA19 (also as known as HDA1) were reported as positive regulators in ABA and drought stress responses. T-DNA insertion mutants of HDA19 displayed hypersensitivity to ABA. Additionally, compared with wild type plants, expression of several ABA-responsive genes, such as *ABI1* and *ABI2*, was decreased in the HDA19 mutant plants when treated with ABA (Chen and Wu, 2010). Similar to the HDA19 mutant, the HDA6 mutant and HDA6 RNA-interference plants also displayed a hypersensitive phenotype to ABA during seed germination (Chen and Wu, 2010; Chen et al., 2010b). HDA9 is another RPD3/HDA1 family member in *Arabidopsis*. Zheng et al. (2016) reported that HDA9 is involved in drought stress response. Loss-of-function mutants of *HDA9* exhibited phenotypes insensitive to PEG-6000 treatment, and *HDA9* mutation led to a higher up-regulation of many drought stress-responsive genes compared to wild type plants (Zheng et al., 2016).

The gene expression pattern of HD2 genes, including *HD2A*, *HD2B*, *HD2C* and *HD2D*, has been revealed in *Arabidopsis* (Zhou et al., 2004), and the expression of *HD2A*, *HD2B*, *HD2C* and *HD2D* was repressed by ABA (Luo et al., 2012). *HD2C* has been identified as a novel regulator of ABA responses. Overexpression of *HD2C* in transgenic plants caused an ABA-insensitive phenotype and enhanced tolerance to drought stress (Sridha and Wu,

2006). Compared to wild type plants, *hd2c-1* and *hd2c-3*, two T-DNA insertion mutant lines of *Arabidopsis*, showed increased sensitivity to ABA during germination (Luo et al., 2012). HD2D is another HD2 family member, which is distantly related to other HD2 genes (Han et al., 2016). Overexpression of *HD2D* enhanced drought tolerance in transgenic *Arabidopsis* plants, suggesting HD2D plays a role in drought stress response (Han et al., 2016).

The involvement of SRT2 HDACs in ABA responses has been demonstrated in plants. Two SRT2-type HDACs, AtSRT1 and AtSRT2, were identified in *Arabidopsis*. AtSRT1 interacted with *Arabidopsis* cMyc-Binding Protein 1 (AtMBP-1) and negatively regulated plant tolerance to stress (Liu et al., 2017). Whether AtSRT2 is involved in drought stress responses remains unclear.

Previous studies have demonstrated that overexpression or expression repression of HDAC genes changes plant sensitivity to drought stress or ABA (Sridha and Wu, 2006; Luo et al., 2012; Zheng et al., 2016; Liu et al., 2017). However, detailed mechanistic knowledge regarding how HDACs are implicated in the regulation of stress-responsive genes needs to be obtained. With great efforts having been made to generate genome-wide landscapes of epigenetic marks in *Arabidopsis*, the global mapping of an epigenetic modification associated with transcriptional activation has been reported. Lysine residue 9 of histone H3 can either be acetylated or methylated (Zhou et al., 2010). These epigenetic states have a diverse impact on chromatin organization and regulate transcriptional activity. In plants, histone H3 Lysine 9 acetylation (H3K9ac) is preferentially enriched at gene transcript start site (TSS) regions, suggesting that H3K9ac is closely correlated with transcriptional activation (Zhou et al., 2010). Increasing evidence has shown that H3K9ac is positively associated with stress-responsive gene activation in plants during stress responses (reviewed by Kim et al., 2015). A recent study showed the presence of H3K9ac patterns on diurnal genes only at times of the day when their expression is required (Baerenfaller et al., 2016). This result demonstrates that stimuli-induced gene expression is associated with changes in H3K9 acetylation. Similarly, drought stress also alters the status of histone modifications and triggers the expression of drought-responsive genes. Higher levels of

H3K9ac at promoters of stress-inducible genes were observed in plants when they were under drought stress (Zheng et al., 2016).

Current evidence indicates that H3K9ac is mediated by several histone deacetylases, and especially RPD3/HDAC1 family members (Zhou et al., 2010; Zheng et al., 2016). Profiling of H3K9ac in *Arabidopsis* revealed a significant increase in the H3K9ac level of selected target genes in an *HDA19* mutant plant, *hda19* (Zhou et al., 2010). Another study reported that the reduction of *HDA19* in *hda19* mutant plants caused an increase in the H3K9ac level on the promoter of three ABA receptor genes, *PYL4*, *PYL5* and *PYL6*, associated with a higher gene expression level (Mehdi et al., 2015). An increased H3K9ac level for many stress-responsive genes also was found in an *HDA9* mutation line, corresponding to an increased transcription level of those genes (Zheng et al., 2016). Previous research indicated that loss-of-function of HDACs led to an increase in the H3K9ac level for selected target ABA or drought-responsive genes. However, information regarding whether HDAC changes the profiling patterns of H3K9ac at the genome-wide level in response to drought stress is still missing. Histone deacetylases repress the transcription level of target genes through the histone deacetylation process. Exploring the relationship between histone acetylation markers and gene expression would provide a link to understand the roles of histone deacetylases in plant drought stress responses.

1.4 *Brachypodium distachyon*, a genetic model system for studying monocots

The responses of plants to drought stress involving histone deacetylase activity have been studied extensively in *Arabidopsis*. Although dicots such as *Arabidopsis* and monocots such as rice share some stress-related processes via the same regulatory networks, there are still many differences (Nakashima et al., 2014). While several HDACs are involved in stress response in *Arabidopsis*, the functions of HDACs in response to drought stress in monocots remain largely unexplored. In rice, the RPD3/HDAC1 family HDACs showed different responses to various abiotic stresses (Fu et al., 2007; Hu et al., 2009). Two RPD3/HDAC1 genes (*HDA703* and *HDA710*) were induced by drought stress while several others, including *HDA701*, *HDA702*, *HDA704*, *HDA705*, *HDA706*, *HDA12* and *HDA714*, were significantly repressed by drought stress (Hu et al., 2009). However, beyond these

preliminary findings, the specific roles of individual HDACs and their corresponding target genes in the drought stress responses of monocot plants have not been well studied.

Drought stress greatly affects the production of agricultural crops, because it occurs in virtually all climatic regions (Elliott et al., 2014; Daryanto et al., 2016). Several important agricultural crops, such as *Zea mays* (corn), *Triticum aestivum* (common wheat) and rice, are monocot plants. These crops provide the bulk of human nutrition, and some highly productive grasses (also monocots) are promising sources of sustainable energy (Somerville, 2006). The grass family (*Poaceae*) comprises over 10,000 species, and grasses dominate many natural and agricultural systems (Kellogg, 2001). With the development of modern biotechnology, great efforts have already made it possible to sequence the genome of some crop species (Matsumoto et al., 2005; Paterson et al., 2009). However, the genomes of many *Poaceae* members, such as common wheat, are characterized by their daunting size and complexity, which makes it much more difficult to perform genome-scale studies on these species (Vogel et al., 2010). Rice has been used as a model plant for monocots. However, rice is not ideal for investigating drought stress, because its semi-aquatic living habit is different from that of the other main monocot crops.

Brachypodium distachyon (*Brachypodium*), a member of the *Poaceae* family, also has been used as a model system for studying questions unique to monocots. It possesses all the desirable features of a model system (Vogel et al., 2010). *Brachypodium* is a self-fertile, inbreeding annual plant with a life cycle of around 3 months. This grass also has a small size (approximately 20 cm tall at maturity), undemanding growth requirements, and a simple working transformation system. More importantly, its genome is diploid and small (247 Mbp), and whole-genome sequencing has been completed (Garvin et al., 2008; Vogel and Hill, 2008; Alves et al., 2009; Vogel et al., 2010). A rapidly growing interest in *Brachypodium* has triggered the establishment of a series of genome resources, including a series of reference genes that are suitable for normalizing gene expression data in *Brachypodium*. These reference genes become particularly useful when it comes to the gene expression analysis of stress-responsive genes. Under drought stress, the S-adenosylmethionine decarboxylase gene (*SamDC*) was ranked as the most stable gene in *Brachypodium* (Hong et al., 2008).

1.5 Hypothesis and objectives

Because no previous study of *Brachypodium* HDAC genes had been conducted, for my research I identified the histone deacetylase genes for this species and selected one RPD3/HDA1 family member, *Bradi3g08060* (*BdHDI*). I aimed to reveal the role of this histone deacetylase and its corresponding target genes involved in the drought stress responses of the monocot species *Brachypodium*. The following hypothesis guided my research:

I hypothesized that *BdHDI* represses expression of drought-responsive genes through H3K9 deacetylation in *Brachypodium distachyon*.

To test my hypothesis, I addressed the following specific objectives:

1. To examine the role of *BdHDI* in the drought stress response
2. To evaluate H3K9ac levels in wild type and *BdHDI*-overexpression plants
3. To identify the gene associated with H3K9 deacetylation caused by drought stress
4. To examine the effects of *BdHDI* expression on the expression of drought-responsive genes

Chapter 2 Materials and Methods

2.1 Plant materials and growth conditions

Brachypodium distachyon (genotype: Bd21-3) seeds were surface-sterilized in 70% (v/v) ethanol for 90 seconds followed by 20% bleach (active ingredient: 1.2% (w/v) sodium hypochlorite) for 3 minutes. The seeds were rinsed with distilled water and placed on wet sterilized filter paper in petri dishes for 3 days at 4 °C in darkness before sowing on soil or on Murasnige and Skoog (MS) (Murasnige and Skoog, 1962) plates (MS salts (Sigma-Aldrich), 0.8% agar with pH 5.8) or in half-strength Hoagland solution (Hoagland and Arnon, 1950). Plants were grown in a growth room with a relative humidity of 60% under long day conditions (20-hour light/4-hour dark). Growth room temperatures 22 °C during the light period and 18 °C during the dark period.

In addition, *Nicotiana benthamiana* plants were grown in soil in a growth room under a 16/8-hour light/dark cycle at 22/16 °C.

2.2 Phylogenetic analysis

Information for the *Brachypodium* and *Arabidopsis* HDAC family members was obtained from EnsemblPlants (<http://plants.ensembl.org/index.html>), and the peptide sequences of all HDACs in *Brachypodium* and *Arabidopsis* were downloaded from the Phytozome database (<https://phytozome.jgi.doe.gov>). The phylogenetic tree was generated using PhyML (Guindon et al., 2010).

2.3 Plant RNA extraction and gene cloning

Total RNA was isolated from ~ 50 mg of plant tissue using a Plant/Fungi Total RNA Purification Kit (Norgen) according to the manufacturer's instructions. All RNA samples were treated with RNase-free DNase (Norgen) to eliminate genomic DNA contamination. RNA (1 µg) was further used to synthesize cDNA by using an iScript Reverse Transcription Supermix (Bio-RAD). The reaction mix was added in a 0.2 mL RNase-free tube, then the tube was loaded onto a thermocycler, initialized for 5 minutes at 25 °C, followed by 42 °C for 30 minutes, 85°C for 5 minutes, and followed by a final phase of 4 °C for 10 minutes.

To clone the cDNA of *BdHDI*, the reaction components were added in a 0.2 mL tube. The reaction system included: 1 µL of 10 µM each of forward and reverse primer, 4 µL of Phusion High Fidelity Buffer (New England Inc.), 0.4 µL of 10 mM dinucleotide triphosphates (dNTPs), 0.2 µL of Phusion DNA polymerase (New England Inc.), 1 µL of cDNA template and H₂O was added to a final volume of 20 µL. The mixture was then loaded onto a thermocycler, initialized for 30 seconds at 98 °C, followed by 30 cycles of 98 °C for 10 seconds, 61 °C for 20 seconds and 72 °C for 2 minutes, followed by a final extension phase of 72 °C for 10 minutes.

2.4 Subcellular localization

The full-length cDNA sequence of *BdHDI* was obtained from the Phytozome database (<https://phytozome.jgi.doe.gov/pz/portal.html>). The cDNA of *BdHDI* was cloned into the pEarlygate101 vector to generate a *BdHDI-YFP* fusion construct driven by a *CaMV35S* promoter. The construct was then transferred into *N. benthamiana* leaves via an *Agrobacterium* GV3101 mediated infiltration method (Tian et al., 2011). The fluorescent signals were detected by confocal microscopy (Leica) at 48 hours after transformation. Three independent experiments were performed for this test.

2.5 Generation of stable transgenic *Brachypodium* plants

To construct the *BdHDI*-overexpression vector, the full-length cDNA without a stop codon was amplified and cloned into the pDONR221 vector (Invitrogen) by performing a BP reaction. Primers used for *BdHDI* cloning are listed in Appendix 1. Vectors containing the insertions were sequenced to ensure that no mutation was introduced during PCR amplification. The insertions were then transferred into pMDC85 vectors (Curtis and Grossniklaus, 2003) by conducting LR reactions to generate *BdHDI*-overexpression constructs ($2 \times 35S::BdHDI-GFP$).

Plant transformation was performed by following an established *Agrobacterium*-mediated transformation protocol (Alves et al., 2009). Briefly, *Brachypodium* Bd21-3 plants were grown for 7-9 weeks to produce immature seeds (swollen, but still green). Immature seeds were collected and surface-sterilized in 70% (v/v) ethanol for 30 seconds followed by 20%

bleach (active ingredient: 1.2% (w/v) sodium hypochlorite) for 4 minutes. After rinsed with distilled water, immature embryos were harvested from the surface-sterilized immature seeds and cultured on basic MSB3 + Cu 0.6 solid medium (MS salts (Sigma-Aldrich), 30 g/L sucrose, Fe-ethylenediaminetetraacetic acid (Fe-EDTA), 2.5 mg/L 2,4-D, vitamins M5, 0.6 mg/L CuSO₄, 2 g/L Phytigel, pH 5.8) in the dark for 3 weeks. Compact embryogenic callus (CEC) with a creamy color was generated from the immature embryos at week 3 and transferred onto fresh MSB3 + Cu 0.6 medium for another 2 weeks in the dark. CEC was split in 4-6 pieces and grown on fresh MSB3 + Cu 0.6 medium for 1 week. CEC was split one last time in 4-6 pieces and placed on fresh MSB3 + Cu 0.6 medium before inoculation with *Agrobacterium tumefaciens* (AGL1 strain).

A. tumefaciens, carrying the pMDC85-*BdHDI-GFP* vector, was cultured in LB liquid medium in an incubator-shaker at 28 °C and 200 r.p.m overnight. *A. tumefaciens* was harvested from the overnight culture followed by a suspension using MSB + AS45 liquid medium (MS salts (Sigma-Aldrich), 10 g/L sucrose, Fe-EDTA, 45 mg/L acetosyringone, 10 g/L mannitol, pH 5.5). The suspension was cultured in an incubator-shaker at 28 °C and 200 r.p.m for 2 hours to disperse *A. tumefaciens*. CEC plates were flooded with 13 mL of *A. tumefaciens* (OD₆₀₀=1) and left for a 5-minute inoculation in a laminar flow hood. The bacterial suspension was completely removed from the plates and CECs were left uncovered under the laminar flow hood for 7 minutes as a desiccation treatment. CECs were co-cultured with *A. tumefaciens* on MSB + AS60 solid medium (MS salts (Sigma-Aldrich), 30 g/L sucrose, Fe-EDTA, 2.5 mg/L 2,4-D, vitamins M5, 60 mg/L acetosyringone, 2 g/L Phytigel, pH 5.8) plates for 2 days in the dark.

Co-cultured CECs were transferred onto MSB3 + Cu 0.6 + H100 + T225 solid medium (MS salts (Sigma-Aldrich), 30 g/L sucrose, Fe-EDTA, 2.5 mg/L 2,4-D, vitamins M5, 0.6 mg/L CuSO₄, 2 g/L Phytigel, 225 mg/L timentin, 100 mg/L hygromycin B, pH 5.8) for selection for 3 weeks. Hygromycin-resistant calli were transferred onto MSR26 + H50 + T225 solid medium (MS salts (Sigma-Aldrich), 30 g/L sucrose, Fe-EDTA, 0.2 mg/L kinetin, vitamins M5, 225 mg/L timentin, 50 mg/L hygromycin B, 2 g/L Phytigel, pH 5.8) for 3 weeks under a 16-hour photoperiod. Shoots were regenerated from the hygromycin-resistant calli and transferred onto MSR63 + Ch7 + T112 solid medium (MS salts (Sigma-

Aldrich), 10 g/L sucrose, Fe-EDTA, 7 g charcoal, 112 mg/L timentin, vitamins B5, 6 g/L agar, 2 g/L Phytigel, pH 5.8) to generate roots. Fully rooted plantlets were transferred to soil to finish vegetative growth and reproduction. Mature seeds were harvested from plants individually and stored for later experiments.

To knock down the expression of *BdHDI* in *Brachypodium*, RNA-interference (RNAi) lines were generated. A segment of the *BdHDI* transcript sequence that is located from 1576 to 1885 bp of the downstream of the start codon was amplified and introduced into pDONR221 by conducting a BP reaction. The inserts were then transferred into a pHellsgate12 vector (Helliwell and Waterhouse, 2003) by LR reaction to generate the RNAi construct. The constructs were introduced into *A. tumefaciens* AGL1 to produce *BdHDI*-RNAi *Brachypodium* plants by using the same transformation method for generating overexpression plants. Primers used for gene cloning and confirmation of DNA insertion are listed in Appendices 1&2.

2.6 Homozygous transgenic plant selection using a progeny test

The regenerated transgenic (*BdHDI*-overexpression) plants were named the T0 generation. The phenotype of the T0 plants was hygromycin-resistant (Hyg R). The plants grown from seeds, harvested from self-pollinated T0 transgenic plants, were named the T1 generation. The phenotypes of T1 plants were either hygromycin-resistant (Hyg R) or hygromycin-sensitive (Hyg r). The ratio of the phenotype classes was Hyg R: Hyg r = 3:1. This ratio suggested that T1 plants were mixtures of homozygous R/R, heterozygous R/r and homozygous r/r. The r/r individuals were eliminated and the hygromycin-resistant plants were grown for producing seeds. I grew 50 T2 seeds from each T1 plant on medium containing hygromycin. All 50 seeds showed hygromycin resistance, suggesting that the T1 parent of this T2 population was homozygous R/R. Not all 50 seeds showed hygromycin resistance, suggesting that the T1 parent of this T2 population was heterozygous R/r. The homozygous R/R plants were grown for seed production. The homozygous *BdHDI*-RNAi plants were selected by using a progeny test with paramomycin selection.

2.7 Plant genome DNA isolation

Leaf tissue (~ 100 mg) samples were collected then ground in liquid nitrogen into fine powder. Ground samples were transferred into a 2 mL Eppendorf tube containing 0.5 mL genomic DNA extraction buffer (2% hexadecyltrimethylammonium bromide (CTAB), 1.4 M NaCl, 0.1 M Tris-HCl pH 8, 20 mM EDTA). Samples were incubated at 60 °C and 0.5 mL chloroform was added, followed by centrifugation at 3,000 rpm for 5 minutes. The upper, aqueous phase was transferred to a new tube and 250 µL isopropanol was added. After gently mixed by continually inverting the tube for 1 minute, the mixed solution was centrifuged at 13,000 rpm for 15 minutes. A small white pellet containing genomic DNA was observed at the bottom of the tube. The supernatant was removed from the tube. To wash the DNA pellet, 300 µL of 70% ethanol was added to the tube. Ethanol was discarded after centrifugation at 13,000 rpm for 5 minutes. The tube was left open for 10 minutes under vacuum at room temperature to allow the remaining ethanol to evaporate. The pellet was re-suspended in 50 µL of ddH₂O.

2.8 General polymerase chain reaction setup

Reaction components were added in 0.2 mL tubes to start the polymerase chain reaction (PCR). The reaction included: 1 µL of 10 µM each of forward and reverse primer, 5 µL of 5 x Go Taq Flexi Buffer (Promega Inc), 0.5 µL of 10 mM dNTPs, 3 µL 25 mM MgCl₂, 1 µL of Go Taq Flexi DNA polymerase (Promega Inc), 1 µL of DNA template, and H₂O was added to a final volume of 25 µL. The mixture was then loaded onto a thermocycler, initialized for 2 minutes at 95 °C, followed by 30 cycles of 95 °C for 15 seconds, 55-60 °C for 30 seconds and 72 °C for 1 minute, followed by a final extension phase of 72 °C for 5 minutes.

2.9 Stress treatments

To measure the expression level of *BdHDI*, 4-leaf stage wild type *Brachypodium* were used for the stress experiments. The soil drying method was conducted by withholding water for 5 days. PEG-6000 (w/v, 20%) and 400 mM mannitol were added into the Hoagland solution for 3 days, separately. For the ABA treatment, *Brachypodium* plants were treated with ABA

(100 μ M) Hoagland solution. In this test, three independent experiments were performed. For each experiment, three plants of control or each stress treatment were pooled together for RNA extraction.

Plants were tested to compare their ABA sensitivities and drought tolerance as described previously (Tang et al., 2012). For the ABA sensitivity test during seed germination, Bd21-3, OE22 and OE30 were surface-sterilized with 70% (v/v) ethanol for 90 seconds followed by 20% bleach (active ingredient: 1.2% (w/v) sodium hypochlorite) for 3 minutes. For each line, 50 seeds were placed on $\frac{1}{2}$ MS medium containing 0 or 2 μ M ABA, followed by 3 days in the dark at 4 $^{\circ}$ C. Plates were transferred to the tissue culture room to allow the seeds to germinate for 6 days. Germinated seeds of each line were recorded, and the germination percentages were calculated. In this test, three independent experiments were performed.

For the ABA sensitivity test during post-germination growth, *Brachypodium* seeds including the wild type Bd21-3, *BdHDI*-overexpression lines and *BdHDI*-RNAi were germinated for 1 day then transferred to either $\frac{1}{2}$ MS or $\frac{1}{2}$ MS medium containing 1 μ M ABA. The lengths of the shoot and root were measured after 2 weeks. In this test, three independent experiments were performed. For each experiment, three replicates (10 plants of each line for one replicate) were used.

For the drought stress tolerance experiment, *Brachypodium* plants were grown in a half-split manner (half side for 10 wild type plants and half side for 10 transgenic plants) in pots filled with sandy soil. Drought stress treatments were conducted at the 4-leaf stage by withholding water for certain days (10 days for the *BdHDI*-overexpression plants and 8 days for the *BdHDI*-RNAi plants). Plants were re-watered after the drought treatment for 1 week to allow them to recover. The survival for each genotype was quantified. Plants with green leaves and a regenerated shoot were considered to have survived. In this test, three independent experiments were performed. For each experiment, three replicates were used for calculating the survival of each genotype.

To collect samples for ChIP-Seq assays, drought stress was simulated by using PEG-6000 solution. Briefly, *Brachypodium* seeds (Bd21-3 and OE22) were germinated on wet filter paper in Petri dishes for 3 days. Then young seedlings were placed on floating boards in

magenta boxes (8 plants for each box, 96 plants per phenotype plants for one ChIP assay) containing Hoagland's solution. Four-leaf stage plants were treated with 20% (w/v) PEG-6000 Hoagland's solution. Plants grown in regular Hoagland's solution were used as control. Samples were harvested after 3 days.

To measure the expression level of drought-responsive genes under drought stress, 4-leaf stage *Brachypodium* plants (Bd21-3, *BdHDI*-OE lines OE22 and OE30, and *BdHDI*-RNAi line *bdhd1-30*) were treated with 20% (w/v) PEG-6000 Hoagland's solution. Plants grown in regular Hoagland's solution were used as control. Samples were harvested after 3 days. In this test, three independent experiments were performed. For each experiment, three plants of each phenotype with drought treatment or control were pooled together for RNA extraction.

To measure the gene expression under ABA treatment, the samples of 4-leaf stage *Brachypodium* plants (wild type Bd21-3, *BdHDI*-OE lines OE22 and OE30, and *bdhd1-30*) were taken after 6 hours of 100 μ M ABA treatment. Plants grown in regular Hoagland's solution and sprayed with water were used as a control. In this test, three independent experiments were performed. For each experiment, three plants of each phenotype with ABA treatment or control were pooled together for RNA extraction.

2.10 Soil water content and leaf water potential (Ψ_1) measurements

Soil water content was measured using a soil sensor reader (Spectrum Technologies). Three measurements were taken for each pot every 24 hours for 5 days. Leaf water potential (Ψ_1 , Mpa) was measured using a SAPS II Portable Plant Water Status Console (Soil Moisture Equipment Corp.) at the same time as measuring soil water content. Measurements were from the 4-leaf stage wild type Bd21-3 plants. Plant leaves were excised from the shoot using a scalpel blade then placed into the pressure chamber with the petiole protruding from the chamber lid. The chamber was pressurized using a nitrogen tank, and water potential was recorded as soon as xylem sap was observed emerging from the cut end of the petiole. In this test, three independent experiments were performed and three replicates were used for each experiment.

2.11 Protein extraction and protein gel blotting

Fresh leaf tissue (0.3 g) was ground in liquid nitrogen and suspended in lysis buffer (0.25 M HCl, 20 mM pH 6.8 Tris-HCl, 2 mM EDTA, 20 mM, β -mercaptoethanol (β -ME) and 0.2 mM phenylmethylsulfonyl fluoride (PMSF)). Proteins were extracted from the supernatant after 2 minutes of sonication followed by 15 minutes of centrifugation, then stored at -80 °C. Protein samples were denatured by adding 18.5 mM dithiothreitol before loading onto SDS-PAGE gels. After separation by electrophoresis using a Biochrom Novaspec Plus Visible Spectrophotometer (Bio-RAD), proteins were transferred to a polyvinylidene difluoride membrane (Bio-RAD) using a Trans-Blot Semi-Dry Electrophoretic Transfer Cell (Bio-Rad). The primary antibodies Anti-H3K9ac and Anti-H3 (Cell Signaling Technology and Millipore) were incubated overnight in the customized dilutions. Secondary rabbit antibody (Millipore) was incubated with the membrane for 2 hours. Proteins were detected using the EI-ECL system (BI industries).

2.12 Chromatin immunoprecipitation assays

Chromatin immunoprecipitation (ChIP) assays were carried out by following a published protocol (Gendrel et al., 2005) with minor modifications. Briefly, 3 g of 21-day-old *Brachypodium* seedlings grown in hydroponic conditions were harvested and cross-linked with 37 mL 1% formaldehyde for 25 minutes under vacuum. Glycine (0.125 M) was added to terminate the fixation reaction. The seedlings were rinsed with water twice and blotted with filter paper to remove the remaining water. The samples were ground in liquid nitrogen into fine powder, which was transferred into a 50-mL Falcon tube containing 30 mL of extraction buffer (0.4 M sucrose, 10 mM Tris-HCl pH 8, 10 mM MgCl₂, 5 mM β -ME, 0.1 mM PMSF), 2 tablets of complete protease inhibitor cocktail tablets (Roche) in 100 mL H₂O). The solution was placed on ice for 5 minutes, then was filtered through a double layer of miracloth (Millipore), followed by centrifugation at 3,000 \times g for 20 minutes at 4 °C. After removing the supernatant, the pellet was re-suspended in 1 mL of extraction buffer 2 (0.25 M sucrose, 10 mM Tris-HCl pH 8, 10 mM MgCl₂, 1% Triton X-100, 5 mM β -ME, 0.1 mM PMSF, 1 tablet of complete mini protease inhibitor cocktail tablet (Roche) in 10 mL H₂O). The re-suspended solution was centrifuged at 12,000 \times g for 10 minutes at

4 °C. The supernatant was removed and the pellet was gently re-suspended with 300 µL of extraction buffer 3 (1.7 M sucrose, 10 mM Tris-HCl pH 8, 0.15% Triton X-100, 2 mM MgCl₂, 5 mM β-ME, 0.1 mM PMSF, 1 tablet of complete mini protease inhibitor cocktail tablet in 10 mL H₂O). The re-suspended solution was loaded into another 300 µL of extraction buffer 3 in new tube, followed by 1 hour centrifugation at 16,000 × g at 4 °C. The pellet was harvested and was re-suspended in 300 µL of nuclei lysis buffer (50 mM Tris-HCl pH 8, 10 mM EDTA, 1% SDS, 0.1 mM PMSF, 1 tablet of complete mini protease inhibitor cocktail tablet in 10 mL H₂O). The solution was sonicated 3 times, for 15 seconds each, with 1 minute incubation on ice between each treatment. To remove the debris, the solution was centrifuged at 12,000 × g for 10 minutes at 4 °C. The supernatant (~ 300 µL) was transferred to a new tube and 10 µL of the supernatant was taken as the input DNA control and saved at -20 °C. The remaining solution was diluted to a final volume 3 mL with CHIP dilution buffer (1.1% Triton X-100, 1.2 mM EDTA, 16.7 mM Tris-HCl pH 8, 167 mM NaCl). The total chromatin solution was equally divided into three 1.5 mL-tubes. For each tube, 40 µL of protein A agarose beads was added to pre-clear the chromatin solution for 1 hour at 4 °C. The supernatant was transferred to a new tube after centrifugation for 1 minute at 4 °C. Another 50 µL of protein A agarose beads was added to the pre-cleared chromatin solution, along with 10 µL antibody anti-H3K9ac (Cell Signaling Technology). The chromatin solution was incubated overnight at 4 °C. After centrifugation for 1 minute at 4 °C, the beads were saved and washed sequentially with 1 mL of each of the following buffers (2 × 10 minutes): (1) Low salt wash buffer (150 mM NaCl, 0.1% SDS, 1% TritonX-100, 2 mM EDTA, 20 mM Tris-HCl (pH 8.0)). (2) High salt wash buffer (500 mM NaCl, 1% TritonX-100, 2 mM EDTA, 20 mM Tris-HCl (pH 8.0), 0.1% SDS). (3) LiCl wash buffer (1 mM EDTA, 1% sodium deoxycholate, 0.25 LiCl, 1% NP40, 10 mM Tris-HCl (pH 8.0)). (4) TE buffer (1 mM EDTA, 10 mM Tris-HCl (pH 8.0)). The immune complexes were eluted with 250 µL of elution buffer (1% SDS, 0.1 M NaHCO₃), incubated for 15 minutes at 65 °C. The elution process was repeated and the supernatants were combined. To reverse the cross-link of DNA and histones or other chromatin components, 20 µL of NaCl was added to the solution. Meanwhile, the input DNA control was made up to 500 µL of elution buffer, followed by adding 20 µL of NaCl. The reverse cross-link processes were undertaken at 65 °C for 6 hours. After that, each

sample was added with 10 μ L of 0.5 M EDTA, 20 μ L of 1 M Tris-HCl (pH 6.5) and 1 μ L of 20 mg/mL proteinase K (New England), followed by 1 hour of incubation at 45 °C. The DNA was purified and recovered by using the MiniElute PCR purification kit (Qiagen).

ChIP assay followed by quantitative PCR (ChIP-qPCR) was performed using a SsoFast™ EvaGreen Supermix kit (Bio-RAD). For each qPCR reaction, the following cycling parameters were used: an initial phase of 98 °C for 2 minutes, followed by 40 cycles of 98 °C for 5 seconds and 60 °C for 10 seconds. The reaction entered the melting curve analysis, which began at 65 °C, and increased incrementally by 0.5 °C until it reached 95 °C. The fluorophore activity was detected by using a CFX96 real-time PCR detection system (Bio-RAD) and the cycle threshold value (C_T) was recorded and analyzed with CFX Manager™ Software (Bio-RAD). Primers used for ChIP-qPCR are listed in Appendix 3.

2.13 ChIP-Seq and data analysis

To obtain 10 ng of DNA for next generation sequencing, DNA from 3 ChIP assays was pooled together as one biological sample. Two biological samples were prepared and sent for next generation sequencing. Next generation sequencing was performed at Sickkids in Toronto. Sequencing of single-end 50 bp reads was carried out on an Illumina HiSeq 2500.

The raw data were uploaded on Galaxy (<https://usegalaxy.org/>) and processed using the Illumina sequence data analysis pipeline GAPIipeline 1.3.2. The reads were mapped to the *Brachypodium* genome (version Ensemble plants v 1.0) by using Bowtie (Langmead and Salzberg, 2012). Only perfectly and uniquely mapped reads were retained for future data analysis. Data were analyzed as described by Lu et al. (2011) and Li et al. (2016). First, the MACS program was employed to convert the alignments to wiggle (WIG) files (Zhang et al., 2008). Then the WIG files were visualized by importing them to the Integrated Genome Browser program (Helt et al., 2009). Next, the ChIP-enriched domains (peaks) were identified by running the SICER program (Zang et al., 2009). The quantitative comparisons between wild type Bd21-3 and BdHD1-OE line were conducted by using the PeakAnalyzer program (Salmon-Divon et al., 2010). Regions with more than two-fold changes were selected for future analysis. Lastly, the distance between each peak summit and the nearby transcription start site (TSS) of a gene was calculated to assign the identified peaks to

proximal genes. Briefly, the peak summit was assigned to the gene if it was mapped within 2 kb upstream of the TSS or 2 kb downstream of the transcription terminate site (TTS). When the peak summit was assigned to multiple genes, the closest TSS was assigned. If there was no TSS to be found in this window, the peak was left unassigned.

2.14 Gene ontology analysis

The PANTHER Classification System (Mi et al., 2013; Mi et al., 2017) was applied to determine for which Gene Ontology (GO) categories the genes were statistically enriched.

2.15 Gene expression analysis

As described previously, total RNA was isolated from plant tissue (~ 50 mg) using the Plant/Fungi Total RNA Purification Kit (Norgen). To obtain cDNA, 100 ng of RNA from each sample was used by using an iScript Reverse Transcription Supermix (Bio-RAD).

The real-time quantitative PCR (RT-qPCR) was performed using a SsoFast™ EvaGreen Supermix kit (Bio-RAD). For each qPCR reaction, the following cycling parameters were used: an initial phase of 95 °C for 30 seconds, followed by 40 cycles of 95 °C for 5 seconds and 60 °C for 10 seconds. The reaction entered the melting curve analysis, which began at 65 °C, and increased incrementally by 0.5 °C until it reached 95 °C. The fluorophore activity was detected by using a CFX96 real-time PCR detection system (Bio-RAD) and the cycle threshold value (C_T) was recorded and analyzed with CFX Manager™ Software (Bio-RAD). Primers used for RT-qPCR are listed in Appendix 4.

RT-qPCR results were shown as the relative expression level. The data analysis procedure is shown below.

ΔC_T values were calculated using the following formula:

$$\Delta C_T = C_T(\text{Target}) - C_T(\text{SamDC}),$$

$\Delta\Delta C_T$ values were calculated as the difference between each treatment or genotypes ΔC_T and wild type (Control) ΔC_T (wild type):

$$\Delta\Delta C_T = \Delta C_T(\text{Overexpression/RNAi}) - \Delta C_T(\text{wild type})$$

Relative expression level was calculated by: $2^{(-\Delta\Delta CT)}$

SamDC was used as the internal reference gene. All RT-qPCR was conducted with three technical replicates for one biological replicate.

2.16 Primer design

All primers were designed by using Primer3Plus (<https://primer3plus.com>). The primer parameters were: melting temperature: 60 °C, GC content: 40-60%.

2.17 Statistical analysis

Microsoft Excel 2013 (Microsoft Corp., Redmond, Washington) was used to compute simple univariate statistics, including means and standard errors. The Student's t-tests were used to determine the significance of difference between two independent data sets. Two-way analysis of variance (ANOVA) followed by post-hoc Tukey's HSD tests were used to perform multiple comparisons with two variances. All statistical analyses were performed using the statistic program "R" version 3.4.4 Copyright © 2018 (The R foundation for Statistical Computing).

Chapter 3 Results

3.1 Characterization of *BdHDI* in response to drought stress in *Brachypodium*

3.1.1 *BdHDI* is an homologous gene of *HDAC1*

First, I identified 12 *HDAC* genes (Table 1) in *Brachypodium*. Based on the protein similarity of HDACs in *Arabidopsis* and *Brachypodium*, a phylogenetic tree was generated to classify the 12 *Brachypodium* HDACs and to identify the closest homologous gene of *HDAC1* in *Brachypodium*. The phylogenetic analysis showed that *Bradi2g14120* was classified with Type II (*HD-tuins*) HDACs, while the other *HDAC* genes were grouped with Type I (*RPD3/HDA1*) *Arabidopsis* HDACs (Figure 4).

Among these *RPD3/HDA1* *Brachypodium* HDACs, two closest homologous genes of *AtHDA19* were identified, namely *Bradi3g08060* and *Bradi1g37290*. Analysis shows that *Bradi3g08060* and *Bradi1g37290* share 78.2% and 76.6% similarity at the protein level with *AtHDA19*, respectively. Although both *Bradi3g08060* and *Bradi1g37260* share high similarity with *AtHDA19*, only *Bradi3g08060* was selected to carry on the following study, based on the higher similarity with *AtHDA19*. It was named *BdHDI*. Like *HDA19* and other *RPD3/HDA1* family members, *BdHDI* possesses one histone deacetylase domain (Figure 5A). Peptide sequences analysis illustrates that *BdHDI* shares a conserved sequence (Figure 5B), which is crucial for histone deacetylase activity (Lusser et al., 2001), as identified in *HDA6*, *HDA9* and *HDA19*.

I investigated the subcellular localization of *BdHDI* protein by expressing *BdHDI-YFP* driven by a double *CaMV35S* promoter (2×35S) (Figure 6A) in *Nicotiana benthamiana* leaves. The result showed that *BdHDI* was localized in the nucleus (Figure 6B).

Taken together, I classified 12 *Brachypodium* HDACs based on similarity to those in the *Arabidopsis* HDAC family. I identified the closest homologous gene of *AtHDA19*, *BdHDI*, and its protein expression was localized in the nucleus.

Table 1. Histone deacetylases in *Brachypodium*

All *Brachypodium* HDACs were grouped into two classes: *RPD3/HDA1* and *HD-tuins*.

Data were collected from *Ensemble Plants*.

Gene family	Gene name	Reference	Chromosome	Peptide size (aa)
	<i>BdHD1</i>	<i>Bradi3g08060</i>	III	518
	<i>BdHD4</i>	<i>Bradi1g37290</i>	I	521
	<i>BdHD9</i>	<i>Bradi5g09190</i>	V	487
	<i>BdHD6</i>	<i>Bradi3g22370</i>	III	457
	<i>BdHD7</i>	<i>Bradi3g44780</i>	III	469
<i>RPD3/HDA1</i>	<i>BdHD10</i>	<i>Bradi1g56740</i>	I	644
	<i>BdHD5</i>	<i>Bradi1g22240</i>	I	709
	<i>BdHD11</i>	<i>Bradi4g40960</i>	IV	444
	<i>BdHD8</i>	<i>Bradi2g24020</i>	II	388
	<i>BdHD3</i>	<i>Bradi4g06630</i>	IV	188
	<i>BdHD2</i>	<i>Bradi1g37510</i>	I	352
<i>HD-tuins</i>	<i>BdHDT1</i>	<i>Bradi2g14120</i>	II	296

Figure 4. Phylogenetic analysis of histone deacetylases of *Brachypodium* and *Arabidopsis*

Unrooted neighbor-joining tree of 12 *Brachypodium* HDACs and 16 *Arabidopsis* HDACs shows the protein similarities between two species. The homologous gene of *AtHDA19* in *Brachypodium* is highlighted with a light orange color. All the protein sequences of HDAC were obtained from *Phytozome V12.1*.

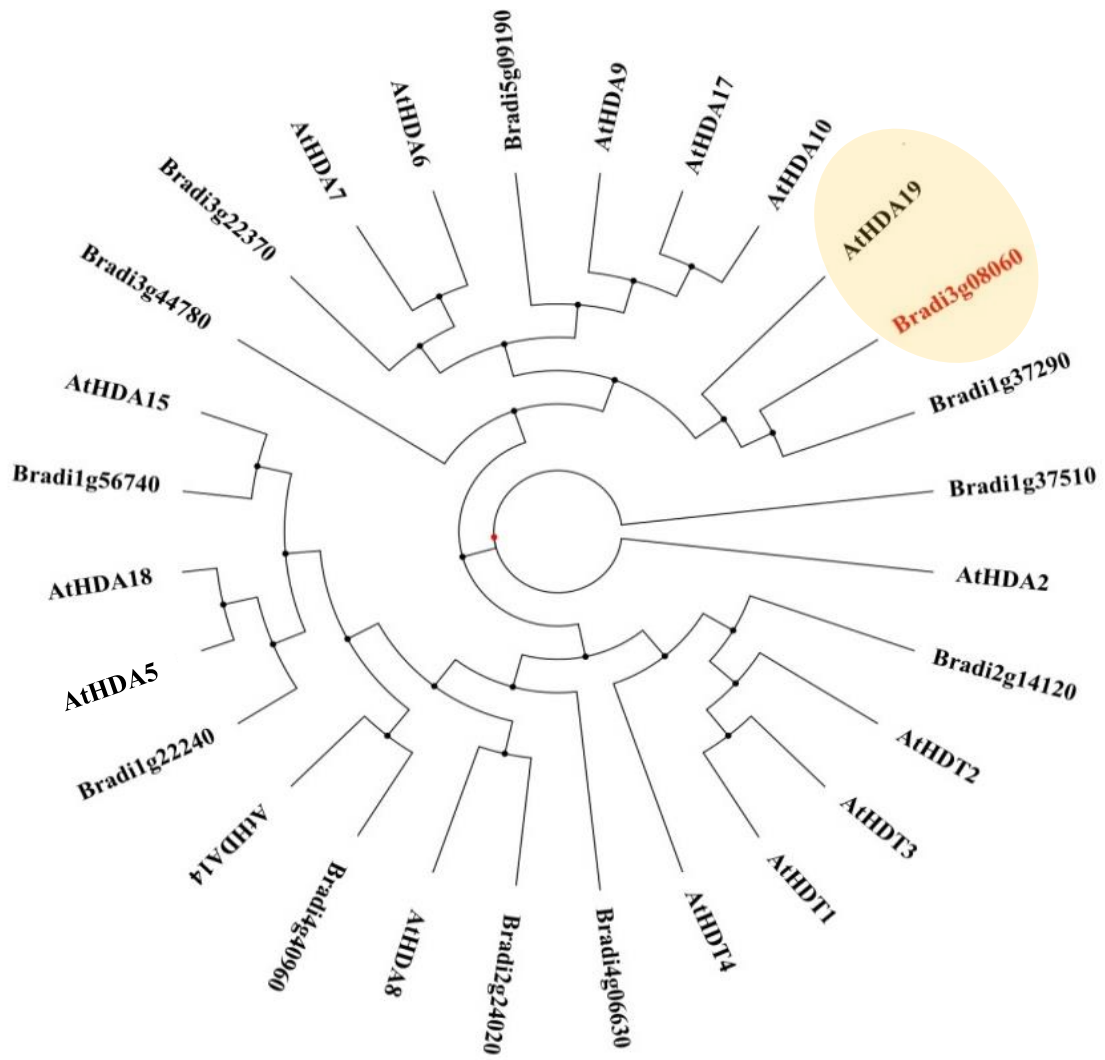


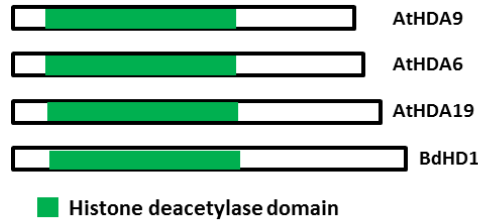
Figure 5. Domain organization of HDACs in HDA6, HDA9, HDA19 and BdHD1

(A) Schematic representation of the domain organization of four Type-I (RPD3/HDAC1) HDACs: HDA6, HDA9, HDA19 and BdHD1. The green boxes represent the conserved HDAC domain.

(B) Protein similarities among 4 HDACs (HDA6, HDA9, HDA19 and BdHD1) shown as percentages. BdHD1 shows the highest similarity with HDA19 (highlighted with the red grid).

(C) Alignment of the catalytic domains of HDA6, HDA9, HDA19 and BdHD1. Amino acid residues that are crucial for catalytic activity and conserved in all sequences are boxed in red.

A



B

Percent identity

		1	2	3	4		
Divergence	1		62.1	56.5	78.2	1	BdHD1
	2	52.4		55.3	62.2	2	HDA6
	3	64	66.8		57.3	3	HDA9
	4	25.9	52.1	62.2		4	HDA19
		1	2	3	4		

C

```

HDA9      DLFEFCQLYAGGTIDAARRLNNKLCDAINWAGSLHHAKKCDASGGFCYINDLVLGILELL
HDA6      GLFDFCRASAGGSIGAAVKLNQRQADAIINWAGSLHHAKKSEASGGFCYVNDIVLGILELL
Bradi3g08060 GLYSFCQTYAGASVGSVAVKLNRG-HDIAINWAGSLHHAKKCEASGGFCYVNDIVLAILLELL
HDA19     GLYSFCQTYAGGSVGGSVKLNHGLCDIAINWAGSLHHAKKCEASGGFCYVNDIVLAILLELL
          .*:.*:  **.:...: :**.  *****.*****.:*****:**.*.*****

HDA9      KHHPRVLYIDIDVHGGDVEEAFYFTDRVMTVSFHKFGDKFFPGTGDVKEIGEREGKFYA
HDA6      KMFKRVLVYIDIDVHGGDVEEAFYTTDRVMTVSFHKFGD-FFPGTGHIRDVGAEKGYA
Bradi3g08060 KHHQRVLYVDIDVHGGDVEEAFYTTDRVMTVSFHKFGD-YFPGTGDVDRDIGHSKGYYS
HDA19     KQHERVLYVDIDVHGGDVEEAFYATDRVMTVSFHKFGD-YFPGTGHIQDIGYSGKYY
          * .  **.:**.:***** ***** :*****.:*: * .**.:*

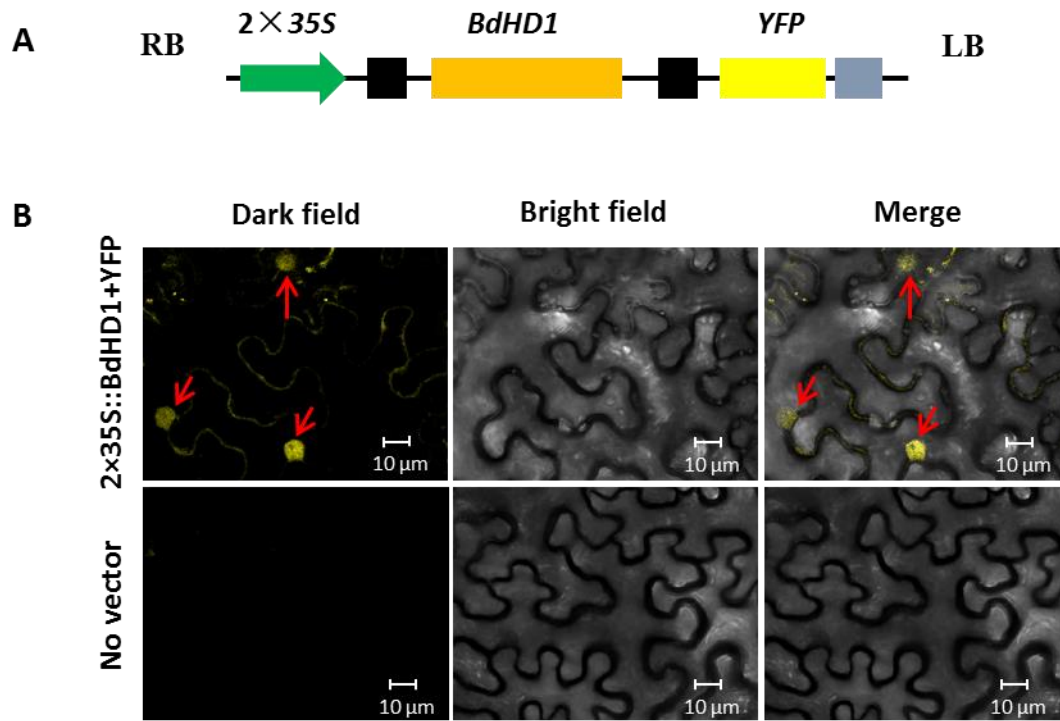
HDA9      INVPLKDGIDSSFNRLFRTIISKVVEIYQPGAIVLQCGADSLARDRLGCFNLSIDGHAE
HDA6      LNVPLNDGMDDESFRSLFRPLIQKMEVYQPEAVVLQCGADSLSGDRLGCFNLSVKGHAD
Bradi3g08060 LNVPLDDGIDDESYSQSLFKPIMAKVMEVFRPGAVVLQCGADSLSGDRLGCFNLSIRGHAE
HDA19     LNVPLDDGIDDESYSHLLFKPIMGVMEIFRPGAVVLQCGADSLSGDRLGCFNLSIKGHAE
          :****.*:*.**.:.  **.: : *:*:*** *:*:*****: *****: ***:

HDA9      CVKFKVKKFNLPLLVTGGGGYTENVARCWTVEIGILLDTELPNEIPENDYIKYFAPDFSL
HDA6      CLRFLRSYNVPLMVLGGGGYTIRNVARCWCYETAVAVGVEPDNKLPHYNEYFEYFGPDYTL
Bradi3g08060 CVKYMRSFNVPLLLLGGGGYTIRNVARCWCYETGVALGQLELDKMPINEYFEYFGPDYTL
HDA19     CVKFMRSFNVPLLLLGGGGYTIRNVARCWCYETGVALGVEVEDKMPHEHYEYFGPDYTL
          *:.....*:**.: ***** .***** **.: . * :*: * ** :**.*:*.
    
```

Figure 6. Subcellular localization of BdHD1-YFP fusion proteins

(A) Schematic diagram of the region of the *BdHD1-YFP* vector used for subcellular localization. The green arrow represents the *CaMV35S* promoter ($2\times 35S$). The orange bar represents the sequence of the coding region of *BdHD1*. The yellow bar represents the DNA sequence of the yellow fluorescence protein gene *YFP*. RB and LB indicate the right and the left border of the T-DNA region, respectively.

(B) A $2\times 35S::BdHD1-YFP$ translational fusion construct was introduced into *Nicotiana benthamiana* leaf epidermis cells via Agro-infiltration using *Agrobacterium* GV3101 (upper row). The yellow spots (pointed by red arrows) indicate the yellow fluorescent protein signal. *N. benthamiana* leaf epidermis cells were infiltrated by *Agrobacterium* without the GV3101 $2\times 35S::BdHD1-YFP$ vector, and were used as control (lower row). This test was performed with three independent experiments. Scale bars: 10 μm .



3.1.2 Expression of *BdHDI* is reduced by drought stress and ABA

To investigate how *BdHDI* responds to drought stress, I measured the expression level of *BdHDI* under drought stress. Progressive drought and osmotic solution were used to administer drought stress.

For the progressive method, drought stress treatments were conducted on 4-leaf stage plants by withholding water for 5 days. At day 5, drought-treated plants had wilting leaves (Figure 7A). Soil water content was measured daily to confirm the water loss in each pot. Soil water content was maintained at 12.0% in the control group, but for the drought-treated group it rapidly dropped to 5.5% on the second day, then reached 0.5% by day 5 (Figure 7B). Leaf water potential was measured to assess the water status of the plants. Under control conditions, leaf water potential was -1.0 Mpa in the *Brachypodium* plants (Figure 7C). As shown in Figure 7C, leaf water potential did not show significant changes for the first 3 days, but it decreased by day 4 and dropped to -2.9 Mpa by day 5. Late embryogenesis abundant (LEA) genes are induced by drought stress and can be used as a drought stress marker (Maitra and Cushman, 1994; Xu et al., 1996; Hundertmark and Hinch, 2008). To confirm the efficiency of the drought stress treatment at the molecular level, the expression level of the LEA gene *BdLEA3* was analyzed. The expression level of *BdLEA3* in drought-treated plants did not show an increase until day 4, and by day 5 it was 15-fold increased (Figure 7D). With the effect of the drought treatment confirmed, I then measured the expression level of *BdHDI* in *Brachypodium*, and the expression level of *BdHDI* was reduced under drought stress (Figure 8A).

For the osmotic solution method, drought treatments were conducted by using PEG-6000 and mannitol independently. Consistent with the progressive drought method result, both the PEG-6000 (Figure 8B) and mannitol (Figure 8C) treatments repressed the expression level of *BdHDI*. I also tested if the expression level of *BdHDI* was regulated by ABA. The result showed that *BdHDI* was down-regulated in the presence of exogenous ABA (Figure 8D). These results suggest that *BdHDI* might be involved in the ABA signaling pathway in the drought stress response.

Figure 7. Drought-induced changes in *Brachypodium* using the soil drying method

(A) Images of the wild type Bd21-3 under control and drought stress conditions at day 1 and day 5.

(B) Measurements of soil water content. The soil water content of each pot was recorded every 24 hours for 5 days. Shown are means \pm standard errors (n=3). Three pots for each independent experiment. The significance of the difference was determined using a Student's t test (** $p < 0.01$).

(C) Measurements of leaf water potential. Leaf water potential was measured every 24 hours for 5 days. Shown are means \pm standard errors (n=3). Three plants for each independent experiment. The significance of the difference was determined using a Student's t test (* $p < 0.05$, ** $p < 0.01$).

(D) Gene expression of *BdLEA3* under control and drought conditions. Data are shown as the expression level relative to the control condition. Shown are means \pm standard errors (n=3). For each independent experiment, three plants from control or drought treatment were pooled together for RNA extraction. The significance of the difference was determined using a Student's t test (* $p < 0.05$, ** $p < 0.01$).

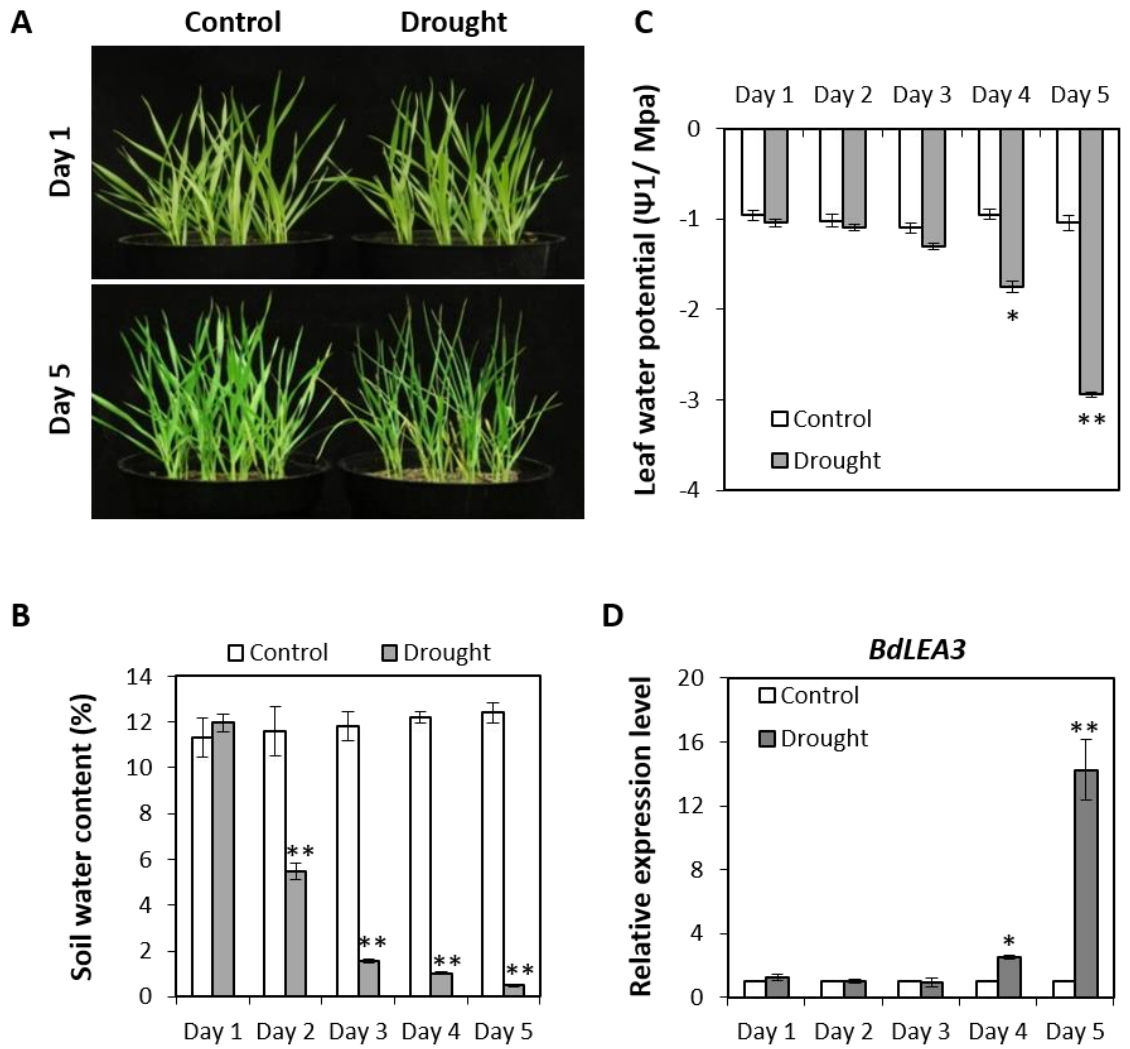
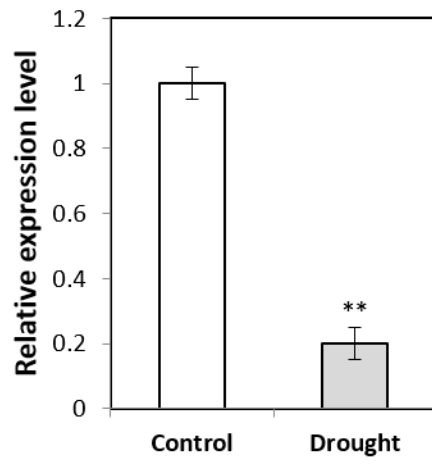
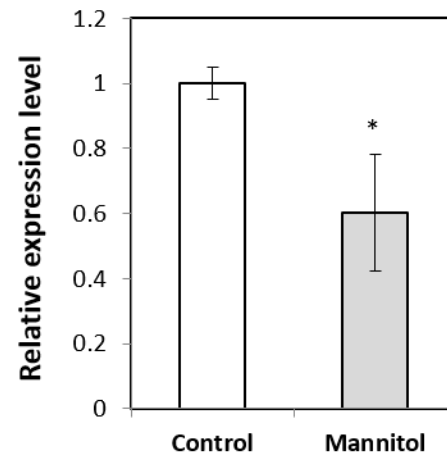
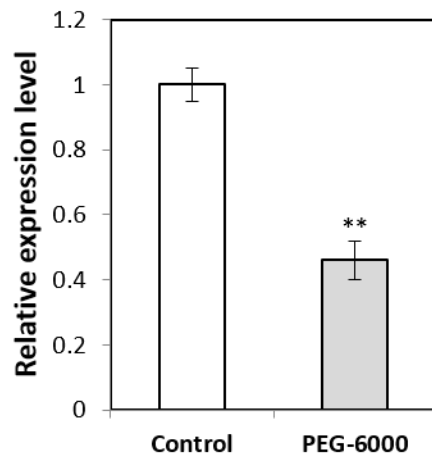
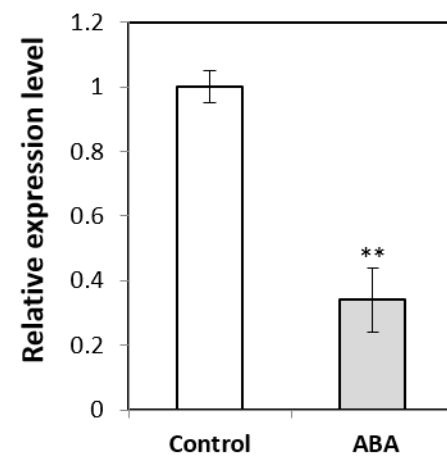


Figure 8. Expression of *BdHDI* under drought, PEG-6000, mannitol and ABA

Expression of *BdHDI* under three drought treatment methods: (A) soil drying method, (B) PEG-6000, (C) mannitol and (D) ABA treatment. Data are shown as the expression level relative to the control condition. Shown are means \pm standard errors (n=3). For each independent experiment, three plants from control or each treatment were pooled together for RNA extraction. The significance of the difference between control and each stress treatment was determined using a Student's t test (* $p < 0.05$, ** $p < 0.01$).

A**C****B****D**

3.1.3 Development of *BdHDI*-overexpression lines and *BdHDI*-RNA interference lines

To further investigate the role of *BdHDI* in the drought stress response of *Brachypodium*, I generated *BdHDI*-overexpression (*BdHDI*-OE) lines and *BdHDI*-RNAi lines.

The construct used for generating *BdHDI*-OE lines is shown in Figure 9A. The expression of the *BdHDI* coding region was driven by a 2×35S promoter, and the expressed protein was attached to a green fluorescent protein (*GFP*) gene. Regenerated transgenic plants were selected with hygromycin. In total, I obtained 44 independently regenerated plants. The transfer-DNA (*BdHDI*-*GFP*) was identified in 10 out of 44 regenerated plants (T-DNA presence in four lines shown in Figure 9B). Green fluorescent protein signals were detected in OE22 and OE30 (Figure 9C). The homozygous plants of OE22 and OE30 were selected after the “Progeny Test”. The gene expression level of *BdHDI* was measured in the two *BdHDI*-OE lines. The RT-qPCR results demonstrated that OE22 and OE30 exhibited higher expression (27.7- and 20.3-fold level, respectively) compared to the wild type Bd21-3 (Figure 9D).

To generate *BdHDI*-RNA interference (*BdHDI*-RNAi) plants, the *BdHDI*-RNAi construct (Figure 10A) was used for plant transformation. Three independent transgenic lines were selected after paromomycin selection and the presence of the transgene (*bdhd1*-PDK) was confirmed by PCR analysis (Figure 10B). The relative expression level of *BdHDI* was measured in different RNAi lines by performing RT-qPCR. The gene expression level of *BdHDI* was knocked down in the three transgenic lines (Figure 10C). Compared to the wild type (100%), *bdhd1-30* had the lowest level (30%) among these three independent lines. The homozygous plants of *bdhd1-30* were selected after the “Progeny Test” for further study. The transgenic lines *bdhd1-31* and *bdhd1-44* were lost during seed propagation.

Figure 9. Generation of *BdHDI*-overexpression lines

(A) Schematic diagram of the region of the *BdHDI*-OE vector used for transformation. The red bar represents the double *CaMV35S* promoter ($2 \times 35S$). The orange bar represents the sequence of the coding region of *BdHDI*. The green bar represents the sequence of the green fluorescent protein gene *GFP*. The dark blue bar represents the sequence of the hygromycin resistance gene *hyg*. RB and LB indicate the right and the left border of the T-DNA region, respectively.

(B) Confirmation of the presence of *BdHDI*-*GFP* in the T1 *BdHDI*-OE lines (OE2, OE8, OE22, and OE30). The genomic DNA of the wild type Bd21-3 was used as a negative control. A fragment (size, 917 bp) of the T-DNA *BdHDI*-*GFP* construct was amplified by using a pair of primers indicated as black arrows in (A). A fragment (size, 325 bp) of the genomic DNA of *SamDC* was amplified as a positive control to indicate the genomic DNA quality.

(C) Green fluorescence protein (GFP) signals were detected in OE22 and OE30 using confocal microscopy. The green spots indicate GFP signals. No GFP signal was detected in the wild type Bd21-3 (negative control).

(D) Relative gene expression of *BdHDI* in Bd21-3, OE22 and OE30. Shown are means \pm standard errors ($n=3$). For each experiment, three plants of each line were pooled together for RNA extraction. The significances of the difference were determined using a Student's *t* test (** $p < 0.01$)

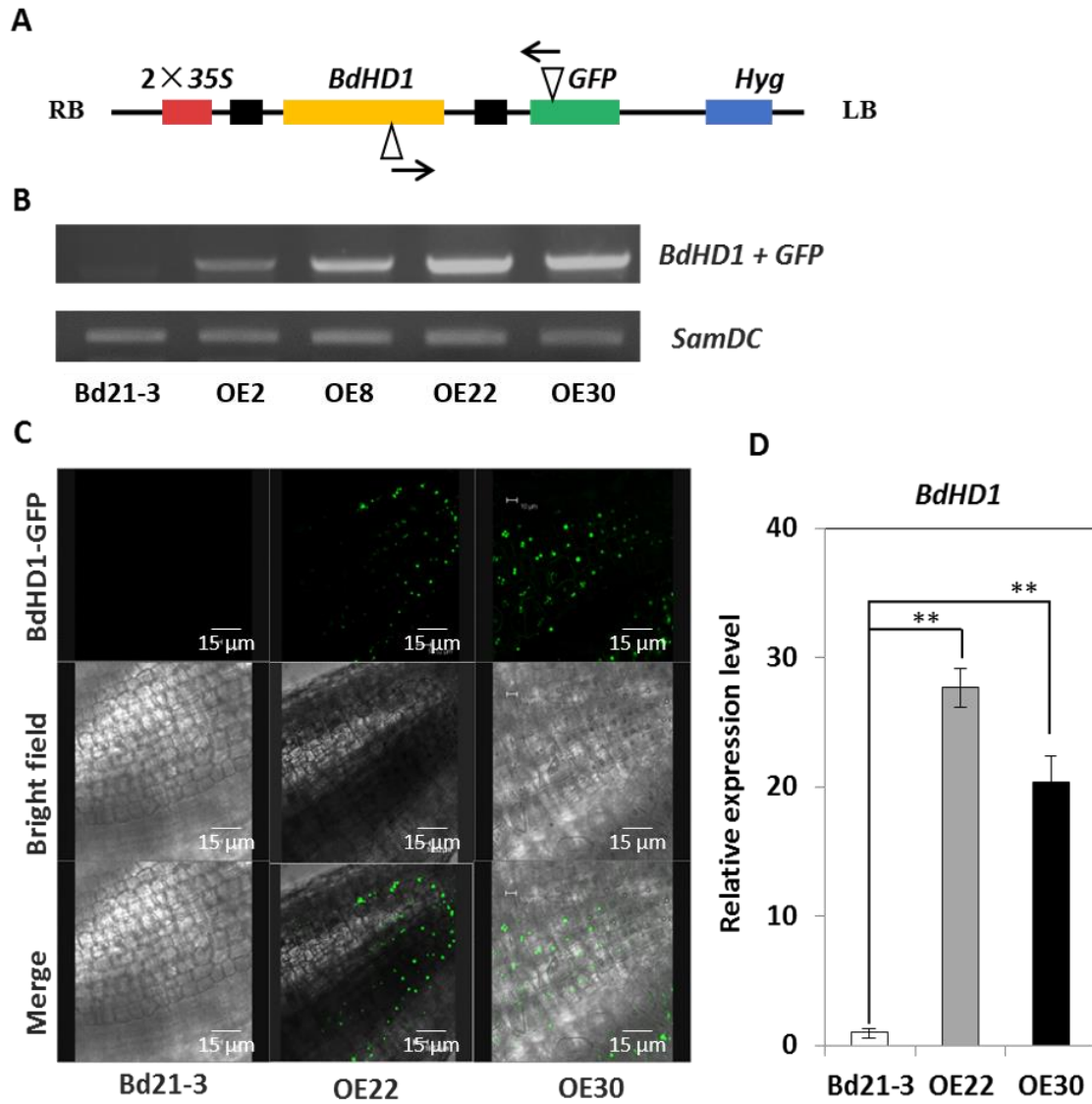


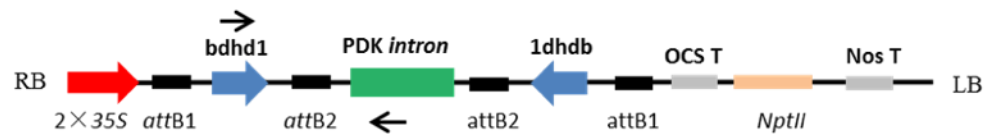
Figure 10. Generation of *BdHDI*-RNAi lines

(A) Schematic diagram of the region of the *BdHDI*-RNAi vector used for generating RNAi plants. The red arrow represents the double *CaMV35S* promoter ($2 \times 35S$). The blue arrows represent the *BdHDI*-specific sequence *bdhd1* (size, 309 bp). The green bar represents the sequence of *PDK* intron. The light brown bar represents the sequence of the paromomycin resistance gene *nptII*. RB and LB indicate the right and the left border of the T-DNA region, respectively.

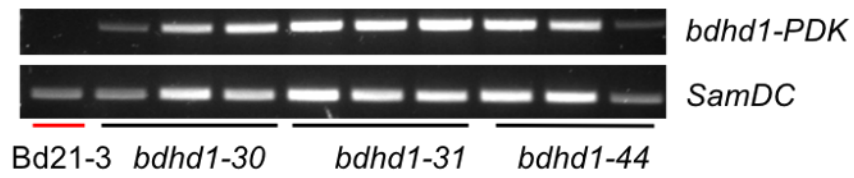
(B) Confirmation of Transfer DNA (*bdhd1-PDK*) presence in the T2 *BdHDI*-RNAi lines (*bdhd1-30*, *bdhd1-31* and *bdhd1-44*). The genomic DNA of Bd21-3 was used as a negative control. A fragment (size, 556 bp) of the RNAi construct was amplified by using a pair of primers indicated as black arrows in (A). A fragment (size, 325 bp) of *SamDC* was amplified as a positive control to indicate the genomic DNA quality.

(C) Relative gene expression of *BdHDI* in Bd21-3, *bdhd1-30*, *bdhd1-31* and *bdhd1-44*. Shown are means \pm standard errors (n=3). For each experiment, three plants of Bd21-3 or each RNAi line were pooled together for RNA extraction. The significances of the difference were determined using Student's t tests (** $p < 0.01$)

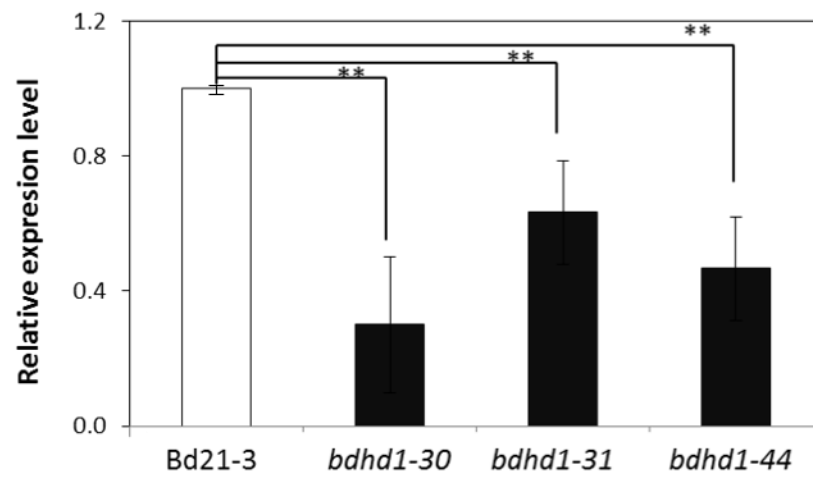
A



B



C



3.1.4 Overexpression of *BdHDI* enhances drought tolerance in *Brachypodium*

I first investigated whether overexpressing *BdHDI* altered the drought tolerance of *Brachypodium*. To answer this question, I conducted drought treatments with the wild type (Bd21-3) and the *BdHDI*-OE plants (OE22 and OE30).

As shown in Figure 11A, the wild type and *BdHDI*-OE plants were grown in the same pot. Plants grown under control conditions served as the control, and plants were treated by withholding water for 10 days, followed by recovery for 1 week. The surviving wild type and *BdHDI*-OE plants were counted and percent survival was calculated (Figure 11B). The survival of the Bd21-3 plants were 43% and 30% while the survival of OE22 and OE30 were 86% and 73%, individually.

3.1.5 *bdhd1-30* plants exhibit lower survival under drought stress

Next, I questioned if knocking down the expression level of *BdHDI* also would reduce drought survival of *Brachypodium*. Then I tested the performance of *BdHDI*-RNAi plants under drought stress. The same drought treatment method was applied to *bdhd1-30* plants. Plants were stressed by withholding water for 8 days, followed by a recovery for 1 week (Figure 12A). The surviving Bd21-3 and *bdhd1-30* plants were counted and percent survival was calculated (Figure 12B). After drought treatment for 8 days, 100% of the Bd21-3 plants survived. Conversely, only 53% of the *bdhd1-30* plants had regenerated green tissue after one-week of recovery. These results indicate that knocking down *BdHDI* reduces *Brachypodium* survival under drought stress.

Figure 11. Survival of *BdHDI*-OE lines under drought stress

(A) Phenotypes of Bd21-3, OE22 and OE30, grown in a split-pot design, before drought stress and after 1 week of re-watering following 10 days of drought stress.

(B) Performance of the two *BdHDI*-OE lines (OE22 and OE30) and the wild type (Bd21-3) after drought stress. Shown are means \pm standard errors (n=3). For each independent experiment, three biological replicates were used to calculate plant survival (10 plants of each genotype were used for each biological replicate) were used to calculate plant survival. The significances of the difference between the Bd21-3 and *BdHDI*-OE line (OE22, OE30) were determined using Student's t tests (* $p < 0.05$, ** $p < 0.01$).

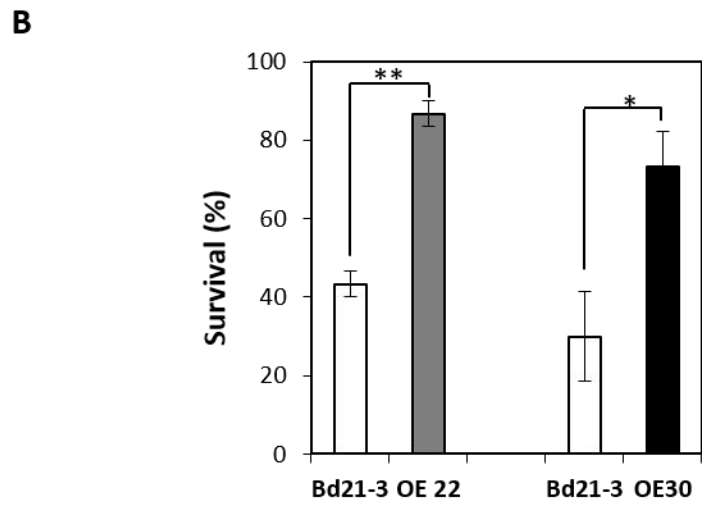
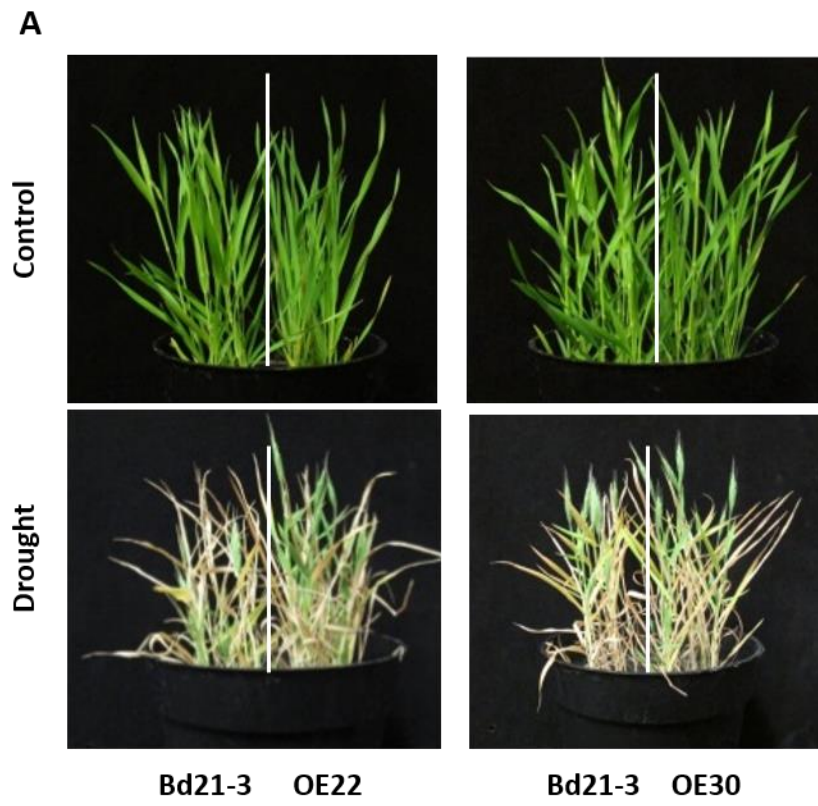
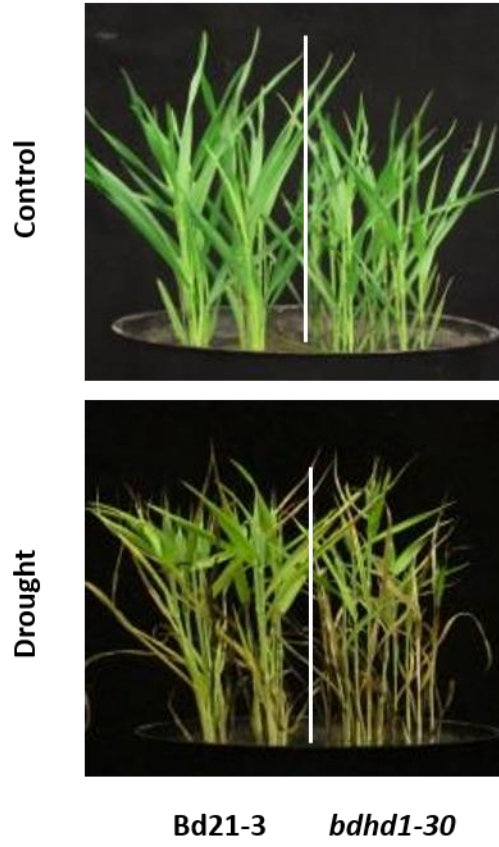
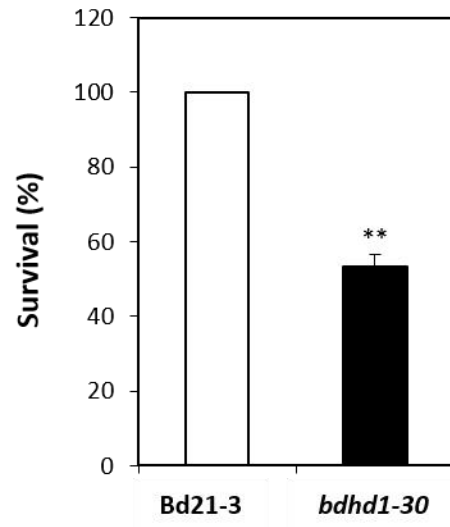


Figure 12. Survival of *BdHDI*-RNAi plants under drought stress

(A) Phenotypes of Bd21-3 and *bdhd1-30*, grown in a split-pot design, before drought stress and after 1 week of re-watering following 8 days of drought stress.

(B) Performance of the Bd21-3 and the *bdhd1-30* plants after the drought stress treatment. Shown are means \pm standard errors (n=3). For each independent experiment, three biological replicates were used to calculate plant survival (10 plants of each genotype were used for each biological replicate). The significance of the difference between Bd21-3 and *bdhd1-30* was determined using a Student's t test (** $p < 0.01$).

A**B**

3.1.6 Overexpression of *BdHDI* leads to an ABA-hypersensitive phenotype during seed germination and during post-germination growth

To examine if *BdHDI* is involved in the ABA pathway, the performance of *BdHDI*-OE lines under ABA treatment were investigated. ABA was applied to the OE lines for a germination test and a post-germination growth test.

For the germination test, germinated seeds were counted at day 6, and the germination percentages of the wild type (Bd21-3) and *BdHDI*-OE lines (OE22 and OE30) were calculated. There was no significant difference in germination between Bd21-3 and the OE lines under control conditions (Figures 13A&B), and the germination percentages of seeds of Bd21-3, OE22 and OE30 reached 100% under control conditions (Figure 13B). However, seeds treated with ABA had lower germination compared to that observed under control conditions (Figure 13A). At day 6, the wild type seeds reached 87% germination, while the OE22 and OE30 seeds exhibited significant lower germination (65% and 59%, respectively) than Bd21-3 under the ABA treatment (Figure 13B).

For the post-germination growth test, the seedlings of wild type (Bd21-3) and *BdHDI*-OE (OE22 and OE30) lines were grown on ABA agar plates for 2 weeks after 2 days of germination (Figure 13C). The lengths of the shoots and roots were measured to assess the post-germination growth. The lengths of the shoots of Bd21-3, OE22 and OE30 were 5.2 cm, 6.0 cm and 5.5 cm, respectively (Figure 13D). The lengths of the roots of Bd21-3, OE22 and OE30 were 7.0 cm, 6.9 cm and 6.6 cm, respectively (Figure 13D). No significant difference in either the length of shoots or roots between the wild type and the *BdHDI*-OE lines was detected when the plants were grown under control growth conditions. In response to ABA, all plants, including Bd21-3, OE22 and OE30, had shorter shoots and roots compared to under control conditions (Figure 13C). However, the *BdHDI*-OE (OE22 and OE30) plants had significantly shorter shoots (1.0 cm and 1.0 cm, respectively) and roots (1.0 cm and 0.9 cm, respectively) than the wild type (Bd21-3) plants (2.3 cm of shoot and 3.1 cm of root) under the ABA treatment (Figure 13E). Taken together, these results demonstrate that overexpressing *BdHDI* increases ABA sensitivity in *Brachypodium*.

Figure 13. *BdHDI*-OE plants are hypersensitive to ABA during germination and during post-germination growth.

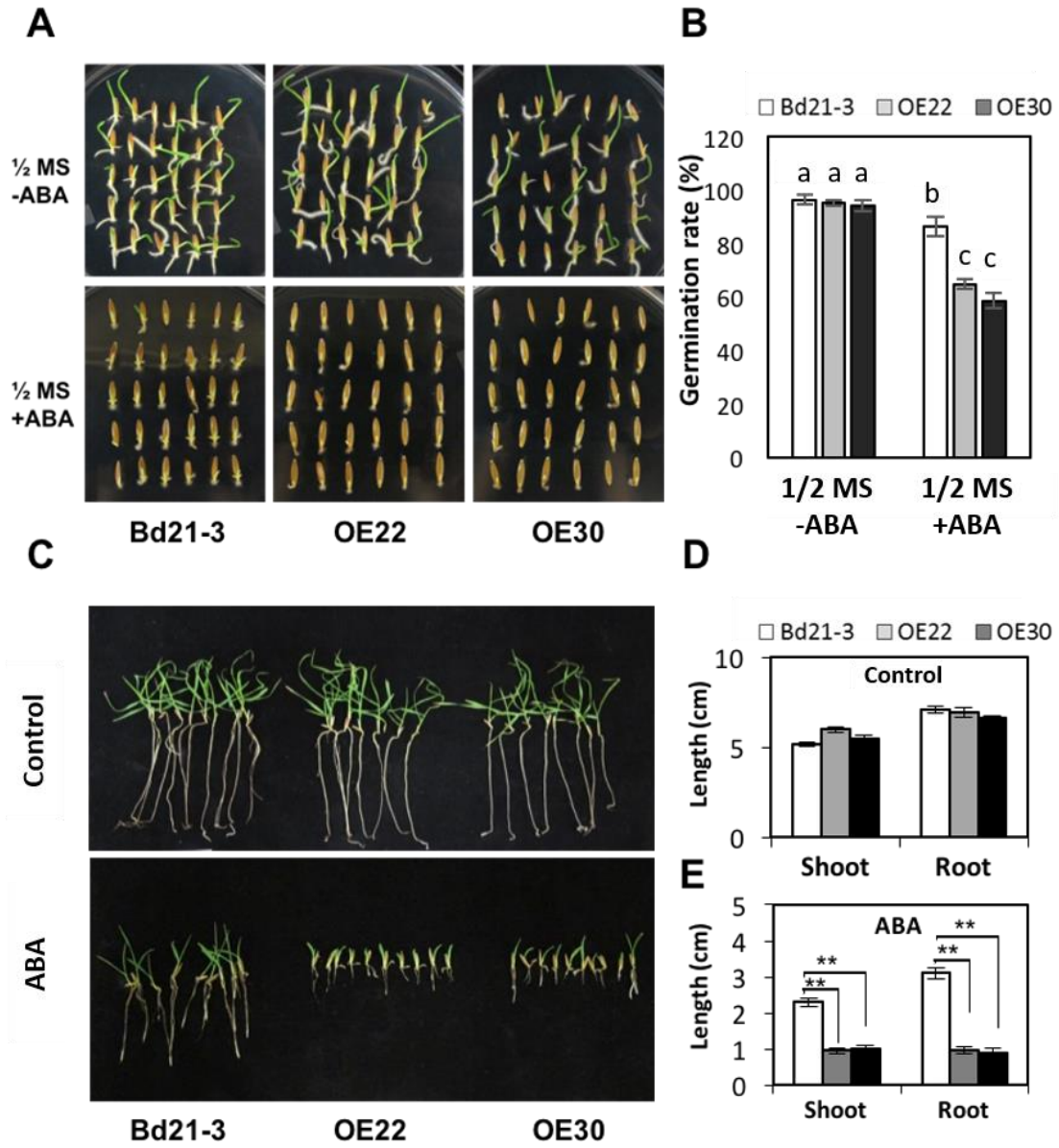
(A) Germination of Bd21-3, OE22 and OE30 on MS medium containing 0 μ M or 2 μ M ABA at day 6.

(B) Germination percentages of *BdHDI*-OE lines (OE22 and OE30) and the wild type (Bd21-3) under control and ABA conditions. Germination percentages were calculated on day 6. Shown are means \pm standard errors (n=3). Fifty seeds of each genotype were used for each independent experiment. The significance of difference was determined by using a two-way ANOVA followed by post-hoc Tukey's HSD tests. Lowercase letters indicate significant differences at the level of $p < 0.05$.

(C) Post-germination growth of the *BdHDI*-OE (OE22, OE30) lines and the wild type (Bd21-3) on MS medium containing 0 μ M or 1 μ M ABA at day 14.

(D) Length of shoots and roots of Bd21-3, OE22 and OE30 grown under control conditions at day 14. Shown are means \pm standard errors (n=3). Ten plants of each genotype were used for each independent experiment. The significances of the difference between Bd21-3 and the *BdHDI*-OE lines (OE22, OE30) were determined using Student's t tests.

(E) Lengths of shoots and roots of Bd21-3, OE22 and OE30 grown on 1 μ M ABA at day 14 after germination. Shown are means \pm standard errors (n=3). Ten plants of each genotype were used for each independent experiment. The significances of the difference between Bd21-3 and the *BdHDI*-OE lines (OE22, OE30) were determined using Student's t tests (** $p < 0.01$).



3.1.7 *BdHDI*-RNAi plants show insensitivity to ABA

To investigate the performance of *BdHDI*-RNAi plants under ABA treatment, I evaluated the post-germination growth of *bdhd1-30* plants. The shoots and roots of *bdhd1-30* and Bd21-3 plants grown on ½ MS medium containing no or 1 µM ABA were measured after 1 week. Under control conditions, Bd21-3 and *bdhd1-30* plants had differences in shoot and root length (Figure 14A), with *bdhd1-30* having significantly shorter shoots (4.2 cm) and shorter roots (5.9 cm) than Bd21-3 plants (5 cm of shoot and 6.5 cm of root) (Figure 14B). With the ABA treatment, no significant difference was observed in the lengths of the shoots between Bd21-3 (3.1 cm) and *bdhd1-30* (3.0 cm) plants; however, longer roots were observed in *bdhd1-30* (4.3 cm) than in Bd21-3 (3.5 cm) seedlings (Figures 14A&C). These results indicated that *BdHDI*-RNAi (*bdhd1-30*) seedlings were less sensitive to ABA than the wild type (Bd21-3) plants.

3.1.8 Overexpressing *BdHDI* does not affect the expression of *PYL4*, *ABI5* and *AGH3*

To gain further insight into the ABA response of the *BdHDI*-OE lines, I analyzed the expression of the ABA receptor gene *PYL4*, ABA-dependent transcription factor gene *ABI5* and the protein phosphatase 2C *AGH3*. Under control conditions, the *BdHDI*-OE lines (OE22 and OE30) had similar expression levels of *PYL4* (Figure 15A), *ABI5* (Figure 15B) and *AGH3* (Figure 15C) to the wild type (Bd21-3) plants. When plants were subjected to the drought treatment, the expression level of *PYL4* was reduced (Figure 15A). On the other hand, both *ABI5* and *AGH3* were induced by drought stress (Figures 15B&C) in the wild type (Bd21-3) and the *BdHDI*-OE lines (OE22 and OE30). However, the data analysis did not reveal significant differences in expression levels of *PYL4*, *AGH3* or *ABI5* between the wild type and *BdHDI*-OE lines under drought stress.

Figure 14. Knocking down *BdHDI* in *bdhd1-30* leads to an ABA insensitive phenotype during post-germination growth

(A) Performance of the *BdHDI*-RNAi line (*bdhd1-30*) and the wild type (Bd21-3) in MS medium containing 0 μ M (Control) or 1 μ M ABA (ABA).

(B) Length of the shoots and roots of Bd21-3 and *bdhd1-30* grown under control conditions at day 14. Shown are means \pm standard errors (n=3). Ten plants of each genotype were used for each independent experiment. The significances of the difference between Bd21-3 and *bdhd1-30* were determined using Student's t tests (* $p < 0.05$, ** $p < 0.01$).

(C) Length of the shoots and roots of Bd21-3 and *bdhd1-30* grown under 1 μ M ABA at day 14. Shown are means \pm standard errors (n=3). Ten plants of each genotype were used for each independent experiment. The significances of the difference between Bd21-3 and *bdhd1-30* were determined using Student's t tests (* $p < 0.05$, ** $p < 0.01$).

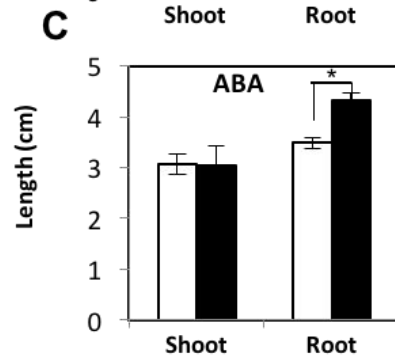
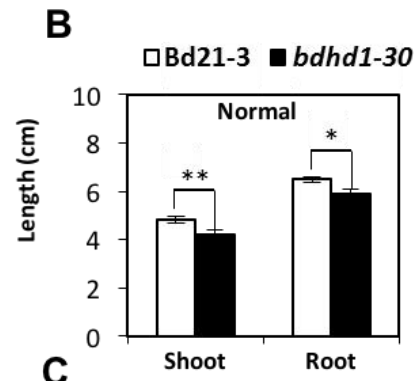
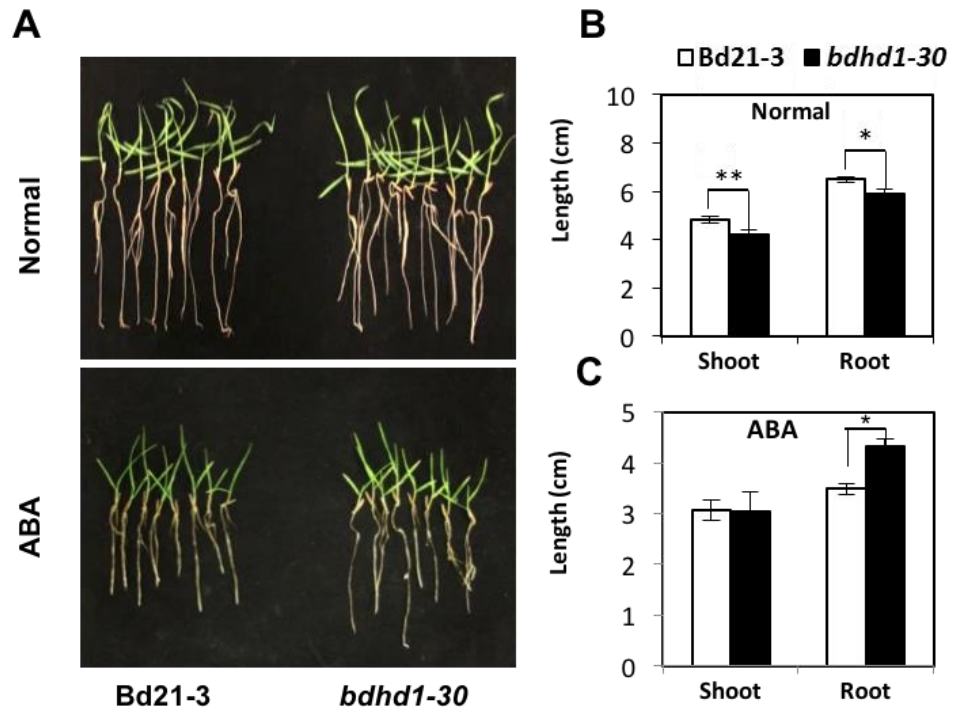
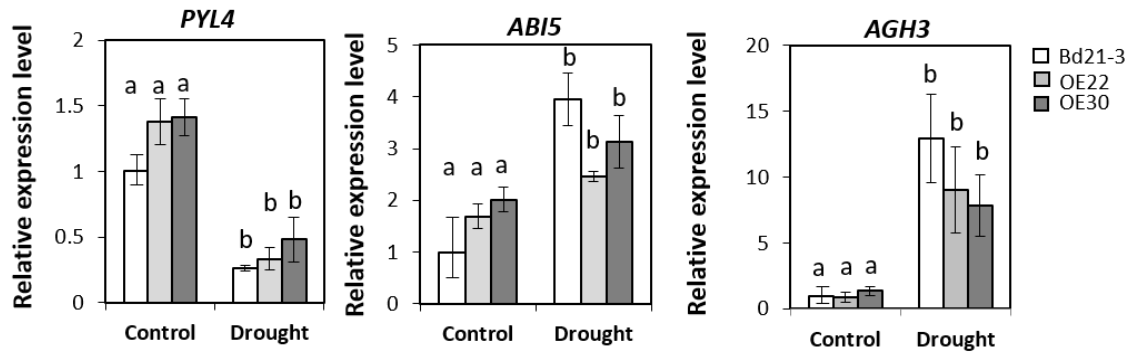


Figure 15. Expression of *PYL4*, *ABI5* and *AGH3* in *BdHDI*-OE plants

Expression of (A) *PYL4*, (B) *ABI5* and (C) *AGH3* in the *BdHDI*-OE (OE22 and OE30) and wild type (Bd21-3) plants under control and drought stress conditions. Shown are means \pm standard errors (n=3). Three plants of each line for each replicate. The significances of the difference were determined by using a two-way ANOVA followed by post-hoc Tukey's HSD tests. Lowercase letters indicate significant differences at the level of $p < 0.05$.



3.2 *BdHDI* reduces H3K9ac and represses gene expression under drought stress

3.2.1 Overexpression of *BdHDI* leads to a decrease of H3K9ac in *Brachypodium*

First, I asked if overexpressing *BdHDI* can affect the H3K9ac level in *Brachypodium*. By performing a Western blot, I detected a lower H3K9ac level in OE22 and OE30 plants compared to the wild type plants (Figure 16A). I measured the blotting signal intensities of H3K9ac and H3. The relative intensity of H3K9ac/H3 was calculated by normalizing to H3. The relative intensity of H3K9ac/H3 in OE22 and OE30 showed 0.86- and 0.89- fold changes of Bd21-3, respectively. (Figure 16B) These results indicate that overexpression of *BdHDI* resulted in the decrease in the H3K9ac level in *Brachypodium*.

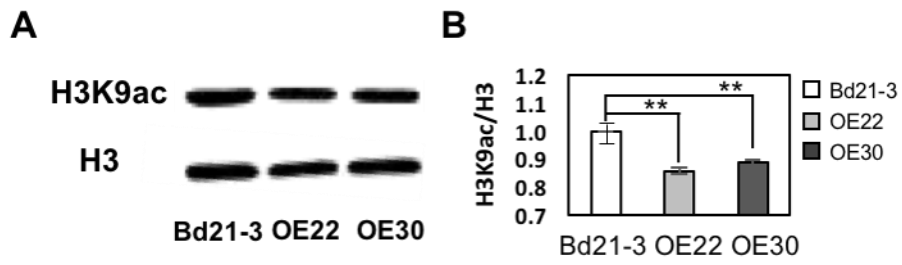
To examine if overexpressing *BdHDI* affects the enrichment level of H3K9ac at the genome-wide scale under control and drought conditions, respectively, ChIP-Seq experiments were performed for Bd21-3 and OE22 plants grown under control and drought conditions. Two independent biological ChIP DNA samples were isolated for sequencing. Sequencing of single-end 50 bp reads was carried out on an Illumina HiSeq 2500. The reads were mapped to the *Brachypodium* genome and H3K9ac-enriched regions were identified in both Bd21-3 and OE22 plants under control and drought conditions. Compared to Bd21-3, 1772 regions showed more than a twofold change ($p < 0.01$) in H3K9ac levels in the OE22 plants under control conditions (Figure 16C). Out of these 1772 regions, 1043 (59%) regions showed more than a two-fold decrease ($p < 0.01$) in H3K9ac in OE22, while 729 (41%) regions showed more than a two-fold increase ($P < 0.01$) in H3K9ac in OE22 (Figure 16C). Under drought conditions, 1449 regions showed more than a two-fold change ($p < 0.01$) in H3K9ac in OE22. Out of these 1449 regions, 1124 (75%) regions showed more than a two-fold decrease ($p < 0.01$) in H3K9ac levels in OE22 and only 375 regions (25%) showed more than a two-fold increase ($p < 0.01$) in H3K9ac levels in OE22 (Figure 16C). The data indicate that overexpression of *BdHDI* mainly acts to reduce H3K9ac levels at the genome-wide scale under drought conditions. However, the increased H3K9ac at some regions in OE22 plants suggests that *BdHDI* also leads to an increase at certain loci.

Figure 16. Overexpressing *BdHDI* leads to a decrease of H3K9ac at the genome-wide level

(A) Western blot analysis of protein extracts from 4-leaf stage plants of Bd21-3, OE22 and OE30, probed with anti-H3K9ac and anti-H3 antibodies. Five plants of each genotype were pooled together for protein extraction. This experiment was repeated independently three time.

(B) Relative intensity analysis of H3K9ac/H3 in Bd21-3, OE22 and OE30. The relative intensities of H3K9ac/H3 in OE22 and OE30 were normalized to Bd21-3. The intensities of blotting signals were quantified using Image J software. Shown are means \pm standard errors (n=3). The significances of the difference between Bd21-3 and the *BdHDI*-OE line (OE22, OE30) were determined using Student's t tests (** $p < 0.01$).

(C) Based on ChIP-Seq data analysis, the numbers of regions with decreased and increased H3K9ac levels (Fold change > 2 , $p < 0.01$) in OE22 compared to Bd21-3 under control and drought conditions.



C

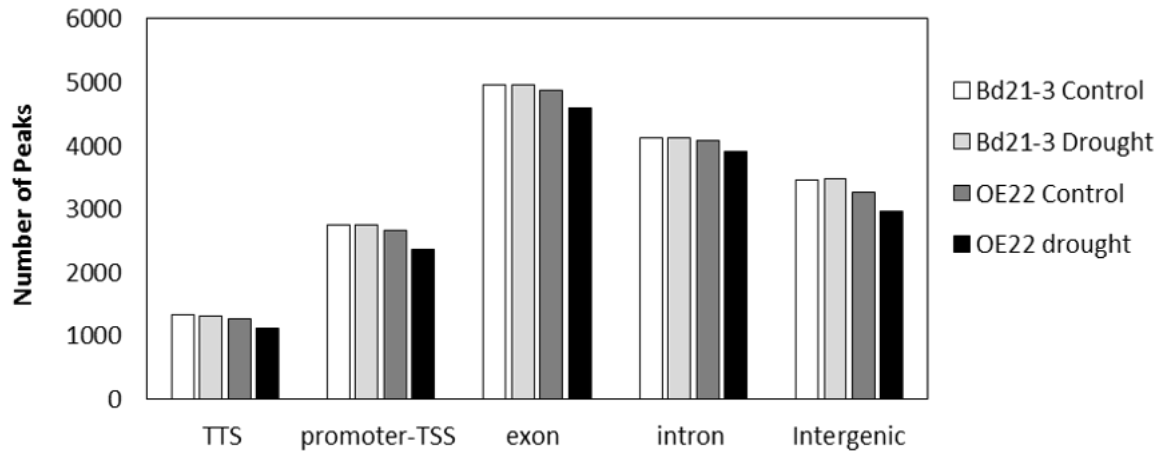
	Decreased	Increased	Total
Control	1043	729	1772
Drought	1124	375	1449

3.2.2 H3K9ac modification patterns under drought stress conditions

H3K9ac-enriched regions were identified based on ChIP-Seq data. Whether overexpressing *BdHDI* affects the distribution patterns of H3K9ac under control and drought stress conditions still was not clear. To address this unknown, the distribution of peaks identified in the ChIP-Seq along the *Brachypodium* genome was characterized. The *Brachypodium* genome was characterized into five classes that included four classes of genic regions (promoter-TSS (1kb upstream of TSS), TTS, exon and intron) and intergenic regions. I calculated the distribution of H3K9ac associated with the different genome categories (Figure 17). The results showed that H3K9ac modification was predominantly enriched in the generic regions, especially in the exon and intron. In each category, there was less enrichment of H3K9ac in OE22 than in the wild type under both control and drought conditions. However, Bd21-3 and OE22 had the same distribution pattern of H3K9ac along the genome, as shown by their same percentages of H3K9ac for each genome category: promoter-TSS (16%), TTS (8%), coding exon (30%), intron (25%) and intergenic regions (21%). The data analysis indicated that overexpressing *BdHDI* did not affect the distribution pattern of H3K9ac in *Brachypodium* either under control or drought stress conditions.

Figure 17. The distribution of H3K9ac modification in Bd21-3 and OE22 plants under control and drought conditions

A histogram displaying the numbers of H3K9ac peaks in Bd21-3 and OE22 plants under control and drought conditions. The numbers of peaks are shown in the different *Brachypodium* genome categories, including promoter-TSS, TTS, coding exon, intron and intergenic regions.



3.2.3 Identification of differentially H3K9ac-modified genes under drought stress in OE22

Next, I analyzed how many H3K9ac-enriched genes there were with a more than two-fold decrease in OE22 than in Bd21-3 under control and drought conditions, respectively. I identified 749 regions, corresponding to 372 genes, which showed lower H3K9ac levels in OE22 under both control and drought stress conditions (Figure 18A). In addition, 380 regions that corresponded to 230 genes showed a more than two-fold decrease under drought condition and 294 regions showed a more than two-fold decrease in OE22 under control conditions. To examine the difference of these 230 genes in H3K9ac levels between Bd21-3 and OE22 under drought conditions, I plotted ChIP-Seq reads from the Bd21-3-drought and OE22-drought plants on the 230 H3K9ac target genes and found that the enrichment level of H3K9ac on TSSs was lower in OE22 compared to Bd21-3 (Figure 18B)

To gain insight into the possible biological roles of the 230 genes that showed decreased H3K9ac in OE22 under drought stress, their potential functional associations were examined by performing a Gene Ontology analysis using the PANTHER Classification System (<http://pantherdb.org/>). These genes were classified according to both metabolic process and cellular processes. By running this program, 185 out of 230 genes were successfully mapped into different categories. In terms of the biological processes, 44 genes were placed in the “cellular process” category and 40 genes were matched to the category of “metabolic process” (Figure 19). Regarding molecular processes, 36 genes were placed in the category of “catalytic activity” and 18 genes were identified in the category of “binding activity” (Figure 19). Due to the limited information on *Brachypodium* genes, 45 out of 230 genes were not matched in the PANTHER Classification System. The gene ontology analysis provided information regarding the potential biological and metabolic functions of 185 out of 230 genes identified from the ChIP-Seq assays.

Figure 18. Regions with decreased H3K9ac in OE22

(A) Numbers of regions with reduced H3K9ac levels in OE22 (Fold change > 2 , $p < 0.01$) comparing to the wild type under control and drought stress conditions.

(B) Peak distribution of H3K9ac on 230 drought-specific genes relative to ± 2 kb around TSS in Bd21-3 and OE22.

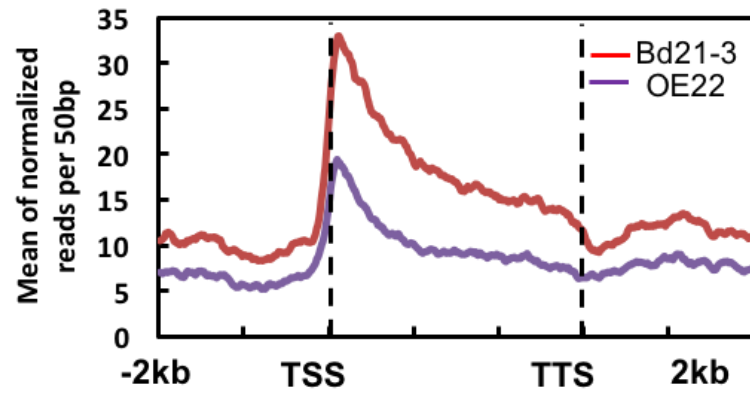
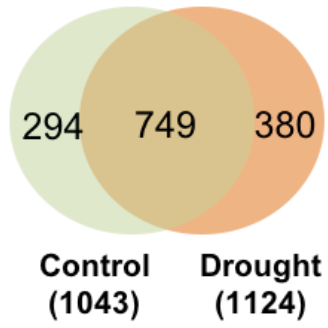
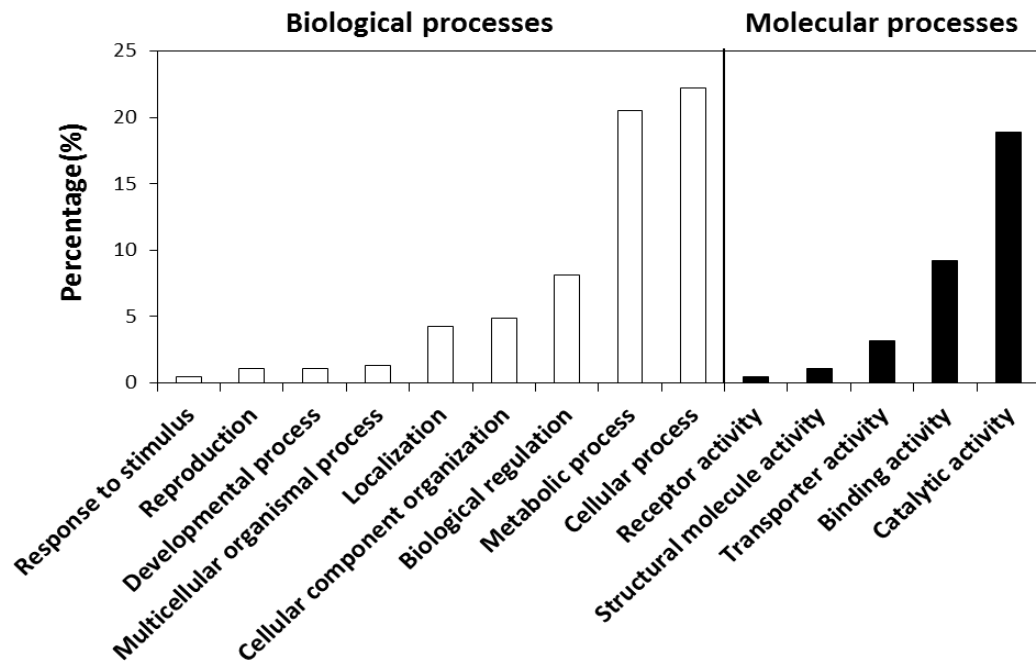


Figure 19. Gene ontology analysis of the 230 drought-specific genes

Gene ontology analysis of 230 drought-specific genes: percentages of genes involved in various biological processes and percentages of genes involved in molecular processes.



3.2.4 Association of H3K9ac modification changes with differential gene expression under drought stress

Transcription factors are master regulators in a transcriptional regulatory system. A single transcription factor can regulate the expression of many target genes through specific binding. According to the gene ontology analysis results, 18 genes were grouped into the “binding activity” category (Figure 19). Ten out of 18 genes, namely *BdMYB1*, *1G25105*, *2G09970*, *3G52260*, *BdORG2*, *BdMYB75*, *3G52320*, *BdE2F2*, *5G12330* and *BdWYRK24*, are transcription factor genes in *Brachypodium*. The distribution of H3K9ac in Bd21-3 and OE22 was visualized at the genome-wide level. Figure 20A shows the distribution of H3K9ac on the 10 genes in Bd21-3 and OE22 under control conditions. The ChIP-Seq data were validated by performing qPCR, and there was no significant difference in the relative H3K9ac enrichment on the 10 genes between Bd21-3 and OE22 (Figure 20B). As shown in Figure 21A, less H3K9ac was enriched on the 10 genes in OE22 than in Bd21-3 under drought conditions (fold change > 2, $p < 0.01$). The ChIP-qPCR results confirmed that lower H3K9ac levels were observed in OE22 than in Bd21-3 under drought stress (Figure 21B). This result suggests that *BdHDI* causes relatively lower H3K9ac levels of target genes in OE22 plants than in Bd21-3 under drought stress.

Next, I tested whether the lower H3K9ac level in the *BdHDI*-overexpression plants causes down-regulation of the corresponding genes. I measured the expression levels of these 10 genes in the wild type and the OE22 plants by performing RT-qPCR. Under control conditions, *BdMYB1*, *1G25105*, *2G09970*, *3G52260*, *BdORG2*, *BdMYB75*, *3G52320*, *BdE2F2*, *5G12330* (Figure 22A) and *BdWYRK24* (Figure 23A) did not show significant differences in expression levels between Bd21-3 and OE22. However, under drought conditions, *BdMYB1*, *1G25105*, *2G09970*, *3G52260*, *BdORG2*, *BdMYB75*, *3G52320*, *BdE2F2* (Figure 22B) and *BdWYRK24* (Figure 23A) showed significantly lower expression in OE22 than in Bd21-3. However, there was no significant difference in the expression of *5G12330* between Bd21-3 and OE22 under drought conditions (Figure 22B). These results indicated that lower H3K9ac levels on these drought-specific genes affected their expression levels. They suggest there was a positive correlation between reduced H3K9ac levels and repressed gene expression.

Figure 20. Profiling of H3K9ac on the 10 transcription factor genes under control conditions

(A) ChIP-Seq data showing different enrichment of H3K9ac for 10 selected genes in OE22 (blue) and the wild type (green) under control conditions. Gene structures are shown underneath each panel. (+) means positive strand, (-) means negative strand. The profiling of H3K9ac for the 10 transcription factor genes was visualized by IGB. Red bars represent the fragments used as qPCR templates for each gene.

(B) ChIP-qPCR validation under control conditions. Data are shown as the relative enrichment of H3K9ac relative to the gene *SamDC*. Shown are means \pm standard errors (n=3). Ninety-six plants of each genotype were used for each independent experiment. The significance of the difference of each gene between OE22 and Bd21-3 was determined using a Student's t test.

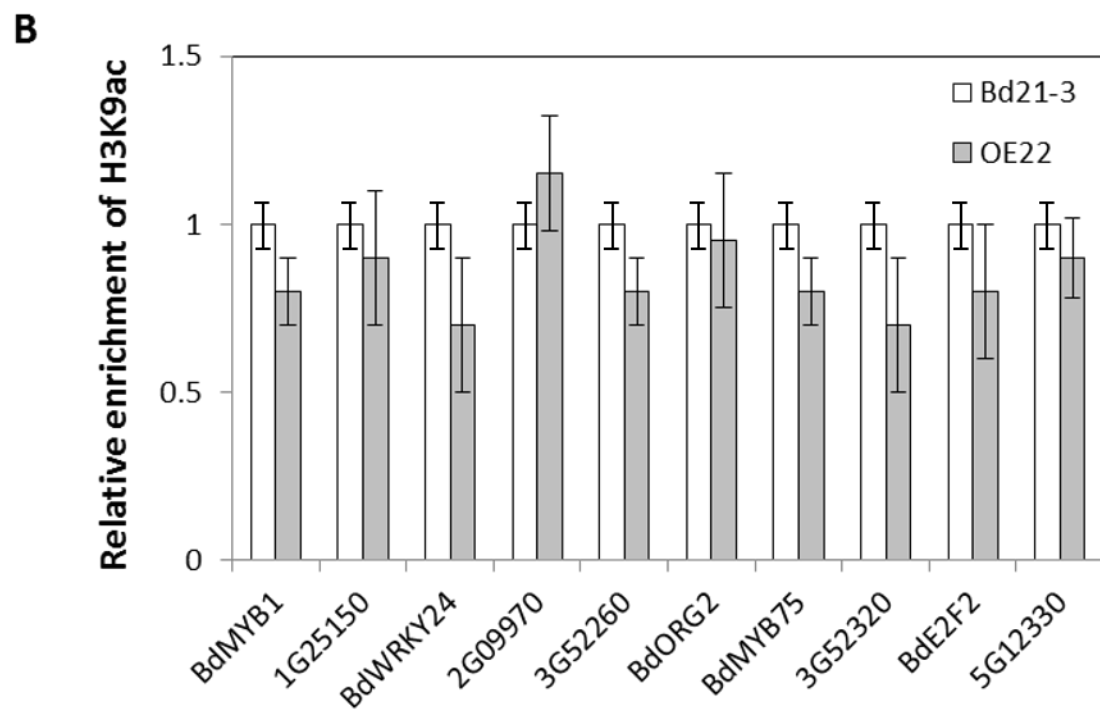
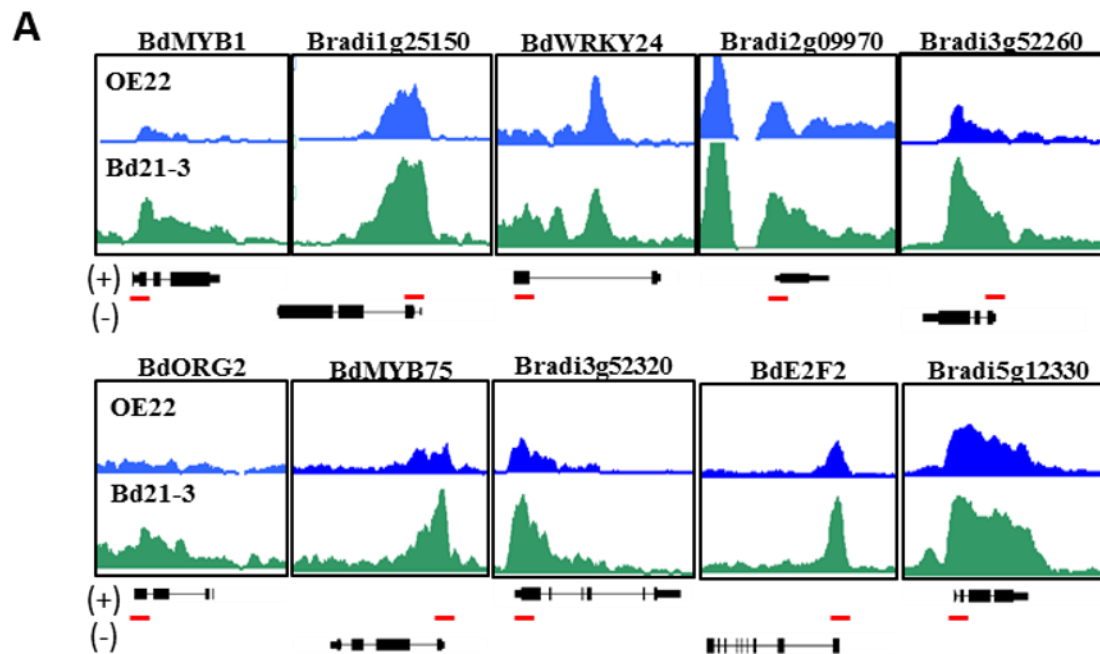


Figure 21. Profiling of H3K9ac on the 10 transcription factor genes under drought conditions.

(A) ChIP-Seq data showing different enrichment of H3K9ac at 10 selected genes in OE22 (orange) and the wild type (red) under drought conditions. Gene structures are shown underneath each panel. (+) means positive strand, (-) means negative strand. The profiling of H3K9ac on 10 transcription factor genes was visualized by IGB. Red bars represent the fragments used as qPCR templates for each gene.

(B) ChIP-qPCR validation under drought stress conditions. Data are shown as enrichment of H3K9ac relative to the gene *SamDC*. Shown are means \pm standard errors (n=3). Ninety-six plants of each genotype were used for each independent experiment. The significance of the difference of each gene between OE22 and Bd21-3 was determined using a Student's t test (* $p < 0.05$, ** $p < 0.01$).

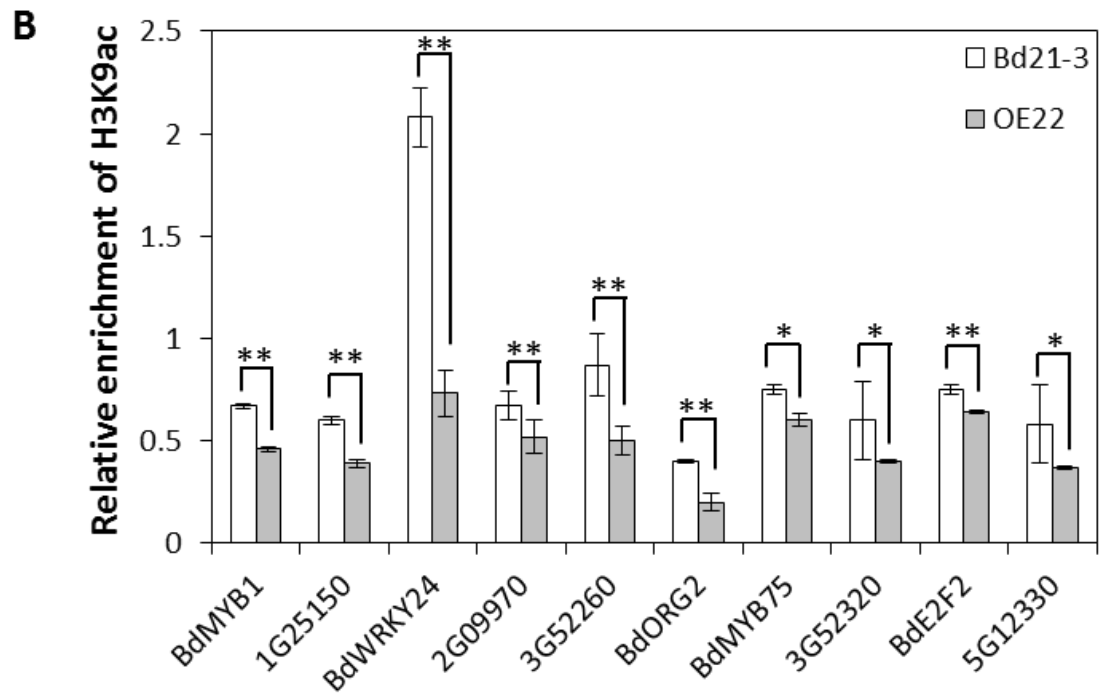
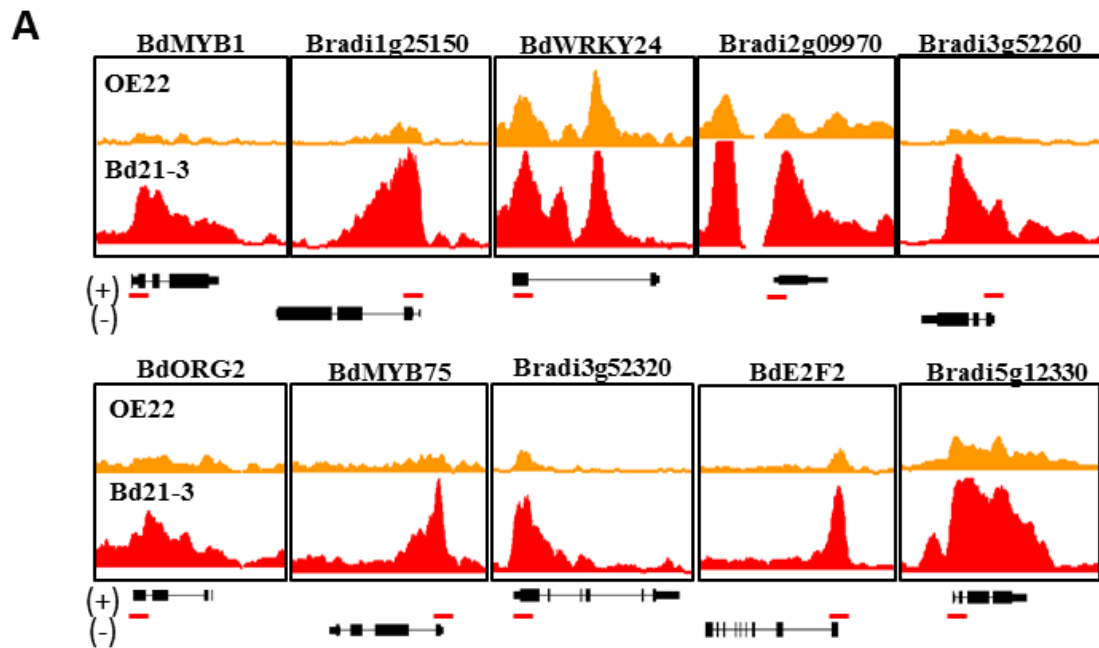
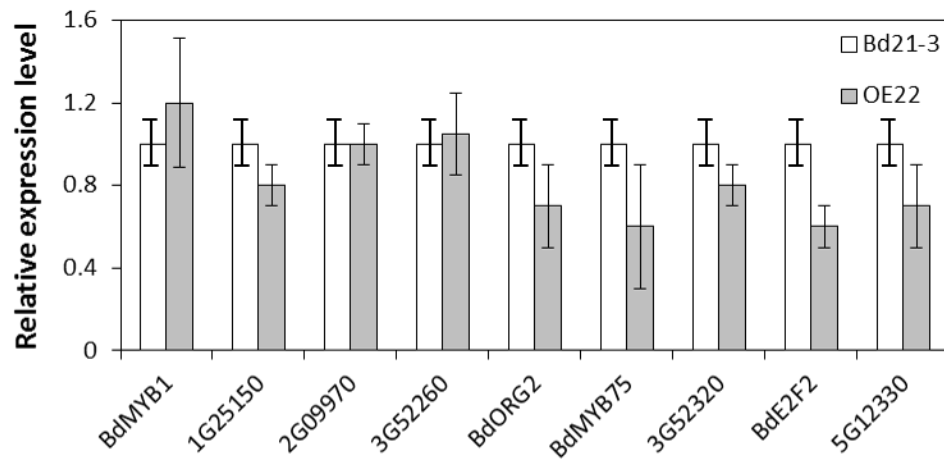
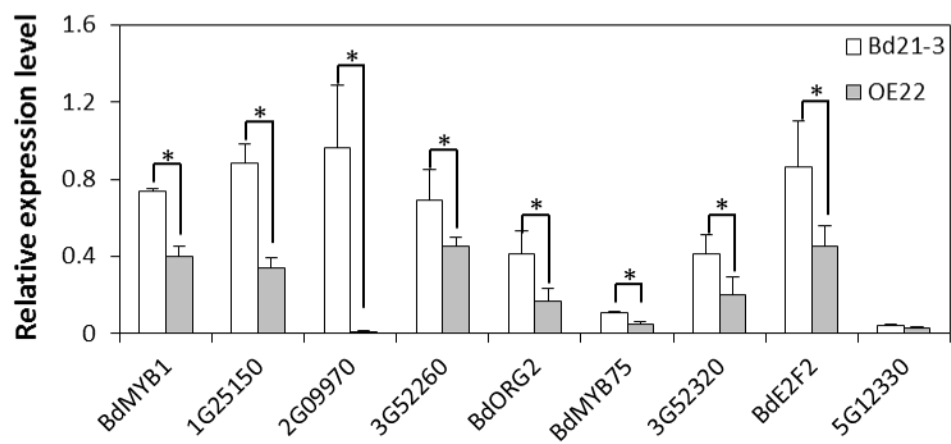


Figure 22. Expression of the “binding activity” genes

RT-qPCR expression analysis of selected genes. The expression of each gene was normalized to that of *SamDC*, and the expression level in wild type Bd21-3 plants grown under control conditions was set to 1. (A) Expression of *BdMYB1*, *1G25105*, *2G09970*, *3G52260*, *BdORG2*, *BdMYB75*, *3G52320*, *BdE2F2*, *5G12330* in Bd21-3 and OE22 under control conditions. (B) Expression of *BdMYB1*, *1G25105*, *2G09970*, *3G52260*, *BdORG2*, *BdMYB75*, *3G52320*, *BdE2F2*, *5G12330* in Bd21-3 and OE22 under drought conditions. Shown are means \pm standard errors ($n = 3$). Three plants of each genotype were pooled together for RNA extraction in one independent experiment. The significance of the difference of each gene between OE22 and Bd21-3 was determined using a Student's t test ($*p < 0.05$).

A**B**

3.2.5 *BdWRKY24* is a drought- and ABA-inducible transcription factor

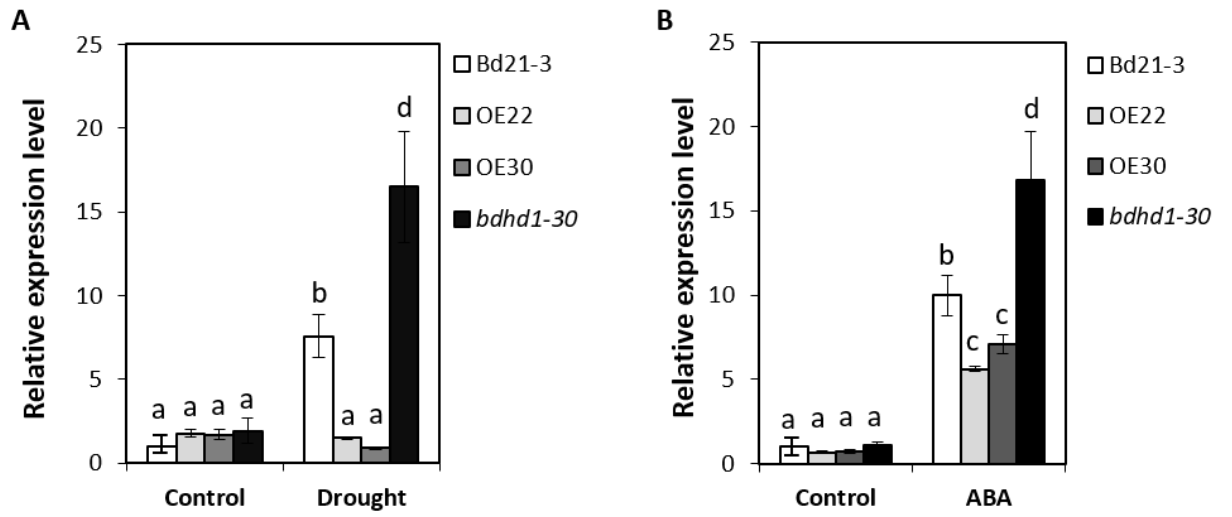
The drought and ABA response phenotypes of the *BdHDI*-OE plants suggested that the expression of some ABA-responsive genes might have been altered in the *BdHDI*-OE plants. Based on the ChIP-Seq data, one WRKY transcription factor gene, *BdWRKY24*, was identified with significantly decreased H3K9ac levels in the OE22 plants. To examine if the gene expression of *BdWRKY24* is regulated by *BdHDI*, I analyzed the transcription level of *BdWRKY24* in the wild type, *BdHDI*-OE lines and *BdHDI*-RNAi plants under control and drought stress conditions by conducting RT-qPCR. Under control conditions, no significant difference was detected between Bd21-3 and transgenic plants (OE22, OE30 and *bdhd1-30*) (Figure 23A). As shown in Figure 23A, the expression levels of *BdWRKY24* were highly induced by drought stress in both Bd21-3 and *bdhd1-30* plants. Significantly higher expression levels of *BdWRKY24* were detected in *bdhd1-30* plants than in Bd21-3 plants. Meanwhile, the expression levels of *BdWRKY24* in the *BdHDI*-OE plants were significantly lower than in Bd21-3 plants under drought stress. This result suggests that *BdHDI* negatively regulated the expression level of *BdWRKY24* under drought stress.

I tested if the expression level of *BdWRKY24* is induced by ABA, in Bd21-3, OE22, OE30 and *bdhd1-30*. The different genotypes of plants were treated with 100 μ M ABA or without ABA. Without ABA, *BdWRKY24* showed a similar expression level in each genotype (Figure 23B). The data showed that the expression level of *BdWRKY24* was induced by ABA in the wild type, Bd21-3 (Figure 23B). This result indicates that *BdWRKY24* is an ABA-inducible gene and might be involved in the ABA signaling pathway. Additionally, compared to Bd21-3, significantly lower expression levels and higher levels of *BdWRKY24* were detected in *BdHDI*-OE (OE22 and OE30) and *BdHDI*-RNAi (*bdhd1-30*), respectively (Figure 23B). The expression patterns of *BdWRKY24* in the different genotypes of plants suggest that *BdHDI* has a negative effect on the expression of *BdWRKY24* in response to ABA.

Figure 23. Expression analysis of *BdWRKY24* under drought stress and ABA

(A) The expression level of *BdWRKY24* in Bd21-3, OE22, OE30 and *bdhd1-30* plants. Data are shown as the relative expression level of *BdWRKY24* to the reference gene, *SamDC*. Shown are means \pm standard errors ($n = 3$). For each independent experiment, 3 plants of each genotype were pooled together for RNA extraction. The significance of difference was determined by using a two-way ANOVA followed by post-hoc Tukey's HSD tests. Lowercase letters indicate significant differences at the level of $p < 0.05$.

(B) The expression levels of *BdWRKY24* in Bd21-3, OE22, OE30 and *bdhd1-30* after 6 hours of the 100 μ M ABA treatment. Shown are means \pm standard errors ($n = 3$). For each independent experiment, 3 plants of each genotype were pooled together for RNA extraction. The significance of difference was determined by using a two-way ANOVA followed by post-hoc Tukey's HSD tests. Lowercase letters indicate significant differences at the level of $p < 0.05$.



Chapter 4. Discussion

4.1 *BdHDI* positively regulates ABA sensitivity and drought tolerance in *Brachypodium*

Previous studies indicate that many HDACs, including HDA6, HDA9, HDA19, HD2C, HD2D and SIR1, are involved in abiotic stress responses in *Arabidopsis* (Chen and Wu, 2010; Chen et al., 2010b; Luo et al., 2012; Mehdi et al., 2015; Han et al., 2016; Zheng et al., 2016). HDACs regulate the expression of the stress-responsive genes that are involved in the transcriptional regulatory networks that respond to environmental stresses (Chinnusamy and Zhu, 2009; Kim et al., 2015). The transcriptional regulatory networks that respond to drought stress differ between dicots and monocots (Nakashima et al., 2009). In rice, the expression patterns of HDACs under different stress conditions have been analyzed, and most of the HDACs are responsive to drought stress (Fu et al., 2007). However, the specific roles of individual HDACs, and their corresponding target genes that respond to drought stress in monocot plants, have not been studied.

In this study, I identified and classified 12 *HDAC* genes in *Brachypodium* (Table 1). The phylogenetic analysis of *HDACs* in *Arabidopsis* and *Brachypodium* indicated that *BdHDI* is a homologous gene of *HDA19*, based on the high similarity at the protein level (Figures 4&5). I also detected that *BdHDI* was localized in the nucleus (Figure 6), which suggests that the nucleus-localized *BdHDI* functions similarly to *HDA19*. The down-regulation of *BdHDI* under drought stress (Figures 7&8) suggests that *BdHDI* is a drought-responsive gene.

To study the role of *BdHDI* in response to drought stress, I generated *BdHDI*-OE (Figure 9) and *BdHDI*-RNAi (Figure 10) plants. Analysis confirmed that *BdHDI*-OE plants had higher expression levels of *BdHDI* than the wild type (Figure 9C), while *BdHDI*-RNAi plants had reduced expression levels of *BdHDI* than the wild type (Figure 10C). To investigate the role of *BdHDI* in the drought stress response of *Brachypodium*, the survival of the *BdHDI*-OE and the *BdHDI*-RNAi plants with the wild type plants under drought stress was determined. *BdHDI*-OE (OE22 and OE30) plants had better survival than the wild type plants under drought stress (Figure 11), while the *bdhd1-30* plants had lower

survival in response to drought stress than the wild type plants (Figure 12).

The down-regulation of *BdHDI* observed in the *Brachypodium* Bd21-3 plants under the drought and ABA treatments might be related to the ABA-dependent drought stress response (Figure 8). Previous research has indicated that an *Arabidopsis* HDA19 T-DNA mutant, *hda19-1*, displayed a phenotype that was hypersensitive to ABA during seed germination (Chen and Wu, 2010). I investigated the *BdHDI*-OE plants under ABA. The *BdHDI*-OE plants did not show any significant difference in germination compared with the wild type plants under control conditions (Figures 13A&B). However, the germination of *BdHDI*-OE seeds was arrested with the application of exogenous ABA (Figure 13A). In the presence of ABA, *BdHDI*-OE plants had significantly shorter shoots and roots than the wild type plants (Figure 13B). These results demonstrate that overexpressing *BdHDI* enhanced sensitivity to ABA during germination and during post-germination growth. In my study, *bdhd1-30* had decreased sensitivity to ABA. Under control conditions, *bdhd1-30* plants had significantly shorter shoots and roots than the wild type Bd21-3 (Figure 14). However, with ABA treatment, the *bdhd1-30* plants exhibited longer roots and a similar length of shoot to the wild type plants (Figure 14). This result indicates that knocking down the expression level of *BdHDI* in *Brachypodium* led to an ABA insensitive phenotype.

Expression of stress-responsive genes has been analyzed to explain the ABA-hypersensitivity of the loss-of-function HDA19 mutant. It was reported that the reduction of HDA19 levels caused down-regulation of ABA responsive genes, including ABI1 and ABI2, but increased the expression of ABA receptor genes (Chen and Wu, 2010; Mehdi et al., 2015). In plants, ABA signaling is mediated by a family of PYR/PYL/RCAR receptor proteins (Pizzio et al., 2013). PYL4 is one of the key ABA receptors (Mehdi et al., 2015). In the absence of ABA, PP2Cs bind and inactivate SnRK2. When ABA is present, ABA binds to PYR/PYL/RCARs, which increases their ability to bind and inhibit PP2Cs (Umezawa et al., 2004). Inactivation of PP2Cs by PYR/PYL/RCARs activates SnRK2, which leads to the activation of the basic leucine zipper (bZIP) transcription factor and switches on the stress response genes (Umezawa et al., 2004; Fujita et al., 2009). *ABI5* encodes a bZIP transcription factor and is required for some ABA-regulated gene expression in plants (Finkelstein, 2000). In *hda19* plants, the reduction of *HDA19* increased

the transcript level of *PYL4* and repressed several ABA-responsive genes involved in core ABA signaling, including *ABI1* and *ABI2* (Chen and Wu, 2010; Mehdi et al., 2015). I analyzed the expression of three ABA-responsive genes in *BdHd1*-overexpression plants: *PYL4*, an ABA receptor gene, *AGH3*, which encodes a PP2C protein, and *ABI5*. The RT-qPCR results indicated that the expression levels of *PYL4*, *ABI5* and *AGH3* were not affected by the overexpression of *BdHd1* (Figure 15). It is possible that *BdHd1* targets different stress-responsive genes from that of *HDA19*, which indicates regulatory networks in *Arabidopsis* and *Brachypodium* may be different. Different functions of HDACs in *Arabidopsis* have been revealed based on the current available evidence. The loss-of-function mutant of *HDA9* was insensitive to PEG treatment. *HDA9* negatively regulated plant responsiveness to dehydration stress by repressing a large number of stress-responsive genes (Zheng et al., 2016). The negative role of *HDA9* in stress response was distinct from that of *HDA19* and *HDA6*, which have a positive role in ABA and salt stress responses. It also is proposed that *HDA9* differs from *HDA19/HDA6* in plant responses by regulating different sets of stress-responsive genes (Zheng et al., 2016).

4.2 *BdHd1* represses gene expression through H3K9 deacetylation

Genome-wide profiling of histone modifications have been revealed in plants (Zhou et al., 2010; Lu et al., 2015; Baerenfaller et al., 2016). Growing evidence indicates that histone modification levels are well correlated with gene expression (Karlic et al., 2010). A recent report identified a differential H3K9ac, H3K27ac and H3S28p signature between the end-of-day and end-of-night that is part of a general mechanism of diurnal transcript level regulation (Baerenfaller et al., 2016). The conserved role of H3K9ac as a gene activation marker has been proposed in plants (Zhou et al., 2010; Du et al., 2013). Genome-wide profiling of H3K9ac has been conducted to investigate its association with general gene expression, but there is still a lack of understanding regarding the association of H3K9ac with the regulation of drought-responsive genes. In rice, drought stress significantly enhanced acetylation of H3K9, H3K18, H3K27 and H4K5 (Fang et al., 2014). This suggests that H3K9ac might be a gene activation marker for drought-responsive genes. In *Brachypodium*, ChIP-Seq data showed that H3K9ac was enriched mainly near the TSS of drought-specific genes. This result is consistent with previous finding that H3K9ac is

enriched near the TSSs of target genes (Zhou et al., 2010). Another study found that H4K16ac is preferentially enriched around TSSs and it positively correlates with gene expression levels in *Arabidopsis* and rice (Lu et al., 2015). Both H3K9ac and H4K16ac are associated with high gene expression.

HDA19 plays an important role in regulating the level of H3K9ac and thereby affects the transcriptional activity of target genes in *Arabidopsis* (Zhou et al., 2010). In the *Arabidopsis* mutant *hda19*, a significant increase of H3K9ac was observed (Zhou et al., 2010). In my study, a decrease of H3K9ac was detected in the *BdHd1*-OE plants (Figures 16A&B). I further revealed the profiling of H3K9ac at the genome-wide level in *Brachypodium* by performing ChIP-Seq. Consistent with the Western blot results, there were more regions with decreased H3K9ac in *BdHd1*-OE plants than in the wild type under control and drought conditions (Figure 16C). This result suggests that *BdHd1* regulates H3K9ac levels in *Brachypodium*. However, the distribution pattern of H3K9ac among different genome categories was not affected by the overexpression of *BdHd1* in *Brachypodium* (Figure 17). In *Arabidopsis*, HDA9 regulates the transcriptional activity of stress-responsive genes. HDA9 mutation leads to the up-regulation of 47 genes related to water-deprivation stress associated with higher H3K9ac in the promoters; thus HDA9 might negatively regulate plant sensitivity to drought stress by regulating the H3K9ac levels of stress-responsive genes in *Arabidopsis* (Zheng et al., 2016). In *Brachypodium*, based on my ChIP-Seq data analysis, 230 genes had lower levels of H3K9ac in *BdHd1*-OE plants compared to the wild type plants under drought stress conditions (Figure 18). Gene ontology analysis of those 230 drought-specific genes indicated that most genes are involved in cellular processes, metabolic processes, catalytic activity and binding activity (Figure 19). I analyzed the H3K9ac levels and the transcriptional activity of 10 transcription factor genes selected from genes classified in the “binding activity”. I found that in the *BdHd1*-OE plants, lower H3K9ac levels on these 10 genes were associated with lower expression levels when compared with the wild type under drought stress (Figures 20-22, 23A). These results suggest that although the *BdHd1* and HDA19 are from different plant species, their negative role in regulating H3K9ac seems to be conserved.

BdHD1 regulates H3K9ac levels, but the target genes of H3K9ac might be different among plant species. Similar to H3K9ac, H4K16ac is another histone modification marker that is positively associated with gene expression levels (Lu et al., 2015). Current evidence has shown the distribution patterns of H4K16ac are generally conserved between *Arabidopsis* and rice, but H4K16ac is associated with different sets of genes in the two species. In *Arabidopsis*, genes with enriched H4K16ac were mostly involved in development, responses to stimuli and signal transduction. In contrast, rice H4K16ac-enriched genes were mostly involved in photosynthesis, metabolic processes and the generation of precursors for metabolites and energy. Because H4K16ac-enriched genes are associated with different biological processes between *Arabidopsis* and rice, suggesting a species-specific role of H4K16ac is suggested (Lu et al., 2015).

RNA sequencing (RNA-Seq) has revealed the genome-wide gene expression in HDA9 mutation in response to drought stress (Zheng et al., 2016). The result showed that HDA9 mutation led to up-regulation of 47 water deprivation stress-related genes, which might be due to the decreased deacetylation activity in the *hda9* mutants. Moreover, 14 up-regulated genes were selected, and significantly higher H3K9ac levels at their promoter regions were detected in the mutant than the wild type plants. There still is a lack of knowledge of genome-wide profiling of H3K9ac under drought stress in plants. My research not only provides information on the genome-wide profiling of H3K9ac in *Brachypodium* under control and drought stress conditions, but also identifies genes with a differential H3K9ac enrichment affected by overexpressing a HDAC gene. The decreased H3K9ac levels of these transcription factor genes (*BdMYB1*, *1G25105*, *2G09970*, *3G52260*, *BdORG2*, *BdMYB75*, *3G52320*, *BdE2F2* and *BdWYRK24*), caused by overexpressing *BdHD1* in plants under drought conditions, probably led to reduced expression of these genes (Figures 21, 22B, 23A). However, the expression of *5G12330* was not significantly lower in OE22 plants than in Bd21-3 under drought stress (Figure 22B). This result suggests that decreased H3K9ac alone in *BdHD1*-OE might not be sufficient for gene repression at some target loci.

4.3 *BdHD1* affects the expression of *BdWRKY24*

In this study, I identified a WRKY transcription factor gene, *BdWRKY24*, which was significantly affected by *BdHD1*. In previous studies, several stress regulatory genes

encoding transcription factors (*AtERF2*, *AtCBF3*, *AtMYB96*, *AtMYB60*, *AtABF2* and *AtABF4*) were found to be the targets of HDA9 (Zheng et al., 2016). This observation suggests that HDA9 plays an important role in drought-responsive gene expression by regulating stress-related transcription factors (Zheng et al., 2016). My ChIP-Seq data analysis identified 230 genes with decreased H3K9ac in *BdHDI*-OE plants under drought conditions. Among these 230 drought-specific genes, several stress regulatory transcription factor genes (such as *BdMYB1*, *BdMYB75* and *BdWRKY24*), were enriched in “binding activity.” The WRKY transcription factors have been mainly associated with plant defense, but increasing evidence suggests the roles of WRKY in plant drought responses (Ülker and Somssich, 2004; Ren et al., 2010; Li et al., 2013). In the wild type *Brachypodium* plants, the expression level of *BdWRKY24* was induced by drought stress (Figure 23A) and ABA (Figure 23B). A similar transcriptional pattern of the WRKY genes *WRKY54* and *WRKY70* was found in the wild type *Arabidopsis* plants, where the *WRKY54* and *WRKY70* transcription factor genes were induced by drought stress (Li et al., 2013). Further study has demonstrated that three WRKY genes, *WRKY46*, *WRKY54*, and *WRKY70*, are involved in drought stress responses, and the triple mutant *wrky46/wrky54/wrky70* is highly tolerant to drought stress in *Arabidopsis*. RNA-sequencing analysis indicated the role of *WRKY46*, *WRKY54* and *WRKY70* in inhibiting drought-responsive genes (Chen et al., 2017). In *Brachypodium*, overexpressing *BdHDI* resulted in a decrease in H3K9ac levels of *BdWRKY24* under drought stress (Figure 21). RT-qPCR results showed that the expression of *BdWRKY24* was significantly repressed under drought stress and ABA treatment in the *BdHDI*-OE plants, but significantly increased in the *bdhd1-30* plants (Figures 23A&B). It is possible that expression of *BdWRKY24* is regulated by *BdHDI*, which affects the sensitivity to ABA and drought tolerance in *Brachypodium*.

4.4 Concluding remarks and perspectives

In conclusion, my work provides a link between histone deacetylase *BdHDI* and an epigenetic marker (H3K9ac) that positively correlates with gene expression in the monocot plant *Brachypodium*. My study revealed that overexpressing *BdHDI* can enhance plant sensitivity to ABA and improve tolerance to drought stress, while knocking-down *BdHDI* leads to an ABA-insensitivity phenotype and decreases drought-tolerance in

Brachypodium. Moreover, the BdHD1 protein is localized in the nucleus and it is responsible for the removal of H3K9 acetylation. This decrease in H3K9 acetylation level leads to a repression of several transcription factor genes in *BdHD1*-OE plants under drought stress.

However, comprehensively understanding the exact role of *BdHD1* in the drought stress response of *Brachypodium* still needs much more exploration. Here, I propose several approaches to further investigate the role of *BdHD1* on drought stress responses.

In my study, I detected the H3K9 acetylation level at a genome-wide level in the OE22 and Bd21-3 plants. Gene expression would need to be explored at the genome-wide level as well to investigate the association between H3K9 acetylation and gene expression. To gain more detailed information regarding gene expression at the genome level under drought stress, a RNA-Seq assay is suggested. RNA-Seq assays could be conducted to reveal the different expression patterns of the drought-responsive genes in the OE22 and Bd21-3 plants. Thus, the expression levels of the 230 genes, identified by the lower H3K9ac level in the OE22 plants than in the wild type plants under drought stress, could be revealed.

It has been reported that several histone acetylation markers, including H3K9ac, H3K27ac, H3K18ac and H3K14ac, respond to drought stress in rice (Fang et al., 2014). In this study, I reported the profiling of H3K9ac in the *Brachypodium* genome, and the H3K9ac-associated genes in *Brachypodium*. However, the profiling of other histone markers is still unexplored in *Brachypodium*. I found that BdHD1 is responsible for the decrease of H3K9ac levels on the target genes. It would be interesting to explore if BdHD1 also targets other histone modification markers.

My study demonstrated that BdHD1 is responsible for the decrease of H3K9ac, which is associated with gene repression. Whether the 230 genes identified in this research are the direct or indirect targets of BdHD1 remains unclear. A ChIP-Seq assay targeting BdHD1 by expressing GFP-labeled BdHD1 driven by its native promoter in *Brachypodium* can be used to explore which of the 230 genes are the direct targets of BdHD1. This would provide more detailed information regarding the direct targets of BdHD1 in *Brachypodium*, and also would show whether BdHD1 targets different group of genes between drought and control conditions.

Histone deacetylases are often recruited as part of larger protein complexes to repress gene expression (Hollender and Liu, 2008). Experimental evidence has shown that HDA19 is involved in such complexes. HDA19 was shown to interact with the repressor complex HISTONE DEACETYLATION COMPLEX1-WD domain protein MSI1(HDC1-MSI1) to repress ABA receptor genes, including *PYL4*, *PYL5* and *PYL6* (Mehdi et al., 2015). Another repressor complex, BES1/TPL/HDA19, also was identified in *Arabidopsis*, and it directly facilitates the histone deacetylation of *ABI3* chromatin, thus leading to the transcriptional repression of *ABI3* and consequently *ABI5* (Ryu et al., 2014). In my study, the 230 drought-specific genes showed lower acetylation levels of H3K9 in the OE22 plants than in Bd21-3 under drought stress. It is possible that BdHD1 interacts with a drought-inducible repressor to reduce the H3K9ac of target genes, thus repressing their gene expression. Alternatively, BdHD1 could be recruited in a repressor complex under control conditions to repress drought-responsive genes; however, the interaction is disrupted under drought conditions because of the lower expression of *BdHD1* when repressed by drought stress. Conversely, overexpressing *BdHD1* can maintain the protein-protein interaction with the gene repressor to maintain the repression of target genes. To identify the BdHD1-interacted protein complexes, two-hybrid screening could be used. BdHD1 would be used as a bait to identify the prey proteins from the screening library that interact with BdHD1. The protein-protein interaction could be further confirmed by using a bimolecular fluorescence complementation (BiFC) assay or a co-immunoprecipitation (Co-IP) assay.

Investigating the role of *BdHD1* in the drought-responsive gene regulatory networks will expand the understanding of the epigenetic regulator in monocot plant stress responses. It will contribute to the understanding of how monocot plants deal with drought stress conditions. My study, along with many others, shows promise in leading to improvement of tolerance to drought stress in monocot crops.

References

- Abe, H., Yamaguchi-shinozaki, K., Urao, T., Iwasaki, T., Hosokawa, D., and Shinozaki, K. (1997). Role of Arabidopsis MYC and MYB homologs in drought- and abscisic acid-regulated gene expression. *Plant Cell Online* **9**:1859–1868.
- Agalou, A., Purwantomo, S., Övernäs, E., Johannesson, H., Zhu, X., Estiati, A., De Kam, R. J., Engström, P., Slamet-Loedin, I. H., Zhu, Z., et al. (2008). A genome-wide survey of HD-Zip genes in rice and analysis of drought-responsive family members. *Plant Mol. Biol.* **66**:87–103.
- Alves, S. C., Worland, B., Thole, V., Snape, J. W., Bevan, M. W., and Vain, P. (2009). A protocol for agrobacterium-mediated transformation of *Brachypodium distachyon* community standard line Bd21. *Nat. Protoc.* **4**:638–649.
- Ariel, F. D., Manavella, P. A., Dezar, C. A., and Chan, R. L. (2007). The true story of the HD-Zip family. *Trends Plant Sci.* **12**:419–426.
- Baerenfaller, K., Shu, H., Hirsch-Hoffmann, M., Fütterer, J., Opitz, L., Rehrauer, H., Hennig, L., and Gruissem, W. (2016). Diurnal changes in the histone H3 signature H3K9ac|H3K27ac|H3S28p are associated with diurnal gene expression in Arabidopsis. *Plant Cell Environ.* **39**:2557–2569.
- Barbosa, E. G. G., Leite, J. P., Marin, S. R. R., Marinho, J. P., de Fátima Corrêa Carvalho, J., Fuganti-Pagliarini, R., Farias, J. R. B., Neumaier, N., Marcelino-Guimarães, F. C., de Oliveira, M. C. N., et al. (2013). Overexpression of the ABA-dependent AREB1 transcription factor from *Arabidopsis thaliana* improves soybean tolerance to water deficit. *Plant Mol. Biol. Report.* **31**:719–730.
- Blunden, J., Arndt, D. S., and Baringer, M. O. (2011). State of the climate in 2010. *Bull. Am. Meteorol. Soc.* **92**:S1–S236.
- Burke, E. J., Brown, S. J., and Christidis, N. (2006). Modeling the recent evolution of global drought and projections for the twenty-first century with the Hadley Centre Climate Model. *J. Hydrometeorol.* **7**:1113–1125.
- Chen, L. T., and Wu, K. (2010). Role of histone deacetylases HDA6 and HDA19 in ABA and abiotic stress response. *Plant Signal. Behav.* **5**:1318–1320.
- Chen, H., Lai, Z., Shi, J., Xiao, Y., Chen, Z., and Xu, X. (2010a). Roles of Arabidopsis WRKY18, WRKY40 and WRKY60 transcription factors in plant responses to abscisic acid and abiotic stress. *BMC Plant Biol.* **10**:281.
- Chen, L. T., Luo, M., Wang, Y. Y., and Wu, K. (2010b). Involvement of Arabidopsis histone deacetylase HDA6 in ABA and salt stress response. *J. Exp. Bot.* **61**:3345–3353.
- Chen, J., Nolan, T. M., Ye, H., Zhang, M., Tong, H., Xin, P., and Chu, J. (2017). Arabidopsis WRKY46, WRKY54, and WRKY70 transcription factors are involved in brassinosteroid-regulated plant growth and drought responses. *Plant Cell* **29**:1425–1439.
- Chinnusamy, V., and Zhu, J. K. (2009). Epigenetic regulation of stress responses in plants. *Curr. Opin. Plant Biol.* **12**:133–139.
- Chinnusamy, V., Gong, Z., and Zhu, J. K. (2008). Abscisic acid-mediated epigenetic processes in plant development and stress responses. *J. Integr. Plant Biol.* **50**:1187–1195.

- Curtis, M. D., and Grossniklaus, U.** (2003). A gateway cloning vector set for high-throughput functional analysis of genes in planta. *Breakthr. Technol.* **133**:462–469.
- Dangl, M., Brosch, G., Haas, H., Loidl, P., and Lusser, A.** (2001). Comparative analysis of HD2 type histone deacetylases in higher plants. *Planta* **213**:280–285.
- Daryanto, S., Wang, L., and Jacinthe, P. A.** (2016). Global synthesis of drought effects on maize and wheat production. *PLoS One* **11**:1–15.
- Du, Z., Li, H., Wei, Q., Zhao, X., Wang, C., Zhu, Q., Yi, X., Xu, W., Liu, X. S., Jin, W., et al.** (2013). Genome-wide analysis of histone modifications: H3K4me2, H3K4me3, H3K9ac, and H3K27ac in *Oryza sativa* L. *J. Mol. Plant* **6**:1463–1472.
- Elliott, J., Deryng, D., Müller, C., Frieler, K., Konzmann, M., Gerten, D., Glotter, M., Flörke, M., Wada, Y., Best, N., et al.** (2014). Constraints and potentials of future irrigation water availability on agricultural production under climate change. *Proc. Natl. Acad. Sci.* **111**:3239–3244.
- Eulgem, T., Rushton, P. J., Robatzek, S., and Somssich, I. E.** (2000). The WRKY superfamily of plant transcription factors. *Trends Plant Sci.* **5**:199–206.
- Fang, H., Liu, X., Thorn, G., Duan, J., and Tian, L.** (2014). Expression analysis of histone acetyltransferases in rice under drought stress. *Biochem. Biophys. Res. Commun.* **443**:400–405.
- Farooq, M., Wahid, A., Kobayashi, N., Fujita, D., and Basra, S. M. A.** (2009). Plant drought stress: effects, mechanisms and management. In *Sustainable Agriculture*. pp. 153–188.
- Finkelstein, R. R.** (2000). The Arabidopsis abscisic acid response gene ABI5 encodes a basic leucine zipper transcription factor. *Plant Cell Online* **12**:599–610.
- Finkelstein, R.** (2013). Abscisic acid synthesis and response. *Arab. B.* **11**:e0166.
- Fita, A., Rodríguez-Burruezo, A., Boscaiu, M., Prohens, J., and Vicente, O.** (2015). Breeding and domesticating crops adapted to drought and salinity: a new paradigm for increasing food production. *Front. Plant Sci.* **6**:1–14.
- Fu, W., Wu, K., and Duan, J.** (2007). Sequence and expression analysis of histone deacetylases in rice. *Biochem. Biophys. Res. Commun.* **356**:843–850.
- Fujita, Y.** (2005). AREB1 is a transcription activator of novel ABRE-dependent ABA signaling that enhances drought stress tolerance in Arabidopsis. *Plant Cell Online* **17**:3470–3488.
- Fujita, Y., Nakashima, K., Yoshida, T., Katagiri, T., Kidokoro, S., Kanamori, N., Umezawa, T., Fujita, M., Maruyama, K., Ishiyama, K., et al.** (2009). Three SnRK2 protein kinases are the main positive regulators of abscisic acid signaling in response to water stress in Arabidopsis. *Plant Cell Physiol.* **50**:2123–2132.
- Garvin, D. F., Gu, Y. Q., Hasterok, R., Hazen, S. P., Jenkins, G., Mockler, T. C., Mur, L. A. J., and Vogel, J. P.** (2008). Development of genetic and genomic research resources for *Brachypodium distachyon*, a new model system for grass crop research. *Crop Sci.* **48**:69–84.
- Gendrel, A. V., Lippman, Z., Martienssen, R., and Colot, V.** (2005). Profiling histone modification patterns in plants using genomic tiling microarrays. *Nat. Methods* **2**:213–218.
- Godfray, H. C. J., Beddington, J. R., Crute, I. R., Haddad, L., Lawrence, D., Muir, J. F., Pretty, J., Robinson, S., Thomas, S. M., and Toulmin, C.** (2010). Food Security: the challenge of feeding 9 billion people. *Science.* **327**:812–818.
- Guindon, S., Dufayard, J. F., Lefort, V., Anisimova, M., Hordijk, W., and Gascuel, O.**

- (2010). New algorithms and methods to estimate maximum-likelihood phylogenies: assessing the performance of PhyML 3.0. *Syst. Biol.* **59**:307–321.
- Han, Z., Yu, H., Zhao, Z., Hunter, D., Luo, X., Duan, J., and Tian, L.** (2016). AtHD2D gene plays a role in plant growth, development, and response to abiotic stresses in *Arabidopsis thaliana*. *Front. Plant Sci.* **7**:1–13.
- Harb, A., Krishnan, A., Ambavaram, M. M. R., and Pereira, A.** (2010). Molecular and physiological analysis of drought stress in *Arabidopsis* reveals early responses leading to acclimation in plant growth. *Plant Physiol.* **154**:1254–1271.
- He, G.-H., Xu, J.-Y., Wang, Y.-X., Liu, J.-M., Li, P.-S., Chen, M., Ma, Y.-Z., and Xu, Z.-S.** (2016). Drought-responsive WRKY transcription factor genes TaWRKY1 and TaWRKY33 from wheat confer drought and/or heat resistance in *Arabidopsis*. *BMC Plant Biol.* **16**:116.
- Hebbes, T. R., Thorne, A. W., and Crane-Robinson, C.** (1988). A direct link between core histone acetylation and transcriptionally active chromatin. *EMBO J.* **7**:1395–1402.
- Helliwell, C., and Waterhouse, P.** (2003). Constructs and methods for high-throughput gene silencing in plants. *Methods* **30**:289–295.
- Helt, G. A., Nicol, J. W., Erwin, E., Blossom, E., Blanchard, S. G., Chervitz, S. A., Harmon, C., and Loraine, A. E.** (2009). Genoviz software development kit: Java tool kit for building genomics visualization applications. *BMC Bioinformatics* **10**:266.
- Hirayama, T., and Shinozaki, K.** (2007). Perception and transduction of abscisic acid signals: keys to the function of the versatile plant hormone ABA. *Trends Plant Sci.* **12**:343–351.
- Hoagland, D. R., and Arnon, D. I.** (1950). The water-culture method for growing plants without soil. *Circ. Calif. Agric. Exp. Stn.* **347**:32 pp.
- Hollender, C., and Liu, Z.** (2008). Histone deacetylase genes in *Arabidopsis* development. *J. Integr. Plant Biol.* **50**:875–885.
- Hong, S.-Y., Seo, P., Yang, M.-S., Xiang, F., and Park, C.-M.** (2008). Exploring valid reference genes for gene expression studies in *Brachypodium distachyon* by real-time PCR. *BMC Plant Biol.* **8**:112.
- Hosy, E., Vavasseur, A., Mouline, K., Dreyer, I., Gaymard, F., Poree, F., Boucherez, J., Lebaudy, A., Bouchez, D., Very, A.-A., et al.** (2003). The *Arabidopsis* outward K⁺ channel GORK is involved in regulation of stomatal movements and plant transpiration. *Proc. Natl. Acad. Sci.* **100**:5549–5554.
- Hu, H., Dai, M., Yao, J., Xiao, B., Li, X., Zhang, Q., and Xiong, L.** (2006). Overexpressing a NAM, ATAF, and CUC (NAC) transcription factor enhances drought resistance and salt tolerance in rice. *Proc. Natl. Acad. Sci.* **103**:12987–12992.
- Hu, Y., Qin, F., Huang, L., Sun, Q., Li, C., Zhao, Y., and Zhou, D. X.** (2009). Rice histone deacetylase genes display specific expression patterns and developmental functions. *Biochem. Biophys. Res. Commun.* **388**:266–271.
- Hundertmark, M., and Hinch, D. K.** (2008). LEA (Late Embryogenesis Abundant) proteins and their encoding genes in *Arabidopsis thaliana*. *BMC Genomics* **22**:118.
- Ingram, J., and Bartels, D.** (1996). The molecular basis of dehydration tolerance in plants. *Annu. Rev. Plant Physiol. Plant Mol. Biol.* **47**:377–403.
- Jenuwein, T.** (2001). Translating the histone code. *Science.* **293**:1074–1080.
- Kapazoglou, A., and Tsiftaris, A.** (2011). Epigenetic chromatin regulators as mediators of abiotic stress responses in cereals. In *Abiotic Stress in Plants - Mechanisms and*

- Adaptations* (ed. Shanker, A.), pp. 395–414. INTECH.
- Karlic, R., Chung, H.-R., Lasserre, J., Vlahovicek, K., and Vingron, M.** (2010). Histone modification levels are predictive for gene expression. *Proc. Natl. Acad. Sci.* **107**:2926–2931.
- Kellogg, E. a** (2001). Evolution evolutionary history of the grasses. *Plant Physiol.* **125**:1198–1205.
- Kim, J.-M., Sasaki, T., Ueda, M., Sako, K., and Seki, M.** (2015). Chromatin changes in response to drought, salinity, heat, and cold stresses in plants. *Front. Plant Sci.* **6**:1–12.
- Komatsu, K., Nishikawa, Y., Ohtsuka, T., Taji, T., Quatrano, R. S., Tanaka, S., and Sakata, Y.** (2009). Functional analyses of the ABI1-related protein phosphatase type 2C reveal evolutionarily conserved regulation of abscisic acid signaling between Arabidopsis and the moss *Physcomitrella patens*. *Plant Mol. Biol.* **70**:327–340.
- Langmead, B., and Salzberg, S. L.** (2012). Fast gapped-read alignment with Bowtie 2. *Nat. Methods* **9**:357–359.
- Lesk, C., Rowhani, P., and Ramankutty, N.** (2016). Influence of extreme weather disasters on global crop production. *Nature* **529**:84–87.
- Leung, J., Merlot, S., and Giraudat, J.** (1997). The Arabidopsis ABSCISIC ACID-INSENSITIVE2 (ABI2) and ABI1 genes encode homologous protein phosphatases 2C involved in abscisic acid signal transduction. *Plant Cell* **9**:759–71.
- Li, J., Besseau, S., and Petri, T.** (2013). Defense-related transcription factors WRKY70 and WRKY54 modulate osmotic stress tolerance by regulating stomatal aperture in Arabidopsis. *new Phytol.* **200**:457–472.
- Li, C., Gu, L., Gao, L., Chen, C., Wei, C. Q., Qiu, Q., Chien, C. W., Wang, S., Jiang, L., Ai, L. F., et al.** (2016). Concerted genomic targeting of H3K27 demethylase REF6 and chromatin-remodeling ATPase BRM in Arabidopsis. *Nat. Genet.* **48**:687–693.
- Liu, X., Yang, S., Zhao, M., Luo, M., Yu, C. W., Chen, C. Y., Tai, R., and Wu, K.** (2014). Transcriptional repression by histone deacetylases in plants. *Mol. Plant* **7**:764–772.
- Liu, X., Wei, W., Zhu, W., Su, L., Xiong, Z., Zhou, M., Zheng, Y., and Zhou, D.-X.** (2017). Histone deacetylase AtSRT1 regulates metabolic flux and stress response in Arabidopsis. *Mol. Plant* **10**:1510–1522.
- Lu, F., Cui, X., Zhang, S., Jenuwein, T., and Cao, X.** (2011). Arabidopsis REF6 is a histone H3 lysine 27 demethylase. *Nat. Genet.* **43**:715–719.
- Lu, L., Chen, X., Sanders, D., Qian, S., and Zhong, X.** (2015). High-resolution mapping of H4K16 and H3K23 acetylation reveals conserved and unique distribution patterns in Arabidopsis and rice. *Epigenetics* **10**:1044–1053.
- Luo, M., Wang, Y. Y., Liu, X., Yang, S., Lu, Q., Cui, Y., and Wu, K.** (2012). HD2C interacts with HDA6 and is involved in ABA and salt stress response in Arabidopsis. *J. Exp. Bot.* **63**:3297–3306.
- Lusser, A., Brosch, G., Loidl, A., Haas, H., and Loidl, P.** (1997). Identification of maize histone deacetylase HD2 as an acidic nucleolar phosphoprotein. *Science.* **277**:88–91.
- Lusser, A., Kölle, D., and Loidl, P.** (2001). Histone acetylation: lessons from the plant kingdom. *Trends Plant Sci.* **6**:59–65.
- Ma, Y., Szostkiewicz, I., Korte, A., Moes, D., Yang, Y., Christmann, A., and Grill, E.** (2009). Regulators of PP2C. *Science.* **324**:1064–1069.
- Maitra, N., and Cushman, J. C.** (1994). Isolation and characterization of a drought-

- induced soybean cDNA encoding a D95 family late-embryogenesis-abundant protein. *Plant Physiol.* **106**:805–6.
- Matsumoto, T., Wu, J., Kanamori, H., Katayose, Y., Fujisawa, M., Namiki, N., Mizuno, H., Yamamoto, K., Antonio, B. A., Baba, T., et al.** (2005). The map-based sequence of the rice genome. *Nature* **436**:793–800.
- Mehdi, S., Derkacheva, M., Ramström, M., Kralemann, L., Bergquist, J., and Hennig, L.** (2015). MSI1 functions in a HDAC complex to fine-tune ABA signaling. *Plant Cell* **29**:TPC2015-00763-RA.
- Melcher, K., Ng, L. M., Zhou, X. E., Soon, F. F., Xu, Y., Suino-Powell, K. M., Park, S. Y., Weiner, J. J., Fujii, H., Chinnusamy, V., et al.** (2009). A gate-latch-lock mechanism for hormone signalling by abscisic acid receptors. *Nature* **462**:602–608.
- Meyer, K., Leube, M. P., and Grill, E.** (1994). A Protein Phosphatase 2C involved in ABA signal transduction in *Arabidopsis thaliana*. *Science*. **264**:1452–1455.
- Mi, H., Muruganujan, A., Casagrande, J. T., and Thomas, P. D.** (2013). Large-scale gene function analysis with the panther classification system. *Nat. Protoc.* **8**:1551–1566.
- Mi, H., Huang, X., Muruganujan, A., Tang, H., Mills, C., Kang, D., and Thomas, P. D.** (2017). PANTHER version 11: Expanded annotation data from Gene Ontology and reactome pathways, and data analysis tool enhancements. *Nucleic Acids Res.* **45**:D183–D189.
- Mickelbart, M. V., Hasegawa, P. M., and Bailey-serres, J.** (2015). Genetic mechanisms of abiotic stress tolerance that translate to crop yield stability. *Nat. Publ. Gr.* **16**:237–251.
- Mikolajczyk, M., Awotunde, O. S., Muszyńska, G., Klessig, D. F., and Dobrowolska, G.** (2000). Osmotic stress induces rapid activation of a salicylic acid-induced protein kinase and a homolog of protein kinase ASK1 in tobacco cells. *Plant Cell* **12**:165–78.
- Murasnige, T., and Skoog, F.** (1962). A revised medium for rapid growth and bio assays with tobacco tissue cultures. *Physiol. Plant.* **15**:473–497.
- Nakashima, K., Tran, L. S. P., Van Nguyen, D., Fujita, M., Maruyama, K., Todaka, D., Ito, Y., Hayashi, N., Shinozaki, K., and Yamaguchi-Shinozaki, K.** (2007). Functional analysis of a NAC-type transcription factor OsNAC6 involved in abiotic and biotic stress-responsive gene expression in rice. *Plant J.* **51**:617–630.
- Nakashima, K., Ito, Y., and Yamaguchi-Shinozaki, K.** (2009). Transcriptional regulatory networks in response to abiotic stresses in *Arabidopsis* and grasses. *Plant Physiol.* **149**:88–95.
- Nakashima, K., Yamaguchi-Shinozaki, K., and Shinozaki, K.** (2014). The transcriptional regulatory network in the drought response and its crosstalk in abiotic stress responses including drought, cold, and heat. *Front. Plant Sci.* **5**:1–7.
- Napoli, C. A. P. M., Selinger, D. A., Pandey, R., Mu, A., Pikaard, C. S., Richards, E. J., Bender, J., Mount, D. W., and Jorgensen, R. A.** (2002). Analysis of histone acetyltransferase and histone deacetylase families of *Arabidopsis thaliana* suggests functional diversification of chromatin modification among multicellular eukaryotes. *Nucleic Acids Res.* **30**:5036–5055.
- Osakabe, Y., Osakabe, K., Shinozaki, K., and Tran, L.-S. P.** (2014). Response of plants to water stress. *Front. Plant Sci.* **5**:1–8.
- Park, S. S.-Y., Fung, P., Nishimura, N., Jensen, D. R., Fujii, H., Zhao, Y., Lumba, S., Santiago, J., Rodrigues, A., Chow, T. F. T. -f. F., et al.** (2009). Abscisic acid inhibits

- type 2C. *Science*. **324**:1068–1069.
- Paterson, A. H., Bowers, J. E., Bruggmann, R., Dubchak, I., Grimwood, J., Gundlach, H., Haberer, G., Hellsten, U., Mitros, T., Poliakov, A., et al.** (2009). The sorghum bicolor genome and the diversification of grasses. *Nature* **457**:551–556.
- Pizzio, G. A., Rodriguez, L., Antoni, R., Gonzalez-Guzman, M., Yunta, C., Merilo, E., Kollist, H., Albert, A., and Rodriguez, P. L.** (2013). The PYL4 A194T mutant uncovers a key role of PYR1-LIKE4/PROTEIN PHOSPHATASE 2CA interaction for abscisic acid signaling and plant drought resistance. *Plant Physiol.* **163**:441–455.
- Price, A. H.** (2002). Linking drought-resistance mechanisms to drought avoidance in upland rice using a QTL approach: progress and new opportunities to integrate stomatal and mesophyll responses. *J. Exp. Bot.* **53**:989–1004.
- Qiu, Y., and Yu, D.** (2009). Over-expression of the stress-induced OsWRKY45 enhances disease resistance and drought tolerance in Arabidopsis. *Environ. Exp. Bot.* **65**:35–47.
- Ren, X., Chen, Z., Liu, Y., Zhang, H., Zhang, M., Liu, Q., Hong, X., Zhu, J. K., and Gong, Z.** (2010). ABO3, a WRKY transcription factor, mediates plant responses to abscisic acid and drought tolerance in Arabidopsis. *Plant J.* **63**:417–429.
- Rosegrant, M.** (2003). Global food security: challenges and policies. *Science*. **1917**:1917–1920.
- Ruijter, A. J. M. de, Gennip, A. H. van, Caron, H. N., Kemp, S., and Kuilenburg, A. B. P. van** (2003). Histone deacetylases (HDACs): characterization of the classical HDAC family. *Biochem. J.* **370**:737–749.
- Rushton, P. J., Somssich, I. E., Ringler, P., and Shen, Q. J.** (2010). WRKY transcription factors. *Trends Plant Sci.* **15**:247–258.
- Rushton, D. L., Tripathi, P., Rabara, R. C., Lin, J., Ringler, P., Boken, A. K., Langum, T. J., Smidt, L., Boomsma, D. D., Emme, N. J., et al.** (2012). WRKY transcription factors: key components in abscisic acid signalling. *Plant Biotechnol. J.* **10**:2–11.
- Ryu, H., Cho, H., Bae, W., and Hwang, I.** (2014). Control of early seedling development by BES1/TPL/HDA19-mediated epigenetic regulation of ABI3. *Nat. Commun.* **5**:1–11.
- Salmon-Divon, M., Dvinge, H., Tammaja, K., and Bertone, P.** (2010). PeakAnalyzer: genome-wide annotation of chromatin binding and modification loci. *BMC Bioinformatics* **11**.
- Santiago, J., Dupeux, F., Round, A., Antoni, R., Park, S. Y., Jamin, M., Cutler, S. R., Rodriguez, P. L., and Márquez, J. A.** (2009). The abscisic acid receptor PYR1 in complex with abscisic acid. *Nature* **462**:665–668.
- Schroeder, J. I., Kwak, J. M., and Allen, G. J.** (2001). Guard cell abscisic acid signalling and engineering drought hardiness in plants. *Nature* **410**:327–330.
- Schweighofer, A., Hirt, H., and Meskiene, I.** (2004). Plant PP2C phosphatases: emerging functions in stress signaling. *Trends Plant Sci.* **9**:236–243.
- Shang, Y., Yan, L., Liu, Z.-Q., Cao, Z., Mei, C., Xin, Q., Wu, F.-Q., Wang, X.-F., Du, S.-Y., Jiang, T., et al.** (2010). The Mg-chelatase H subunit of *Arabidopsis* antagonizes a group of WRKY transcription repressors to relieve ABA-responsive genes of inhibition. *Plant Cell* **22**:1909–1935.
- Shinozaki, K., and Yamaguchi-Shinozaki, K.** (2007). Gene networks involved in drought stress response and tolerance. *J. Exp. Bot.* **58**:221–227.
- Shinozaki, K., Yamaguchi-Shinozaki, K., and Seki, M.** (2003). Regulatory network of gene expression in the drought and cold stress responses. *Curr. Opin. Plant Biol.*

- 6:410–417.
- Somerville, C.** (2006). The billion-ton biofuels vision. *Science*. **312**:1277.
- Sridha, S., and Wu, K.** (2006). Identification of AtHD2C as a novel regulator of abscisic acid responses in Arabidopsis. *Plant J.* **46**:124–133.
- Sternberg, T.** (2011). Regional drought has a global impact. *Nature* **472**:169.
- Tang, N., Zhang, H., Li, X., Xiao, J., and Xiong, L.** (2012). Constitutive activation of transcription factor OsZIP46 improves drought tolerance in rice. *Plant Physiol.* **158**:1755–1768.
- Tian, G., Lu, Q., Zhang, L., Kohalmi, S. E., and Cui, Y.** (2011). Detection of protein interactions in plant using a gateway compatible bimolecular fluorescence complementation (BiFC) system. *J. Vis. Exp.* doi:10.3791/3473.
- Tougane, K., Komatsu, K., Bhyan, S. B., Sakata, Y., Ishizaki, K., Yamato, K. T., Kohchi, T., and Takezawa, D.** (2010). Evolutionarily conserved regulatory mechanisms of abscisic acid signaling in land plants: characterization of ABSCISIC ACID INSENSITIVE1-Like Type 2C Protein Phosphatase in the liverwort marchantia polymorpha. *Plant Physiol.* **152**:1529–1543.
- Tran, L. P., Nakashima, K., Sakuma, Y., Simpson, S. D., Fujita, Y., Maruyama, K., Fujita, M., Seki, M., Shinozaki, K., and Yamaguchi-shinozaki, K.** (2004). Isolation and functional analysis of Arabidopsis stress-inducible NAC transcription factors that bind to a drought-responsive *cis*-element in the early responsive to dehydration stress 1 promoter. *Plant Cell* **16**:2481–2498.
- Ülker, B., and Somssich, I. E.** (2004). WRKY transcription factors : from DNA binding towards biological function. *Curr. Opin. Plant Biol.* **7**:491–498.
- Umezawa, T., Yoshida, R., Maruyama, K., Yamaguchi-Shinozaki, K., and Shinozaki, K.** (2004). SRK2C, a SNF1-related protein kinase 2, improves drought tolerance by controlling stress-responsive gene expression in Arabidopsis thaliana. *Proc. Natl. Acad. Sci.* **101**:17306–17311.
- Umezawa, T., Sugiyama, N., Mizoguchi, M., Hayashi, S., Myouga, F., Yamaguchi-Shinozaki, K., Ishihama, Y., Hirayama, T., and Shinozaki, K.** (2009). Type 2C protein phosphatases directly regulate abscisic acid-activated protein kinases in Arabidopsis. *Proc. Natl. Acad. Sci.* **106**:17588–17593.
- Umezawa, T., Nakashima, K., Miyakawa, T., Kuromori, T., Tanokura, M., Shinozaki, K., and Yamaguchi-Shinozaki, K.** (2010). Molecular basis of the core regulatory network in ABA responses: sensing, signaling and transport. *Plant Cell Physiol.* **51**:1821–1839.
- Umezawa, T., Sugiyama, N., Takahashi, F., Anderson, J. C., Ishihama, Y., Peck, S. C., and Shinozaki, K.** (2013). Genetics and phosphoproteomics reveal a protein phosphorylation network in the abscisic acid signaling pathway in *Arabidopsis thaliana*. *Sci. Signal.* **6**:rs8.
- Valdés, A. E., Övernäs, E., Johansson, H., Rada-Iglesias, A., and Engström, P.** (2012). The homeodomain-leucine zipper (HD-Zip) class I transcription factors ATHB7 and ATHB12 modulate abscisic acid signalling by regulating protein phosphatase 2C and abscisic acid receptor gene activities. *Plant Mol. Biol.* **80**:405–418.
- Vogel, J., and Hill, T.** (2008). High-efficiency Agrobacterium-mediated transformation of *Brachypodium distachyon* inbred line Bd21-3. *Plant Cell Rep.* **27**:471–478.
- Vogel, J. P., Garvin, D. F., Mockler, T. C., Schmutz, J., Rokhsar, D., Bevan, M. W., Barry, K., Lucas, S., Harmon-Smith, M., Lail, K., et al.** (2010). Genome

- sequencing and analysis of the model grass *Brachypodium distachyon*. *Nature* **463**:763–768.
- Wu, F.-Q., Xin, Q., Cao, Z., Liu, Z.-Q., Du, S.-Y., Mei, C., Zhao, C.-X., Wang, X.-F., Shang, Y., Jiang, T., et al.** (2009a). The Magnesium-Chelatase H subunit binds abscisic acid and functions in abscisic acid signaling: new evidence in Arabidopsis. *Plant Physiol.* **150**:1940–1954.
- Wu, X., Shiroto, Y., Kishitani, S., Ito, Y., and Toriyama, K.** (2009b). Enhanced heat and drought tolerance in transgenic rice seedlings overexpressing OsWRKY11 under the control of HSP101 promoter. *Plant Cell Rep.* **28**:21–30.
- Wu, J., Chen, J., Wang, L., and Wang, S.** (2017). Genome-wide investigation of WRKY transcription factors involved in terminal drought stress response in common bean. *Front. Plant Sci.* **8**:1–12.
- Xu, D., Duan, X., Wang, B., Hong, B., Ho, T., and Wu, R.** (1996). Expression of a late embryogenesis abundant protein gene, HVA1, from barley confers tolerance to water deficit and salt stress in transgenic rice. *Plant Physiol.* **110**:249–257.
- Yamaguchi-Shinozaki, K., and Shinozaki, K.** (1993). The plant hormone abscisic acid mediates the drought-induced expression but not the seed-specific expression of rd22, a gene responsive to dehydration stress in Arabidopsis thaliana. *MGG Mol. Gen. Genet.* **238**:17–25.
- Yamaguchi-Shinozaki, K., and Shinozaki, K.** (2005). Organization of *cis*-acting regulatory elements in osmotic- and cold-stress-responsive promoters. *Trends Plant Sci.* **10**:88–94.
- Yoshida, T., Fujita, Y., Sayama, H., Kidokoro, S., Maruyama, K., Mizoi, J., Shinozaki, K., and Yamaguchi-Shinozaki, K.** (2010). AREB1, AREB2, and ABF3 are master transcription factors that cooperatively regulate ABRE-dependent ABA signaling involved in drought stress tolerance and require ABA for full activation. *Plant J.* **61**:672–685.
- Zang, C., Schones, D. E., Zeng, C., Cui, K., Zhao, K., and Peng, W.** (2009). A clustering approach for identification of enriched domains from histone modification ChIP-Seq data. *Bioinformatics* **25**:1952–1958.
- Zhang, Y., Liu, T., Meyer, C. A., Eeckhoute, J., Johnson, D. S., Bernstein, B. E., Nussbaum, C., Myers, R. M., Brown, M., Li, W., et al.** (2008). Model-based analysis of ChIP-Seq (MACS). *Genome Biol.* **9**:R137.
- Zhang, S., Haider, I., Kohlen, W., Jiang, L., Bouwmeester, H., Meijer, A. H., Schlupepmann, H., Liu, C. M., and Ouwkerk, P. B. F.** (2012). Function of the HD-Zip I gene Oshox22 in ABA-mediated drought and salt tolerances in rice. *Plant Mol. Biol.* **80**:571–585.
- Zhen Xie, Zhong-Lin Zhang, Xiaolu Zou, Jie Huang, Paul Ruas, Daniel Thompson, and Q. J. S.** (2005). Annotations and functional analyses of the rice WRKY gene superfamily reveal positive and negative regulators of abscisic acid signaling. *Plant Physiol.* **137**:176–189.
- Zheng, Y., Ding, Y., Sun, X., Xie, S., Wang, D., Liu, X., Su, L., Wei, W., Pan, L., and Zhou, D. X.** (2016). Histone deacetylase HDA9 negatively regulates salt and drought stress responsiveness in Arabidopsis. *J. Exp. Bot.* **67**:1703–1713.
- Zhou, C., Labbe, H., Sridha, S., Wang, L., Tian, L., Latoszek-Green, M., Yang, Z., Brown, D., Miki, B., and Wu, K.** (2004). Expression and function of HD2-type histone deacetylases in Arabidopsis development. *Plant J.* **38**:715–724.

Zhou, J., Wang, X., He, K., Charron, J. B. F., Elling, A. A., and Deng, X. W. (2010). Genome-wide profiling of histone H3 lysine 9 acetylation and dimethylation in arabidopsis reveals correlation between multiple histone marks and gene expression. *Plant Mol. Biol.* **72**:585–595.

Appendices

Appendix 1. Primers used for gene amplification of *BdHD1*.

Constructs	Primers	Sequences (5' > 3')
<i>BdHD1</i>- Overexpression	Bradi3g08060(G1)FOR	GGGGACAAGTTTGTACAAAAAAGCAGGCTCGATGGACCTCTCCT CGGCC
	Bradi3g08060(G1)REV	GGGGACCACTTTGTACAAGAAAGCTGGGTCTGGCTTCTGATAAA CAGCCG
<i>BdHD1</i>-RNAi	Bradi3g08060RNAiFOR	GGGGACAAGTTTGTACAAAAAAGCAGGCTCGCAGGTTCTGGCA CAAAGTT
	Bradi3g08060RNAiREV	GGGGACCACTTTGTACAAGAAAGCTGGGTCTGAGCCACTTTGCAG TTAATGG

Appendix 2. Genes used for genotyping of *BdHDI*-RNAi plants

DNA	Primers	Sequences (5' > 3')
Transfer DNA	RNAiFOR	CAGGTTCTGGCACAAAGTT
	PDKIntronREV	ACAAGCAGATTGGAATTTCTAACA
<i>SamDC</i>	SamDCFOR	TGCTAATCTGCTCCAATGGC
	SamDCREV	GACGCAGCTGACCACCTAGA

Appendix 3 Primers used for ChIP-qPCR

Genes	Primers	Sequences (5' > 3')
<i>SamDC</i>	SamDCchipF	TGCTAATCTGCTCCAATGGC
	SamDCchipR	GACGCAGCTGACCACCTAGA
<i>BdWRKY24</i>	Bd2g49020chipF	TCAGAACGGGGAGAACGA
	Bd2g49020chipR	TCGCTCCTGGTCTGGAAT
<i>BdMYB1</i>	1g07260chipFOR	TATCAACGCCTCTTCCCGTC
	1g07260chipREV	ATGTAGGACTTGAGCGTGCC
<i>1G25150</i>	1g25150chipFOR	TCCTCTCTCCCGTCTCAGTG
	1g25150chipREV	AAGACGTCGTGTGCCTTGAT
<i>2G09970</i>	2g09970chipFOR	CACATACATGGACAGCCCGA
	2g09970chipREV	ATCCTTCAGGTGATCGGGGA
<i>3G52260</i>	3g52260chipFOR	AGCATCAGCAGCAGGAGAAG
	3g52260chipREV	GAACGCCTCCTTGTCTTGA
<i>BdORG2</i>	2g60970chipFOR	TGCTTGGAATCCTGACGCAT
	2g60970chipREV	GTTCTGGTCCTTCATGGCGA
<i>3G52320</i>	3g52320chipFOR	CTGGTCTCCTCCTCACCTCA
	3g52320chipREV	TGGGGAGAGGGAAATACGGT
<i>BdE2F2</i>	5g09640chipFOR	TCACCAATTTCCAGTGCCT
	5g09640chipREV	AGCGTAGAGACCCTGGTACC
<i>5G12330</i>	5g12330chipFOR	AAGCTGAAGGTGGCGATCAA
	5g12330chipREV	CGTGGAGTCGTACTIONGAGCA
<i>BdMYB75</i>	5g16980chipFOR	AGAGGCGGTGTTGATGAAA
	5g16980chipREV	TTCATAACCAGCACCACGGG

Appendix 4. Primers used for RT-qPCR.

Genes	Primers	Sequences (5' > 3')
<i>SamDC</i>	SamDCFOR	TGCTAATCTGCTCCAATGGC
	SamDCREV	GACGCAGCTGACCACCTAGA
<i>BdHD1</i>	BdHD1FOR	ATGGACCTCTCCTCGGCC
	BdHD1REV	CCGCTCTTGAAATTGGACAC
<i>PYL4</i>	PYL4qFOR	GACGATGGTGTGCGATGAAGA
	PYL4qREV	TTGCTATGGCTGCACAAGTC
<i>ABI5</i>	abi5qFOR	GAGTTGGAGACTGAGGTGGC
	abi5qREV	CTGTCAGTGTCTACGCAGG
<i>AGH3</i>	2g45470qFOR	GATAGCGGAACCAGAGGTGA
	2g45470qREV	TAGGCAATTCCTTGCATCT
<i>BdWRKY24</i>	2g49020FOR	GTGGCAAGGAGAAGGCTATG
	2g49020REV	GGTAGCCGTCGTCCAAGATA
<i>BdMYB1</i>	1g07260qFOR	CGATTGCTTCTTCGGCATGG
	1g07260qREV	CCCTACTGCATCCCAAGGTC
<i>1G25150</i>	1g25150qFOR	CGGTGGTTGATACGGACGAT
	1g25150qREV	AACATCAGGCCTAGTGCACC
<i>2G09970</i>	2g09970qFOR	CGCCTTGAGGACGACAGATT
	2g09970qREV	GAGGTGCGTGTACTCCAGAA
<i>3G52260</i>	3g52260qFOR	AGAGGGAAAGGAGTGGTGGT
	3g52260qREV	GAATTGGAAGCAGGGGTGGT
<i>BdORG2</i>	2g60970qFOR	GGTTCAGGTCAGCTTGCTCA
	2g60970qREV	AACGTTGGACACTCTTCGCT
<i>3G52320</i>	3g52320qFOR	GGAAGGGGAGAGCTGAGAGA
	3g52320qREV	CTAGCTAGGCACCATCCACG
<i>BdE2F2</i>	5g09640qFOR	AGGAGCTGGTTGATGTTGCA
	5g09640qREV	ACTTCTGGAGTGATCGTCGC
<i>5G12330</i>	5g12330qFOR	GTCTCAAGAAGACCCTGGC
	5g12330qREV	TGACCTTGACCATGTCGTCG
<i>BdMYB75</i>	5g16980qFOR	GGTTACCCGGTCGTGGATTT
	5g16980qREV	TCACCCAAATGCTCCTCAGG

Curriculum Vitae

Name: Jingpu Song

Post-secondary Education and Degrees: Western University
London, Ontario, Canada
2013- 2018, Ph.D.

Northwest A&F University
Yangling, Shaanxi, China
2009-2013 B.Sc.

Honours and Awards: Western Graduate Research Scholarship
Western University
2013-2018

Travel Award of Department of Biology
Western University
2017

Travel Award of Canadian Association for Plant Biotechnology
Plant Biotech 2016 Conference, Kingston
2016

Related Work Experience: Teaching Assistant
Western University
2013-2018

Research Assistant
Agriculture and Agri-Food Canada
2013-2018

Publications:

Submitted Manuscripts

J. Song, H. Henry, L. Tian. (2018) *Brachypodium* histone deacetylase BdHD1 positively regulates ABA and drought stress responses. Submitted to Plant Science (**Ph.D. Thesis**)

J. Song, H. Henry, L. Tian. (2018) Drought-inducible changes in the histone modification H3K9ac are associated with drought-responsive gene expression in *B. distachyon*. Plan to Plant Molecular Biology. (**Ph.D. Thesis**)